International Conference and Summer School on Silicide Green Technology
(ICSS-SILICIDE 2014) , Jul. 21, 2014
Tokyo University of Science, Katsushika Campus

Light Emission from β-$FeSi_2$

Yoshihito Maeda
Department of Computer Science and Technology
Kyushu Institute of Technology (Kyutech)
Advanced Science Research Center, Japan Atomic Energy Agency

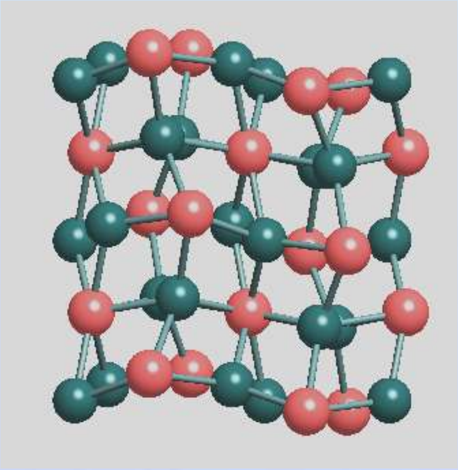

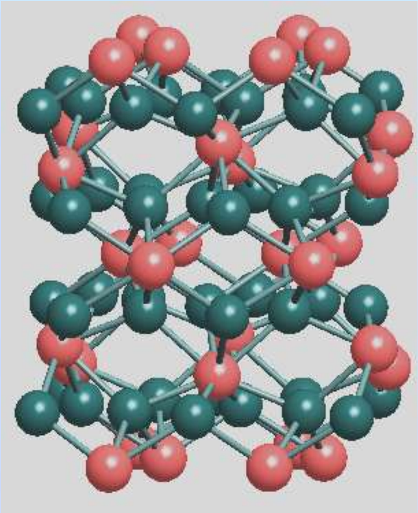

CSSE
Kyushu Institute of technology

Acknowledgements

This lecture is based on many research results on light emission form IBS β-$FeSi_2$ since 1995. YM would like to acknowledge both to dear graduates of Osaka Prefecture University (1995-2003), Kyoto University (2003-2012) and Kyushu Institute of Technology, Kyutech (2012-present) and to students of Kyutech for their serious efforts to sample preparations and optical measurements. And also he would like to give many thanks to Professor Y. Terai of Kagoshima University for continuous and fruitful discussion and suggestion on understanding of PL data. Finally, he expresses his appreciation to organizing committee of ICSS Silicides 2014 for invitation to this international summer school.

CSSE
Kyushu Institute of technology

Outline of my lecture

1. Introduction and Research background

2. Light emission from β-$FeSi_2$ crystals and its fundamental scheme

3. Light emission from β-$FeSi_2$/Si nano-composite phase

4. Some examples of enhancement of PL from β-$FeSi_2$/Si

5. Future study required moreover

CSSE
Kyusyu Institute of technology

1

Introduction and Research background

First, introduction relating to general scheme of semiconducting Silicides and technology toward application to optoelectronics.

Variety of Semiconducting Silicides toward device applications

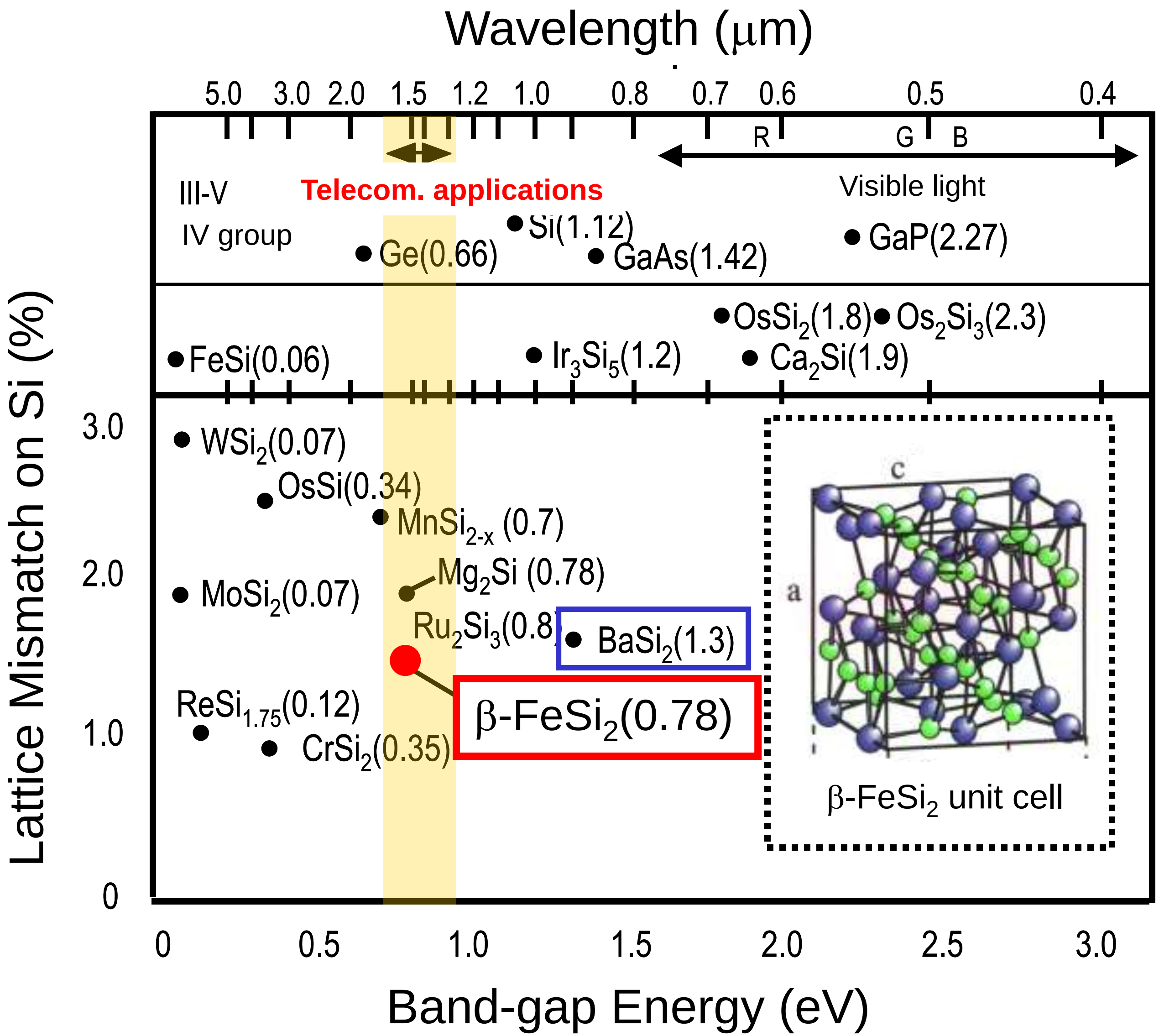

Applications (realized)

Light emitter materials
β-FeSi$_2$/Si, Ru$_2$Si$_3$

Light receiver materials
β-FeSi$_2$/Si, FeSi/Si, Ca$_2$Si/Si

Photonic crystal materials
β-FeSi$_2$/Si waveguide

Photovoltaic materials
β-FeSi$_2$/Si,
BaSi$_2$(Schottky junction)

Thermoelectric materials
Mg$_2$Si,
β-FeSi$_2$(~600K)

Y. Maeda and Y. Terai：Bull. Inst. of Metals Japan, MATERIA 2005 Jun.

Silicon-based approaches for photonics

Full Contribution of Active Silicides

	Standard Materials	Silicon-based approaches: visible	Silicon-based approaches: IR
source	Compound Semiconductors	Nanoparticles Porous Si EL from RE ions	Er-doped pn-junctions β-$FeSi_2$
waveguide	SiO_2 fibers Polymers	Glass/SiO_2/Si Al_2O_3/SiO_2/Si Polymer/SiO_2/Si	Si on SiO_2
modulator or switch	$LiNbO_3$ $BaTiO_3$ etc.	$BaTiO_3$/MgO/Si	Si: thermal Si: free carriers
amplifier	Er:SiO_2	---	Er:Al_2O_3/SiO_2/Si Er:Glass/SiO_2/Si
detector	Compound Semiconductors	Si-MSM	Schottkybarrier SiGe

Table 1: Listing of some Si-based approaches for optoelectronic functions. The waveguides for visible light and most modulators and amplifiers are designed as "breadboard" components, where different materials are deposited or epitaxially grown onto silicon wafers.

Ch. Buchal *et al.*: MRS Proc. 486 (1988) 3-19.

Advanced New silicide technology

Si/β-$FeSi_2$/Si stacking structure

SiO_2/β-$FeSi_2$/Si PhC waveguide

SiO_2/Fe_3Si/Si PhC MO modulator

β-$FeSi_2$ PhC defect amplifier?

β-$FeSi_2$/Si p-n junction

Iron-Silicon binary compounds

Reconsidering their functional properties.

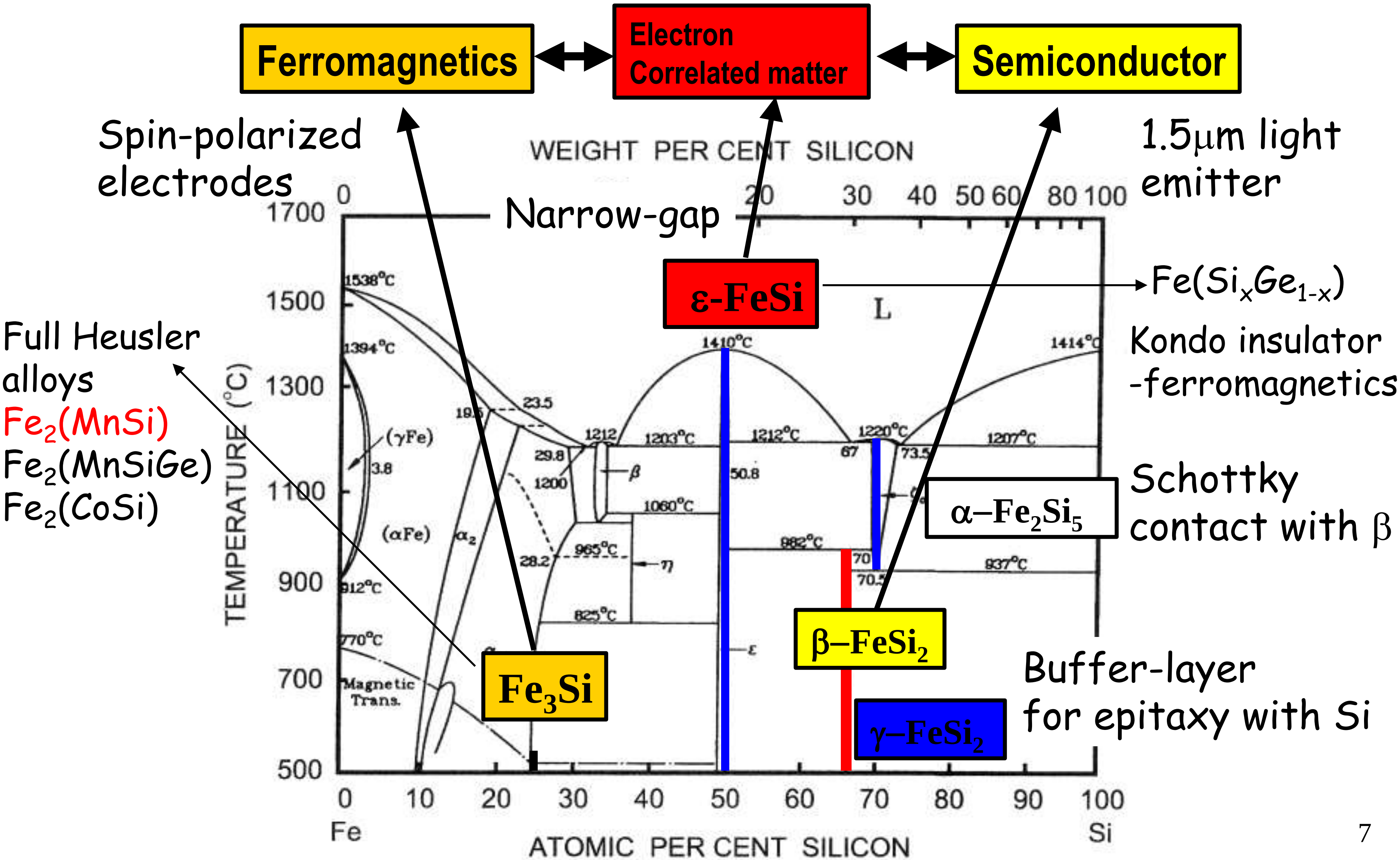

Family of iron silicides

α-FeSi$_2$ (metallic) ⟷ T_c=~950°C ⟷ β-FeSi$_2$ (semiconductor) ⟷ T_c=~600°C ⟷ γ-FeSi$_2$ (metallic)

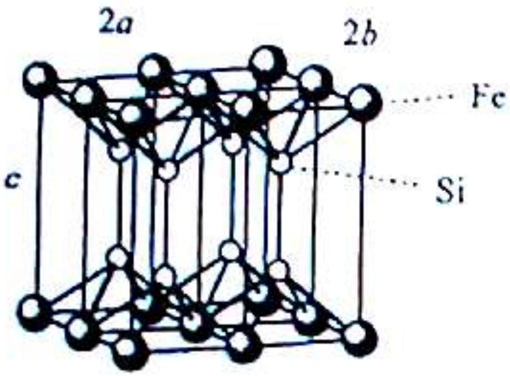

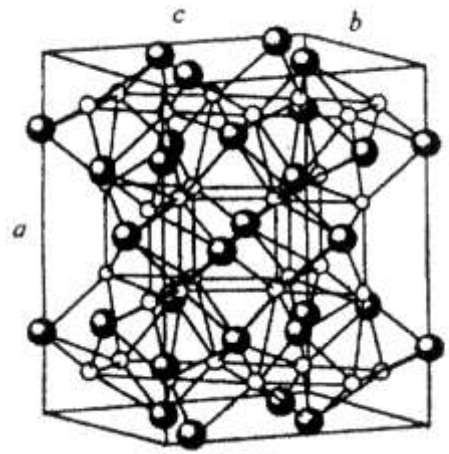

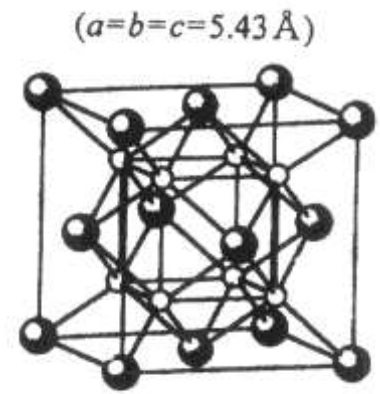

Fe$_3$Si (D0$_3$: Ferromagnetics)

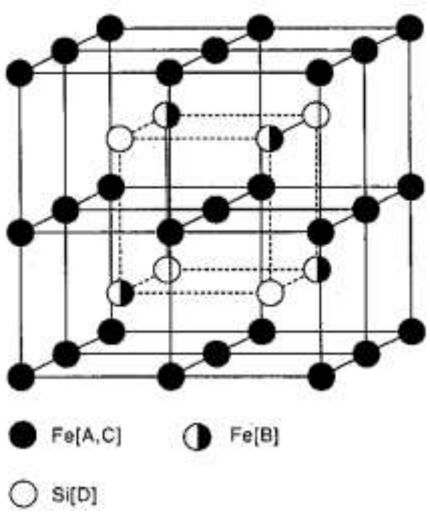

FeSi
(B20 strong electron correlation matter)

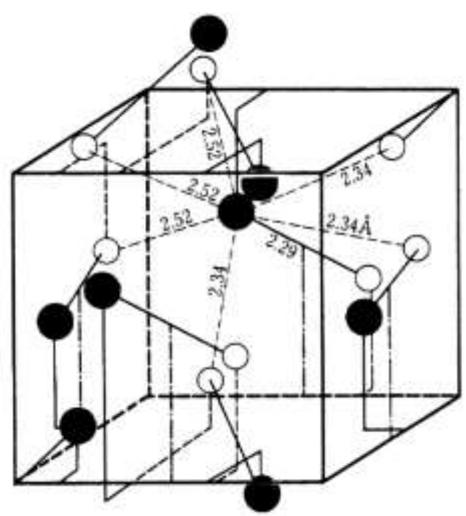

What do we achieve?
Si Optoelectronic Integrated Circuit (OEIC) with Silicides photonics

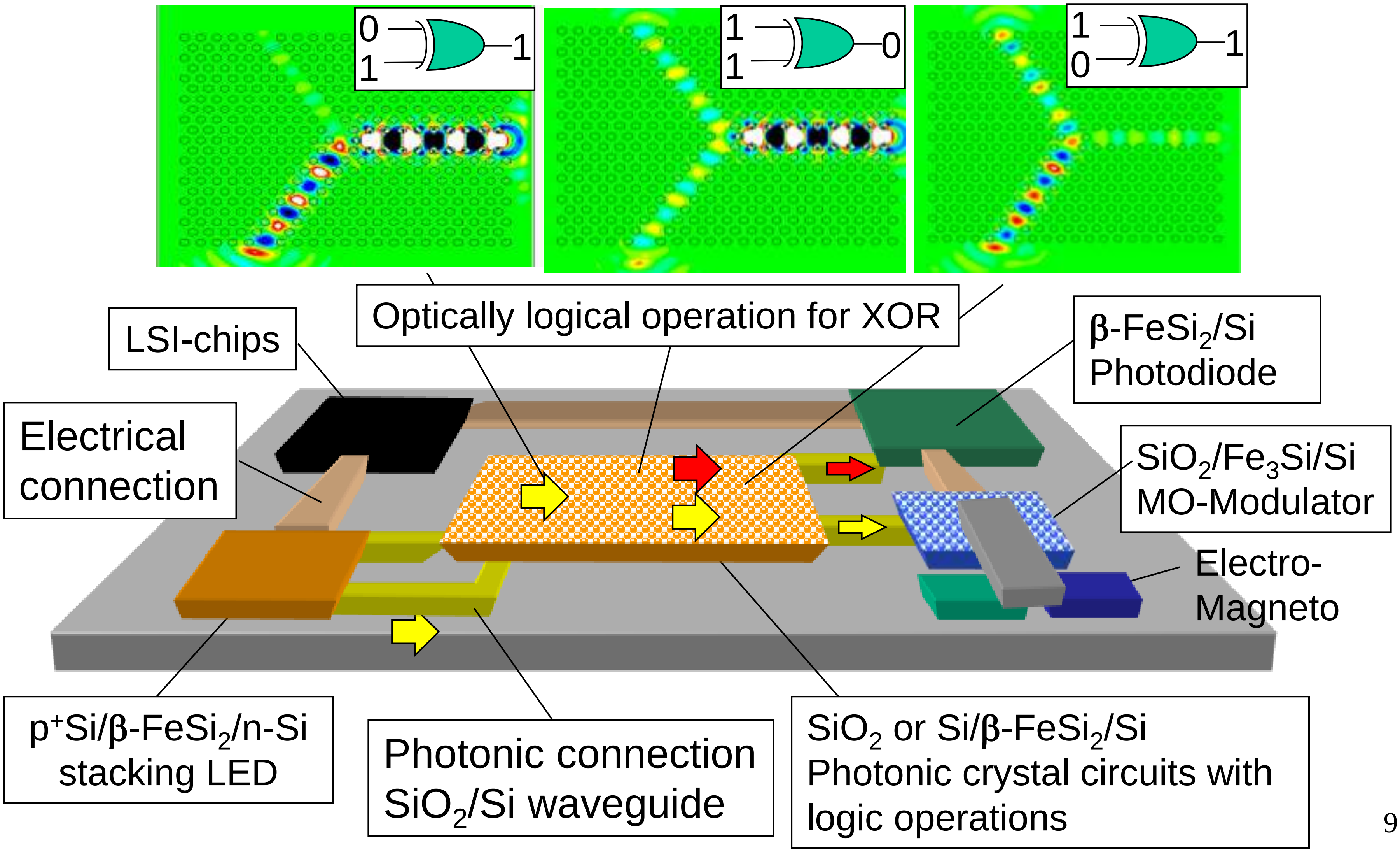

Development of β-$FeSi_2$ LEDs and related LEDs

Univ. of Surrey

MBE

FI

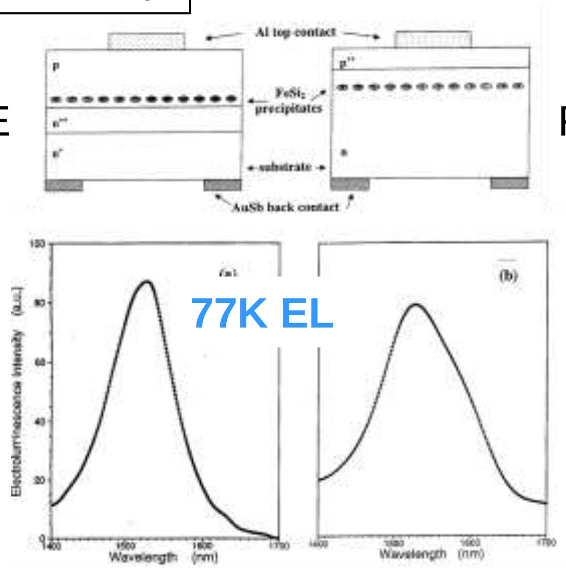

D. Leong et al. :NATURE 387 (1997) 686

Dislocation engineered LED (DELED)

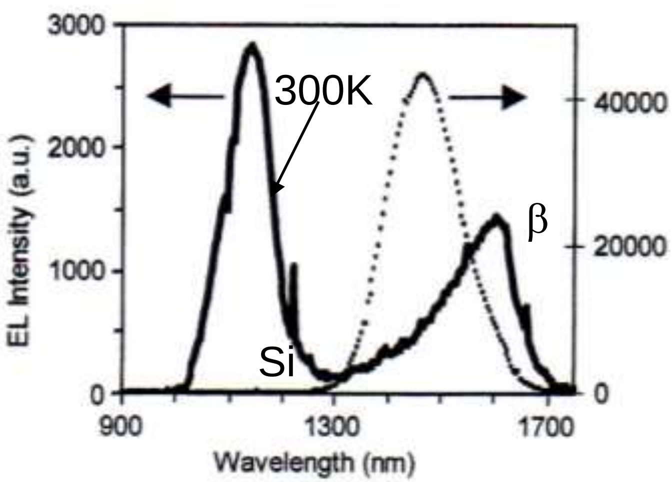

M. Lourenco et al.: Thin Solid Films 461 (2004) 219.

Univ. of Tsukuba

RT-LED

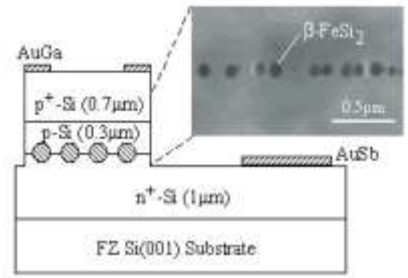

LED structure

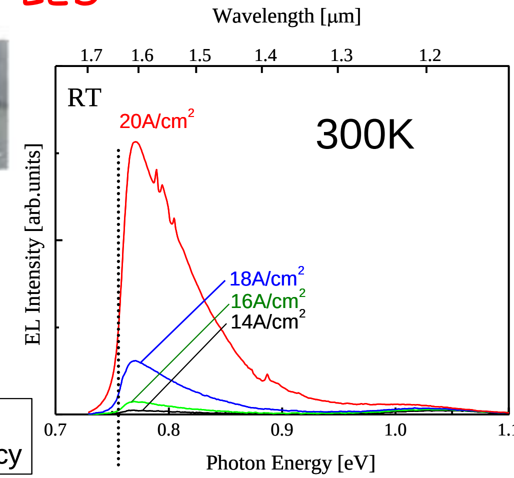

Problem:
Improvement of injection efficiency

Dots -> multi-layers

Low limit of an InGaAs PMT

After T. Suemasu et al. JJAP **39** (2000) L1013.

HAMAMATSU PHOTONICS

RF-magnetron sputter-deposition
Highly oriented film: β(220)//Si(111)

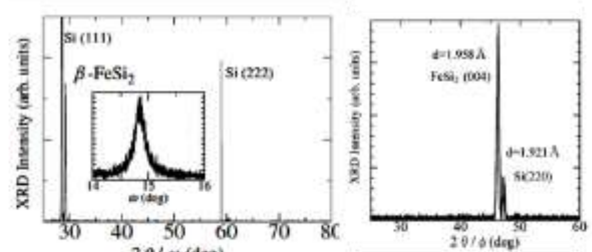

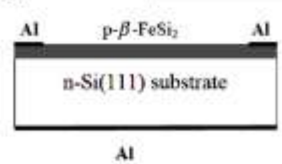

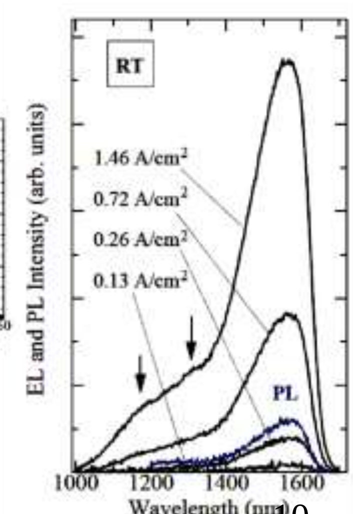

After S. Chu et al.:JJAP 41(2002) L1200.

Fabrication of IBSD-β-$FeSi_2$ photonic patterns on Si

Optical advantage

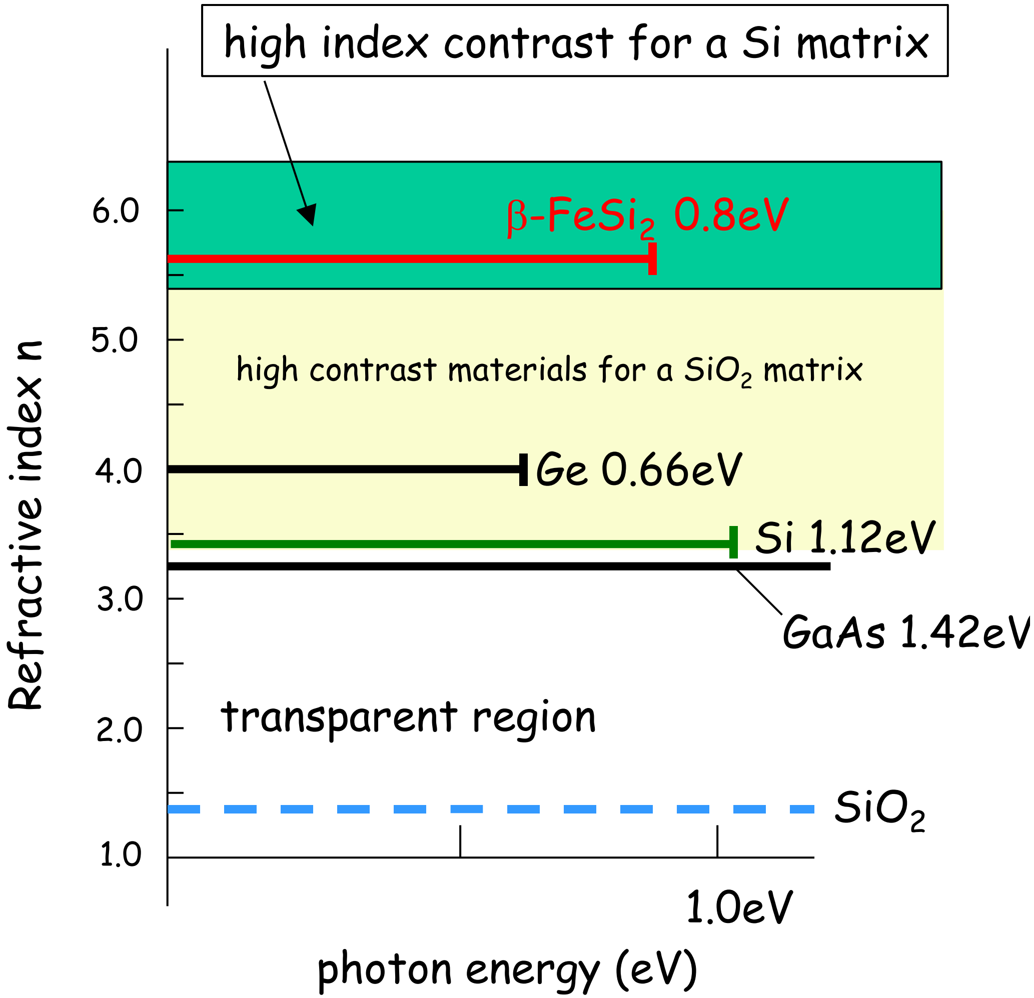

β-$FeSi_2$ PhC waveguides on Si**

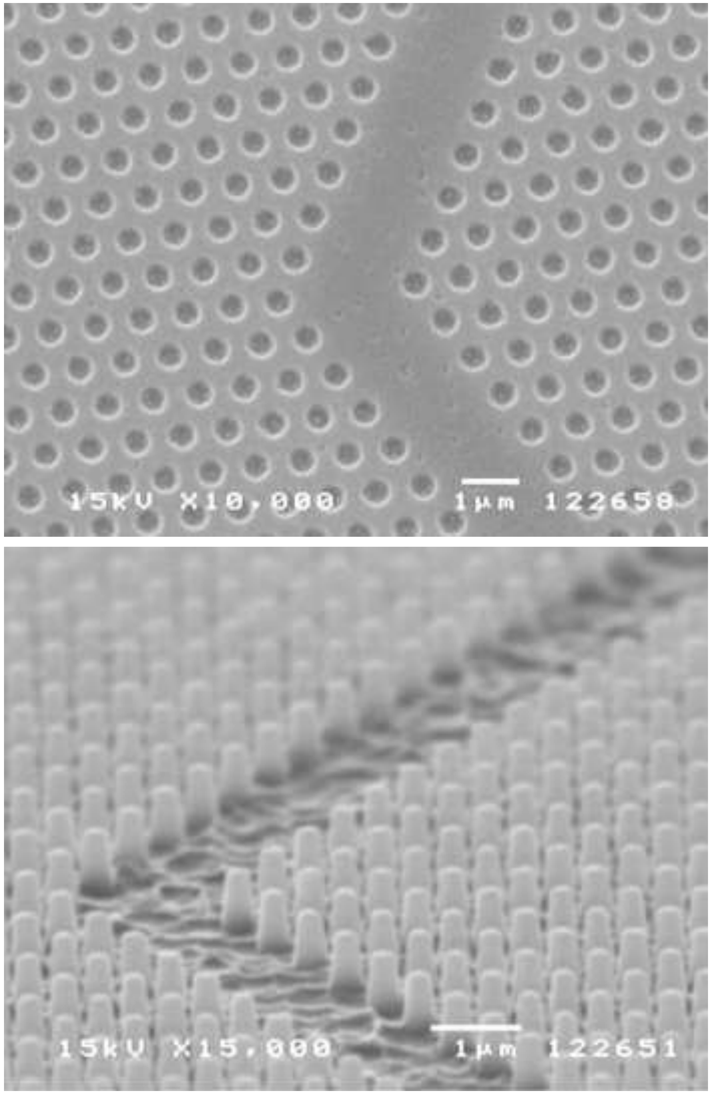

*IBSD: Ion-beam sputtering deposition

**NLD-RIE using a conventional SF_6 gas

Y. Maeda: Appl. Surf. Sci., **254** (2008) 6242.

Perspective of Active Silicides towards Realization of Silicon Photonics and Spintronics

Active Silicides

Semiconducting
β–$FeSi_2$
$BaSi_2$
Mg_2Si

Ferromagnetic
Heusler alloys
$Fe_{3-x}T_XSi$
$Co_{3-x}T'_xSi$
(T=Fe, Mn, Co, Ni)

B20-type
Electron correlation matters

FeSi-FeGe
FeSi-CoSi

Epitaxial Growth Technology

Si | Ge | SiGe

Photonics — Magneto-photonics — Spintronics — Electron correlation

Si-Photonic
LED
PD
Ph-V Th-V

Photonic Crystal Waveguides

Spin Polarized electron injection

Interlayer magnetic coupling devices

Magneto-optical Kerr modulator

Available epitaxial structure for Application of junctions towards Si-photonics or Si-spintronics

(Lattice mismatch <5%)

	Film / Substrate	Si	β-$FeSi_2$	FeSi	Fe_3Si	γ-$FeSi_2$
Semiconductors	Si		1.5 -4.0		4.06	-0.56
	β-$FeSi_2$	-1.42 -3.8		0.09	3.3 2.5	-3.4 3.9
	B20-FeSi		-0.04 -0,29*			
Ferromagnetics	DO_3-Fe_3Si	-3.9	-3.5 -2.8			-4.4
Metal	γ-$FeSi_2$	0.56	-4.2 -4.0		0.64	

***FeSi(111)//β-$FeSi_2$(100)**

A variety of synthesis of β-$FeSi_2$ and properties

Method	Growth/ Epitaxial	Carrier control	Hall Mobility (cm^2/Vs)	Light emission	Photo voltaic
IBS	Epi/Si OR/Si	n(Co), p(Mn,Al)	300 - 450	PL (<120K)	Hetero n-Si
RDE	Epi/Si	n,p	550	PL(RT) **EL(RT)**	----------
MBE	Epi/Si	n,p	2~500	**EL(RT)**	-----------
SPE	Epi/Si	n	~120	-----------	-----------
MOCVD	Epi/Si **/YSZ**	n(P), p(B)	~450	PL(10K)	Hetero
IBSD	OR/Si	n,p	<100	PL(10K)	----------
Sputter	OR/Si	n,p	0.5~300	**EL(RT)**	homo
PLD	OR/Si	n	------	PL(10K)	-----------
VE[1]	OR/Si	n	100~500	----------	-----------
Bulk[2]	needle	n,p	0.1-10	-----------	-----------
Bulk[3]	facet	n,p	~50	PL(10K)	-----------

OR: highly oriented growth, YSZ: Yttria stabilized Zirconia
1: Vacuum evaporation, 2: Chemical vapor transport, 3:Metal solution growth

Ion Beam Synthesis (IBS) : β-$FeSi_2$

(A) High Dose Ion implantation

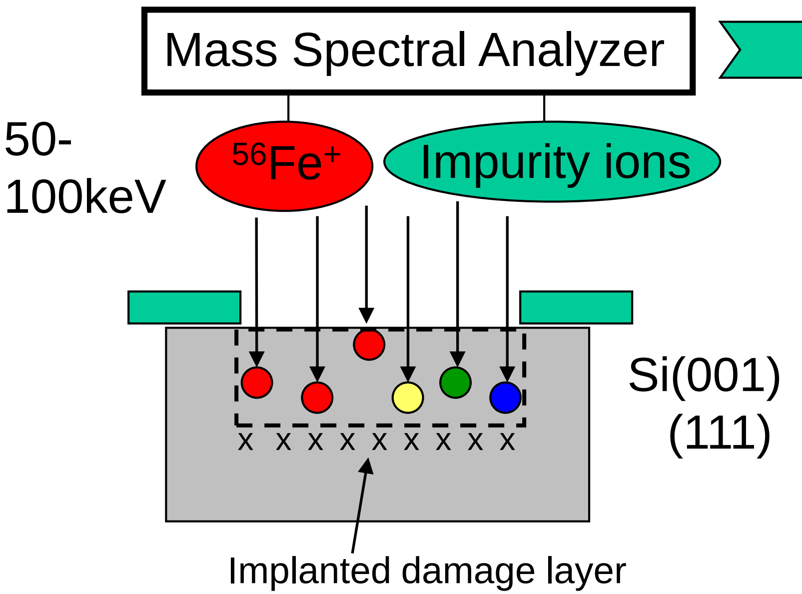

High purity synthesis

Doping control

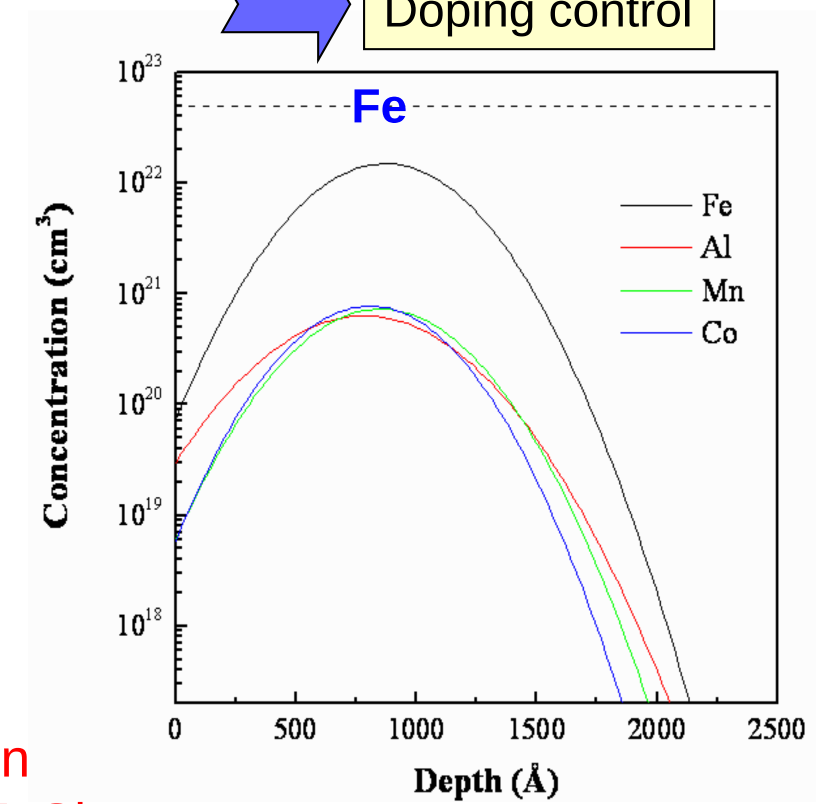

Fe: 100 keV 10^{17} cm^{-2}
Mn, Co: 100 keV 10^{16} cm^{-2}
Al: 50 keV 10^{16} cm^{-2}

(B) Rapid Thermal Annealing >700°C

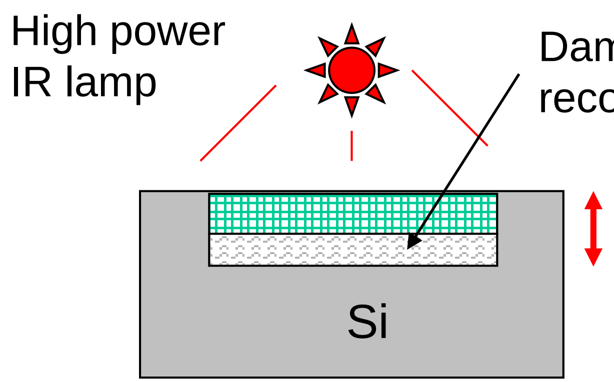

Silicidation
$Fe+2Si=FeSi_2$

Structure and function controls of β-$FeSi_2$ by IBS conditions

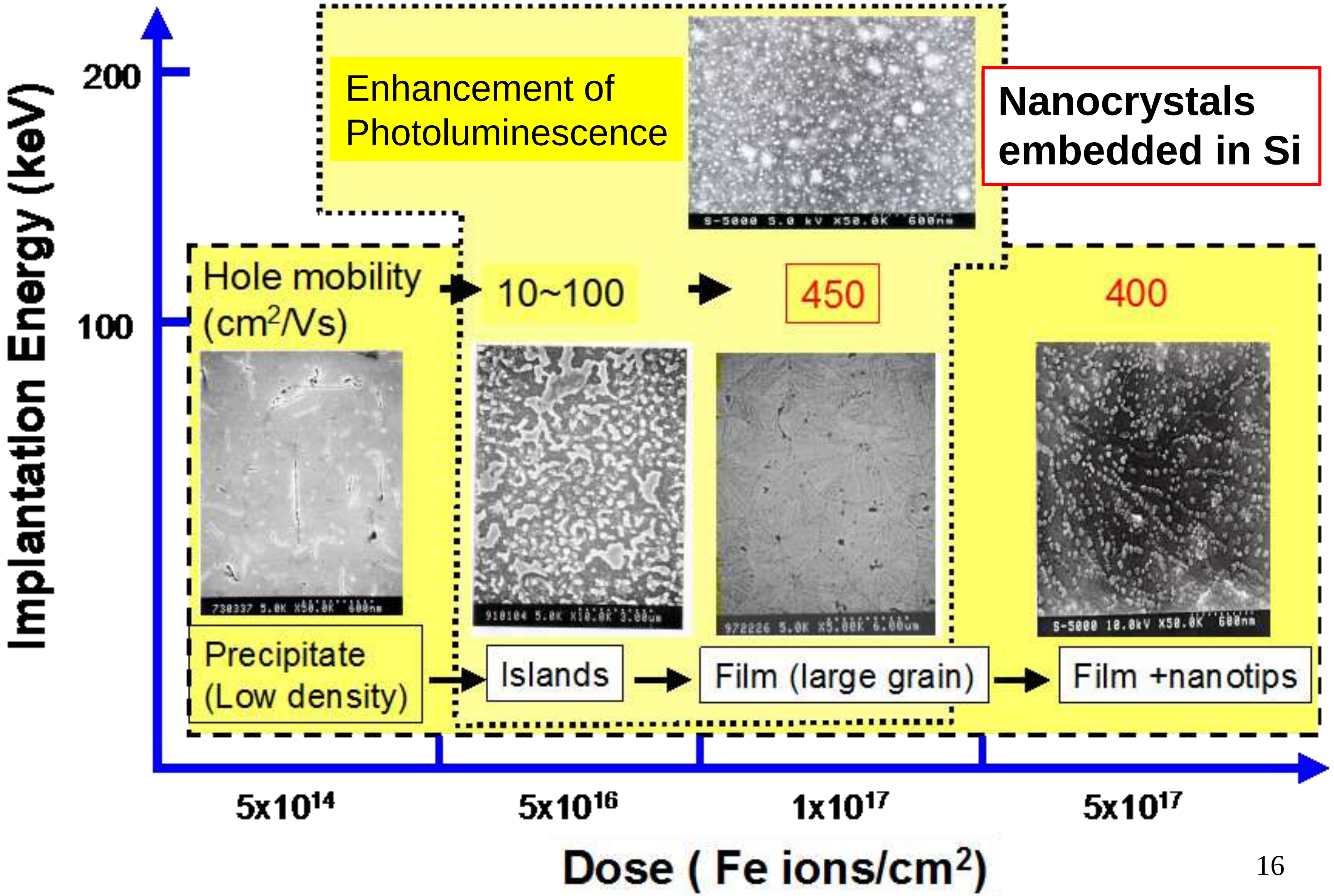

Luminescence spectra corresponding to morphology of IBS β-$FeSi_2$

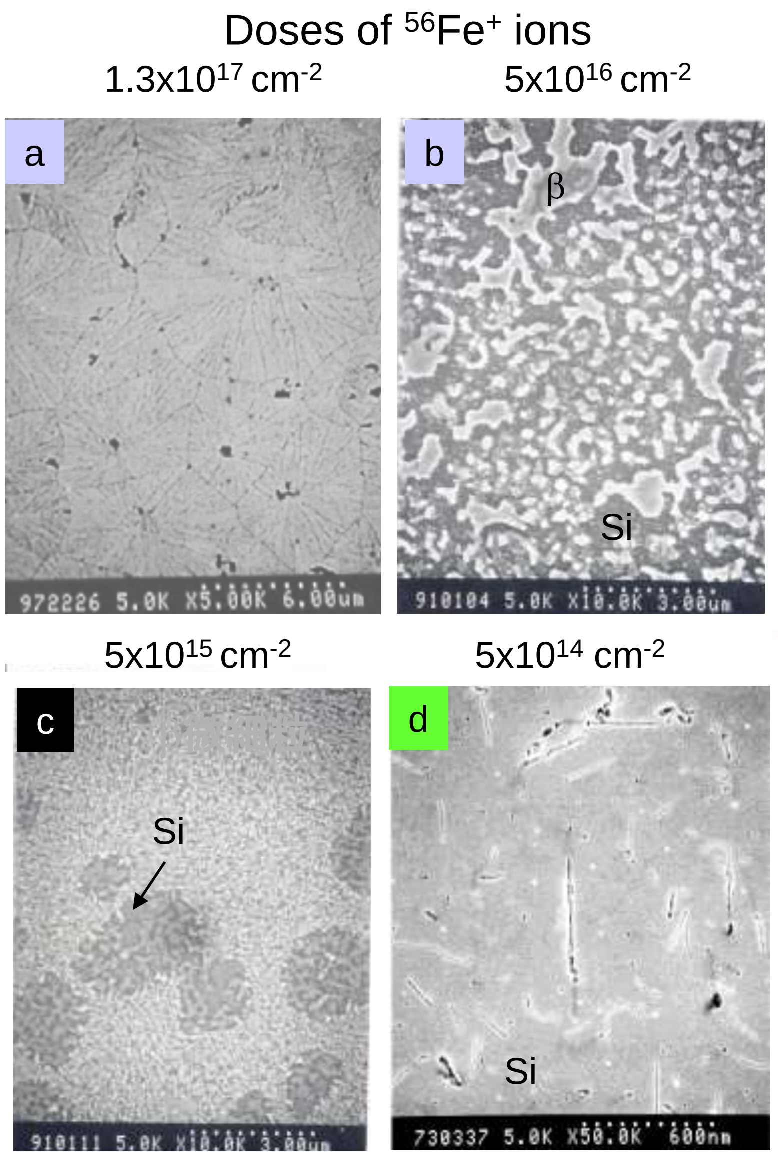

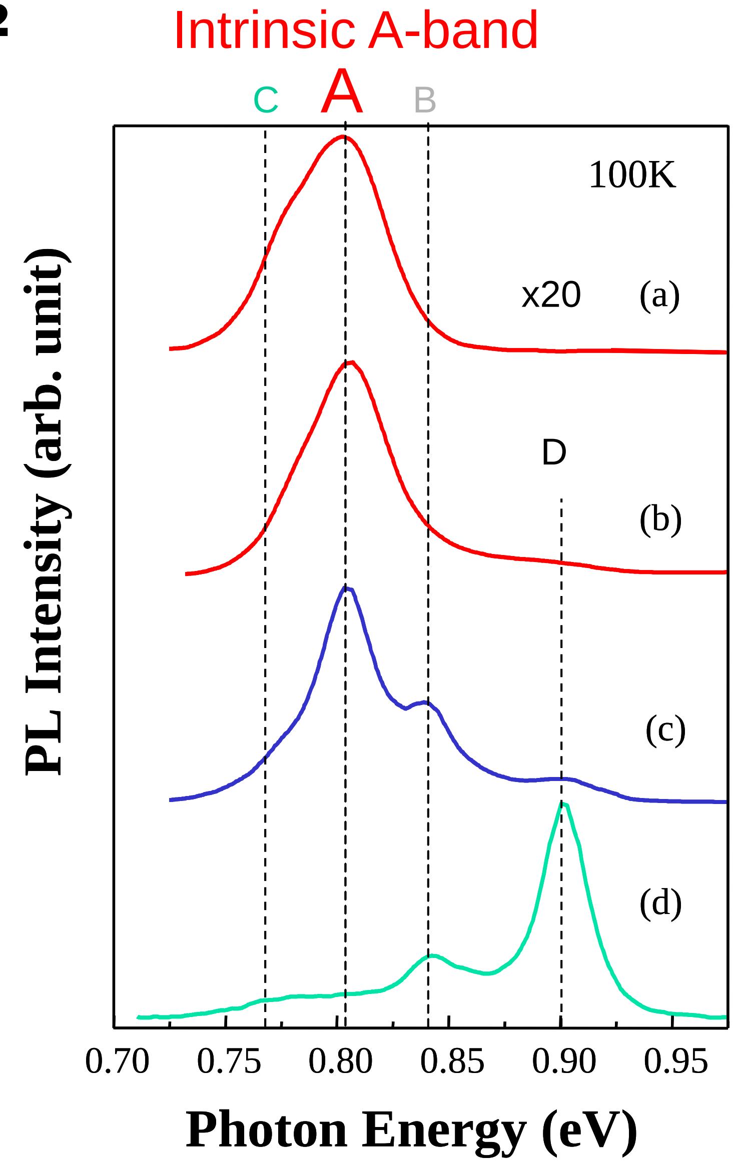

Y. Maeda *et al.* :Thin Solid Films **461** (2004) 160.

Electronic band structure of β-$FeSi_2$

Indirect gap

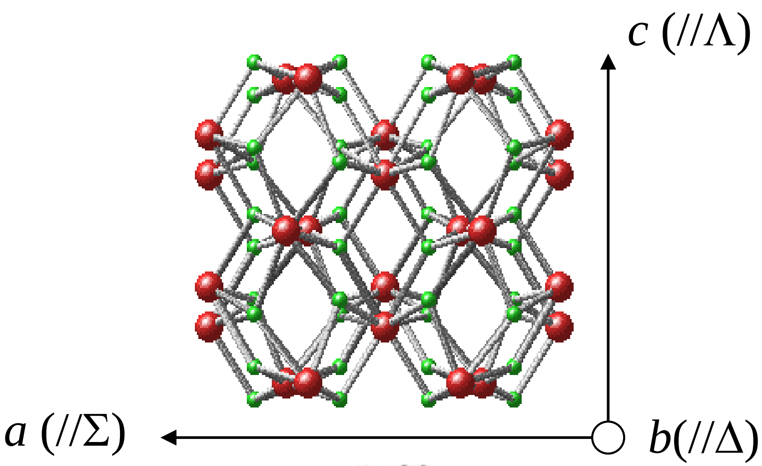

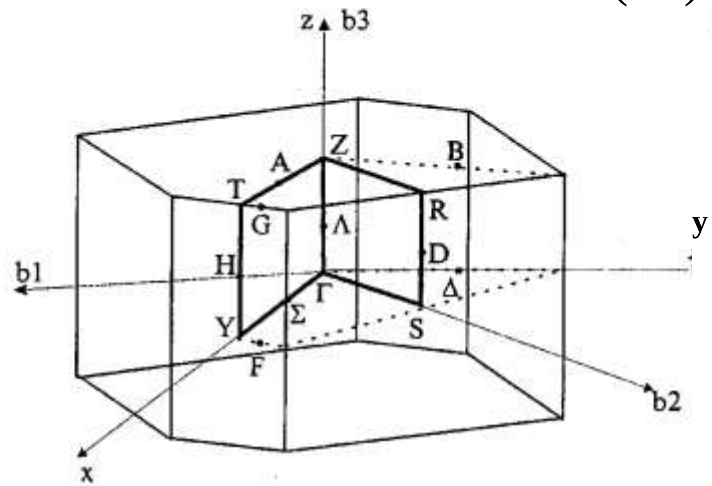

BZ (Rhombic base-centered)

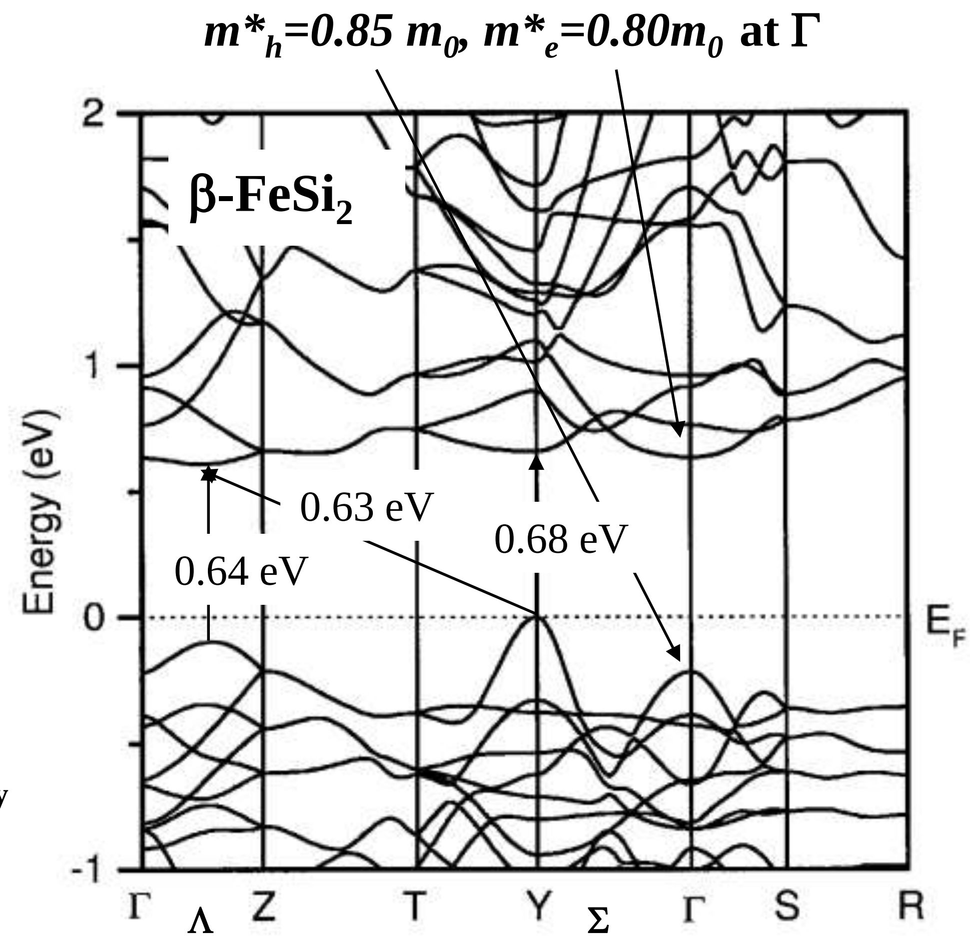

D. B. Migas and Leo Miglio: Phys. Rev. **B62** (2000) 11063.

Optical band-edge and intrinsic PL at 1.54μm

Schematic figures

Direct band-gap | **Indirect band-gap**

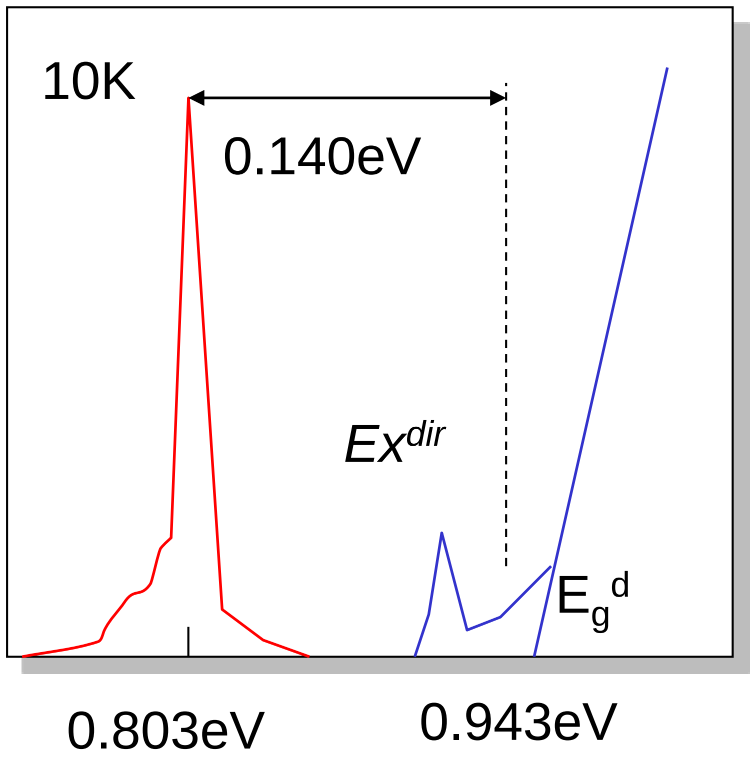

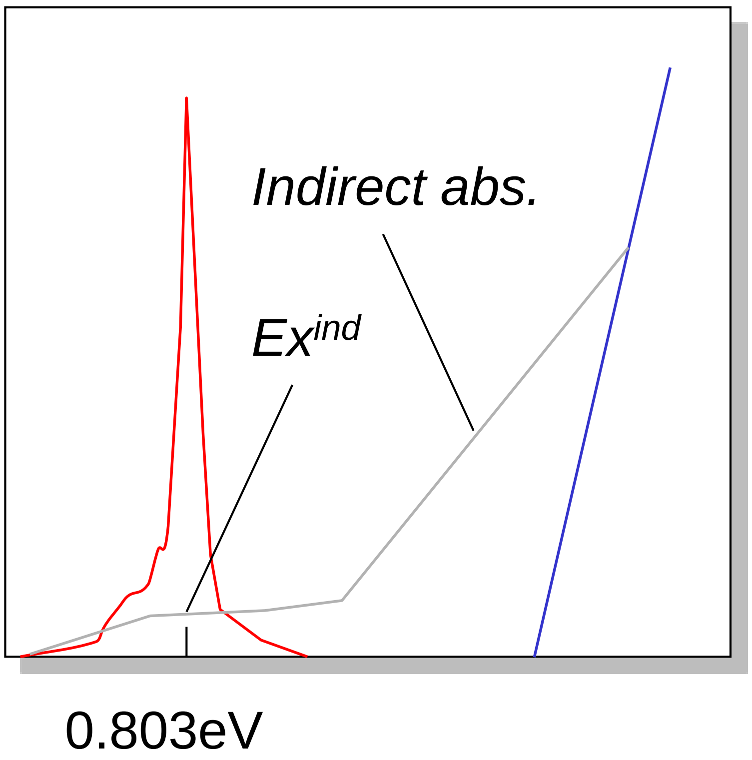

Luminescence is not related to the direct band-gap and excitons.

Luminescence may come from an exciton process at the indirect band-gap via phonon contribution.

CSSE
Kyusyu Institute of technology

2

Light emission from β-$FeSi_2$ crystals and its fundamental scheme

First observation of PLs from β-$FeSi_2$ films deposited on Si substrates

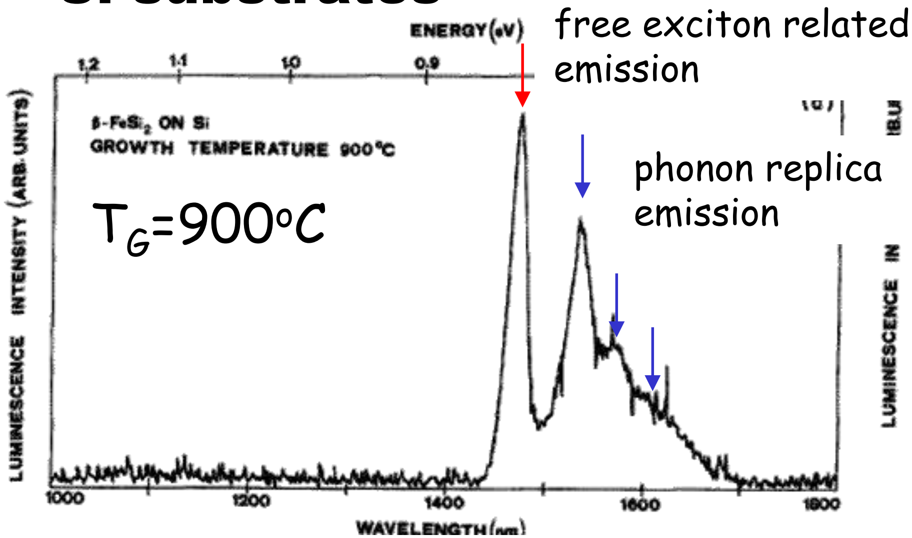

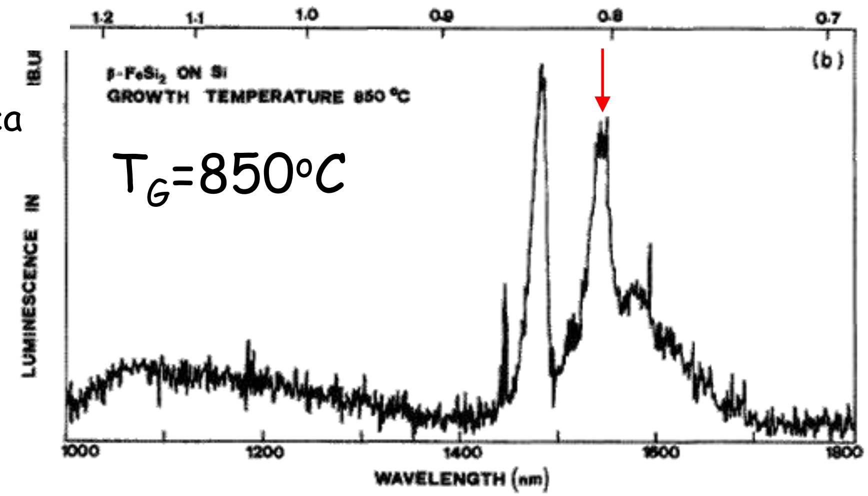

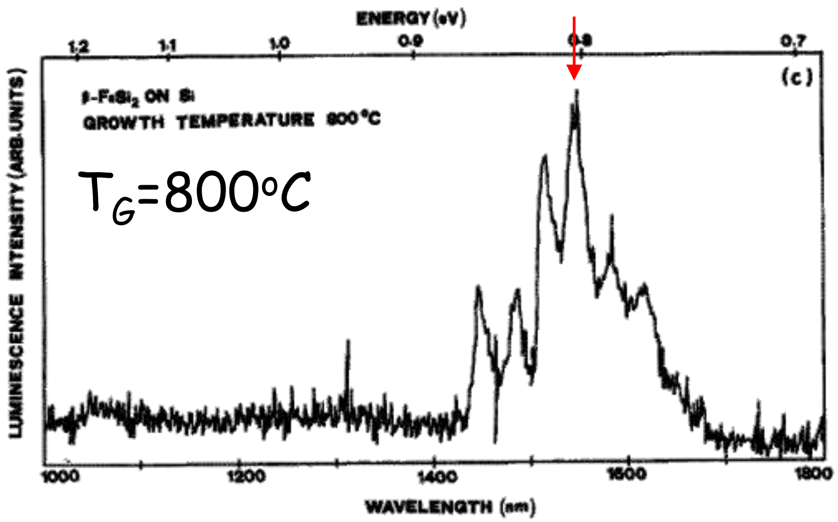

Note

The luminescence at 0.84eV assigned as emission from a free or bound exciton was not observed in other samples.

C. A. Dimitriadis, H. H. Werner, S. Logothetidis and M. Stutzmann, J. Weber and R. Nesper: J. Appl. Phys., **68** (1991), 1726- 1734.

Dislocation related PL spectra on Si(111)

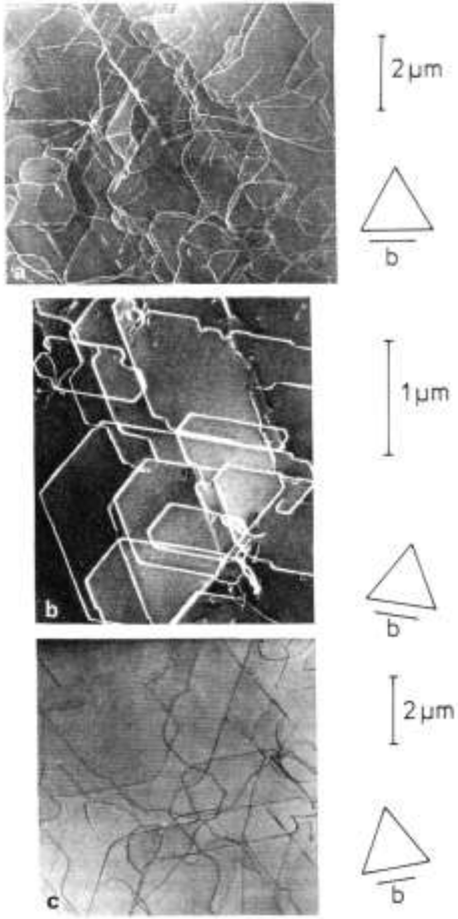

Fig. 1a–c. Transmission electron micrographs of dislocations in silicon crystals deformed by uniaxial compression as specified in Table 1. (a) "Usual" one stage deformation, (b) two stage deformation (LT–HS), (c) two stage deformation (LT–HS) followed by relaxation. The triangles mark the ⟨110⟩ directions in the glide plane, b gives the line of the burgers vector of the primary dislocations. [Micrographs by courtesy of A. Tönnessen (a), E. Heister (b), and F. Sick (c)].

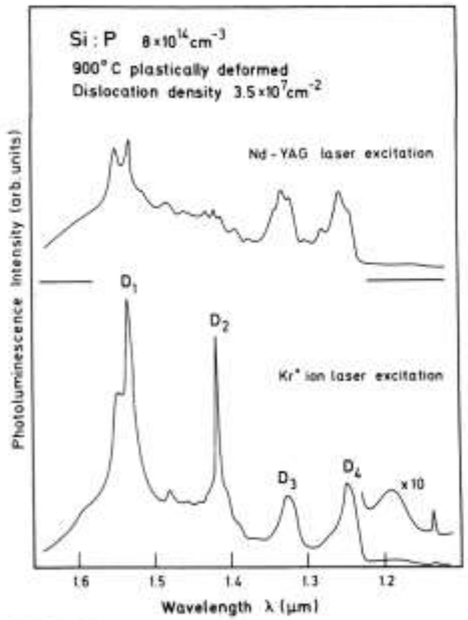

Fig. 5. D line spectra with above – gap excitation ($h\nu = 1.915$ eV Kr^+ laser) and with below – gap excitation ($h\nu = 1.165$ eV Nd–YAG laser). Laser power is 400 mW in both cases focused to similar spot sizes on sample (≈2 mm)

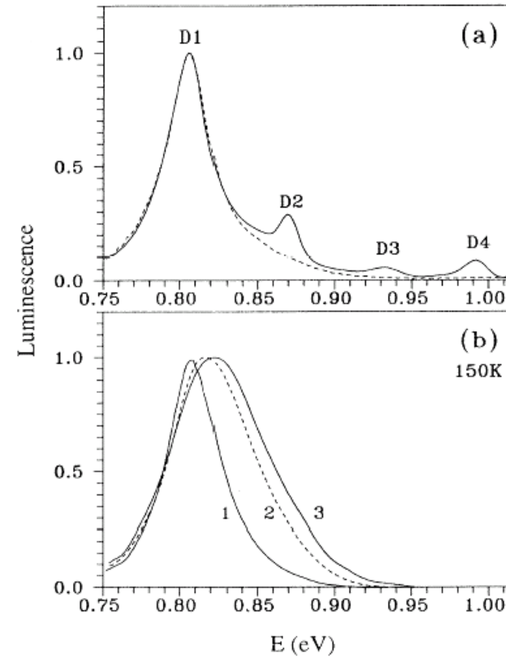

FIG. 1. (a) Normalized photoluminescence (PL) spectra of sample $K3$ at $T = 5$ (solid curve) and 50 K (dashed curve). The Ar-laser excitation density was 6 mW/mm². (b) normalized spectra of sample $K3$ at $T = 150$ K for different excitation densities: Curve 1: Ar laser, 20 mW/mm²; curve 2: electroluminescence (EL) spectrum, current density 100 mA/mm²; curve 3: EL spectrum, current density 400 mA/mm². The energy scale is shifted by $E_g(0\text{ K}) - E_g(150\text{ K})$, where $E_g(T)$ is the energy gap of Si at temperature T.

V. V. Kvederet al., PRB, 51, 10520 (1995)

R. Sauer, J. Weber, and J. StolzAppl. Phys. A, 36, 1 (1985)

1.55μm-Light emission from various samples of β-$FeSi_2$

β-$FeSi_2$ nanometer sized precipitates formed by ***Ion Beam Synthesis (IBS)***

K. Homewood et al.: Thin Solid Films 381 (2001) 188.

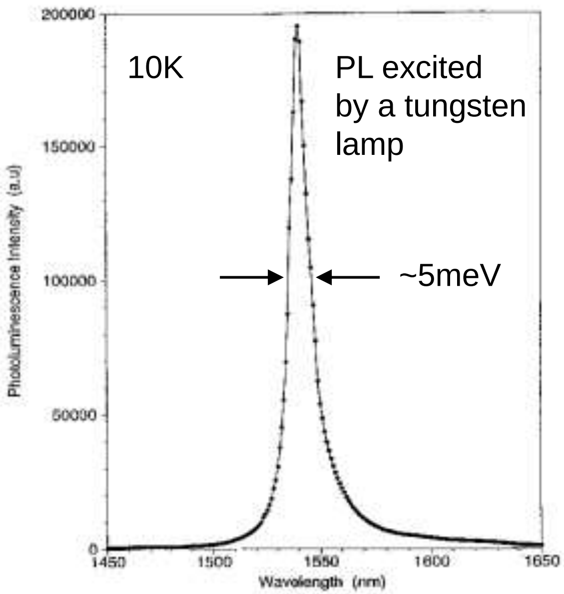

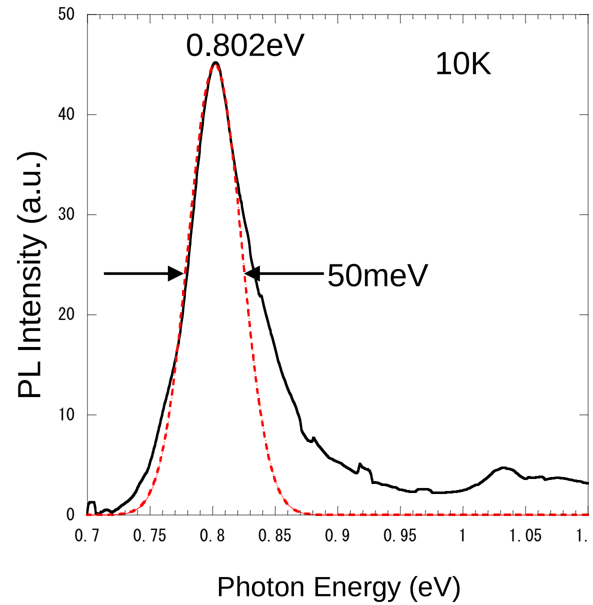

(β-$FeSi_2$/Si) multilayer formed by MBE

T. Sumemasu et al.
Univ. of Tsukuba
(private communication)

Epitaxially grown β-$FeSi_2$ film on Si(111) by MOCVD

K. Akiyama:
Doctoral thesis
Tokyo Tech. 2003

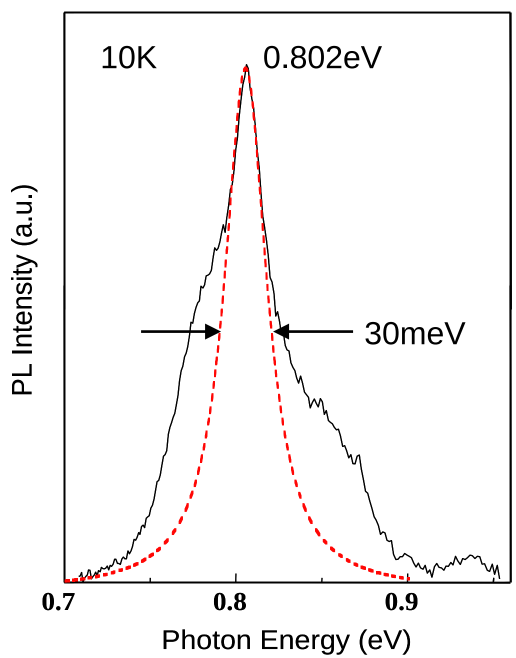

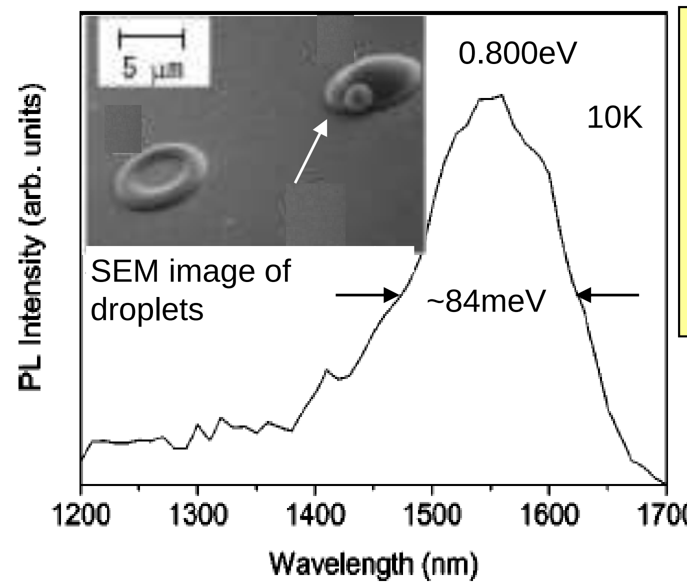

β-$FeSi_2$ droplets formed by excimer laser ablation

A. Narazaki et al.
AIST

A. Narazaki et al.: Appl. Phys. Lett. 82 (2003) 3078.

Defect-related Photoluminescences

Very confusing situation near 1.5 μm of wavelength in IBS samples

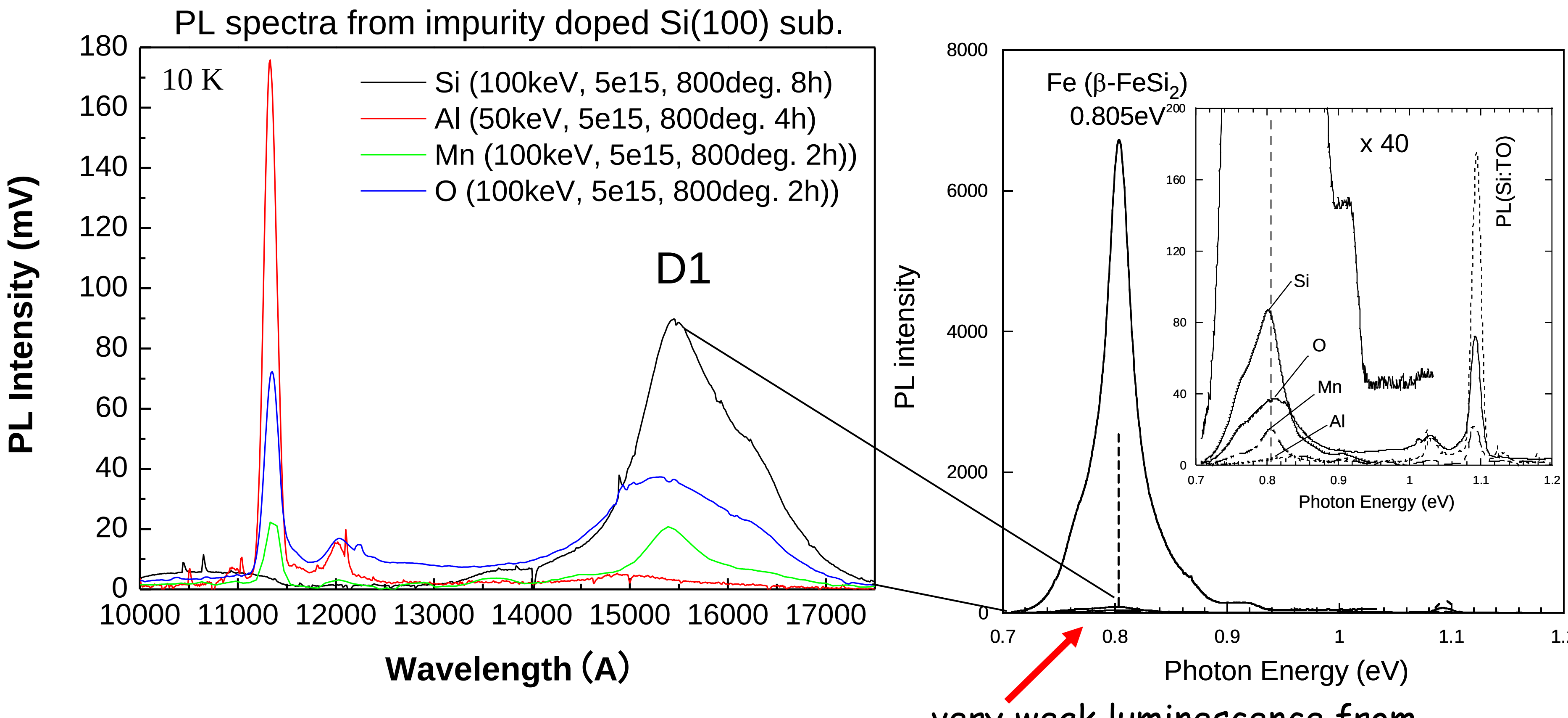

very weak luminescence from these impurity implanted Si(100) substrates.

Note The intensity of the intrinsic photoluminescence from β-$FeSi_2$ is much larger than that of defect-related emissions.

Y. Maeda: Appl. Surf. Sci., **254** (2008) 6242.

PL spectra corresponding to morphology

Surface precipitates

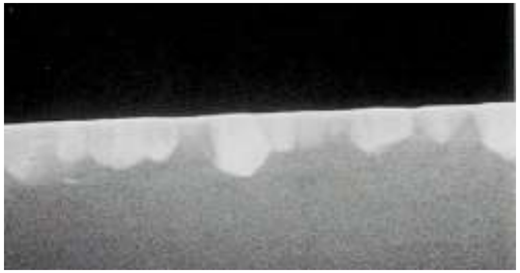

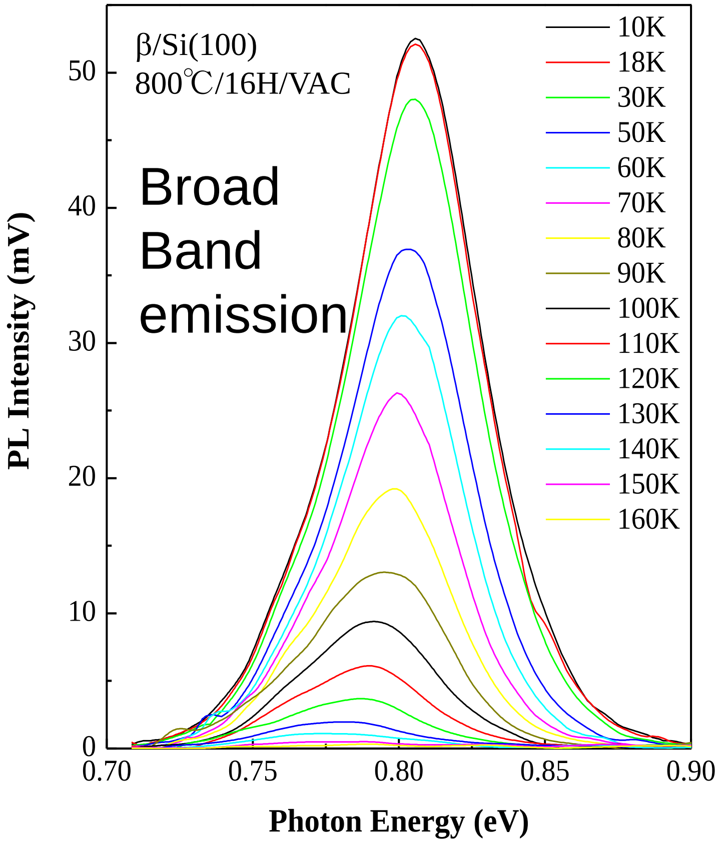

Nanocrystals in Si

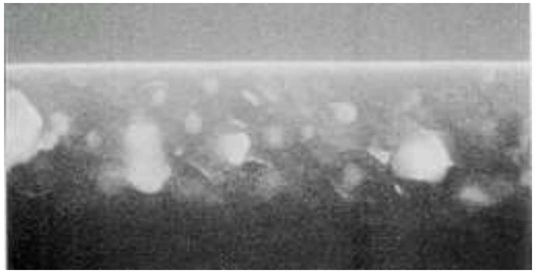

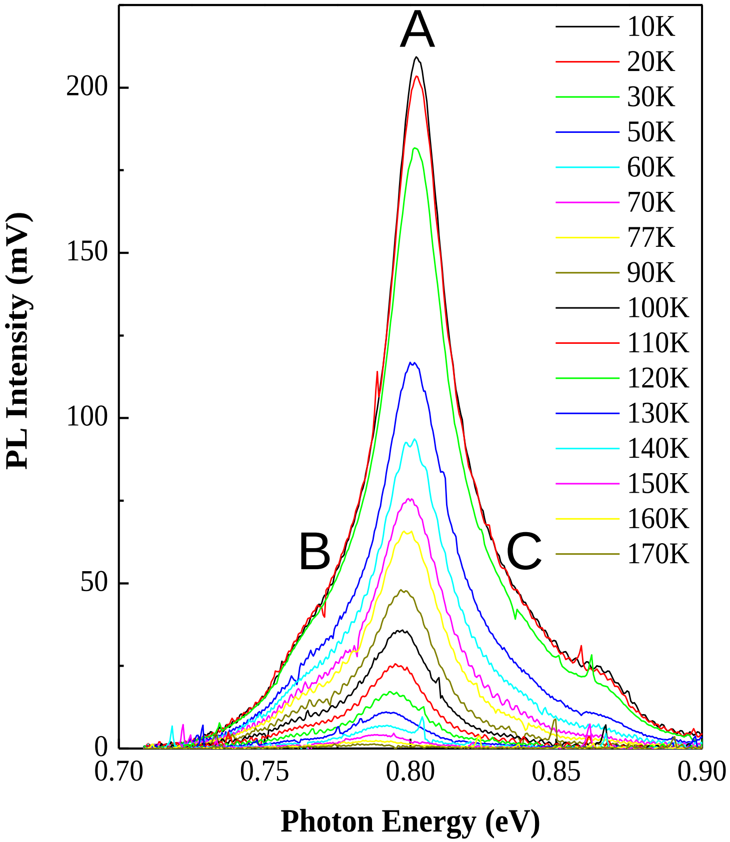

Inhomogeneous spectra of combination of PL bands; A, B, C, and D

The peak separation was not unique.

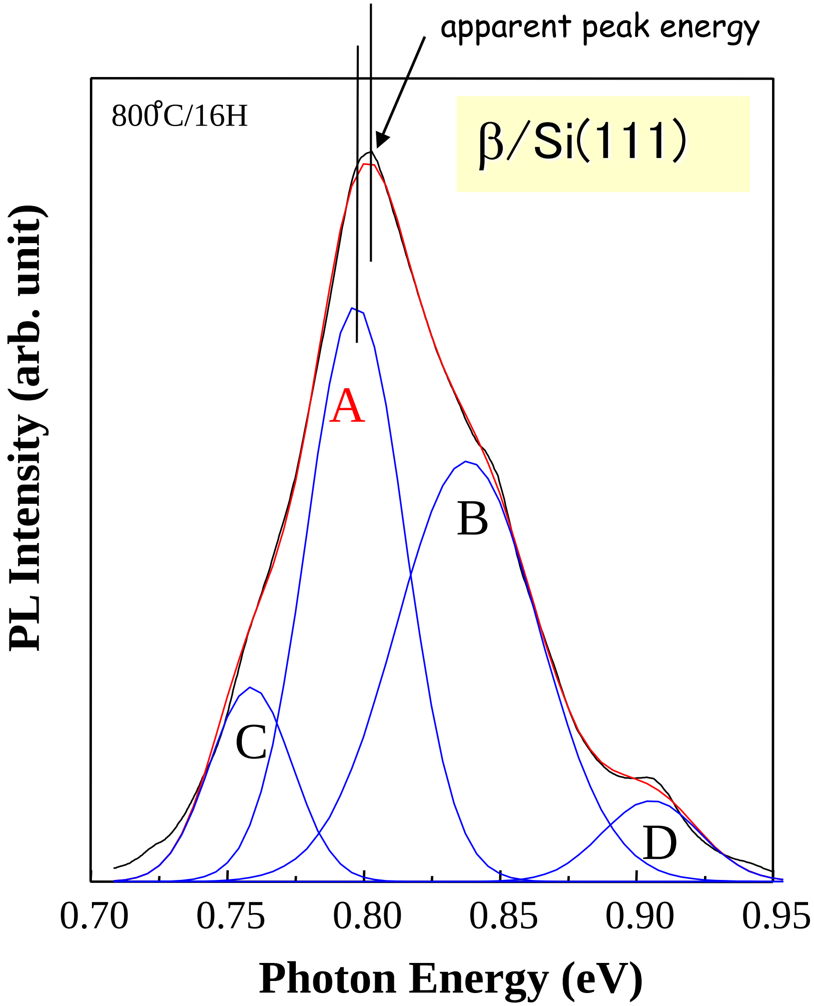

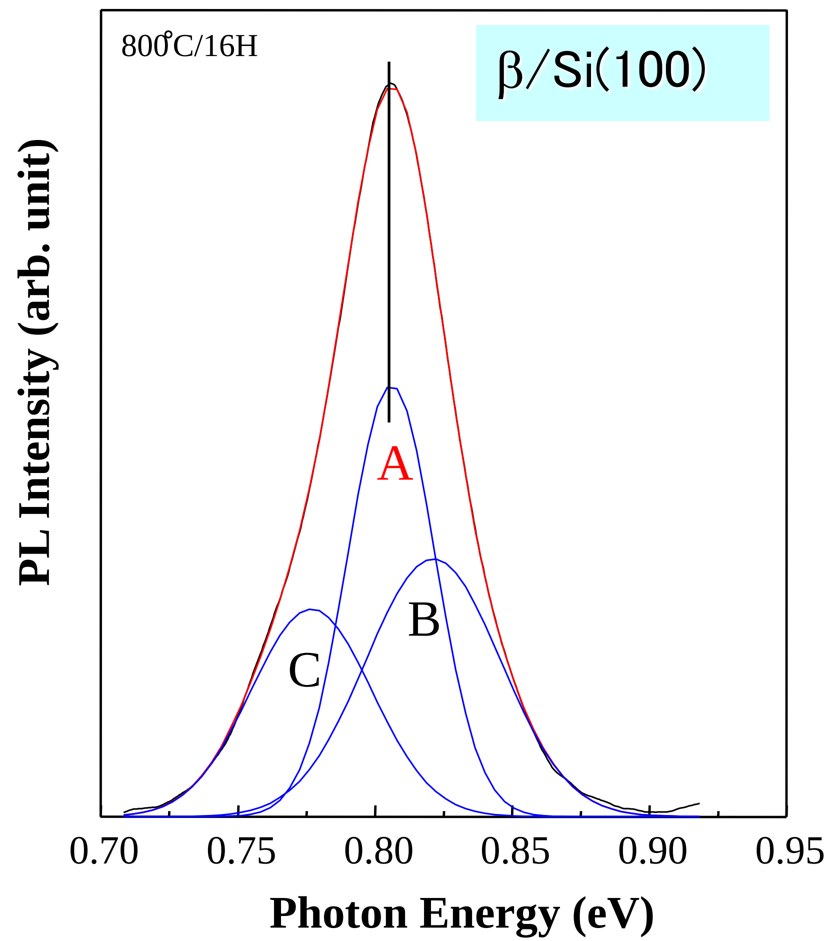

Note The apparent spectrum is a usually inhomogeneous shape by changing of combination of A, B, C and D emission bands.

Inhomogeneous spectrum due to IBS conditions

100keV

94K

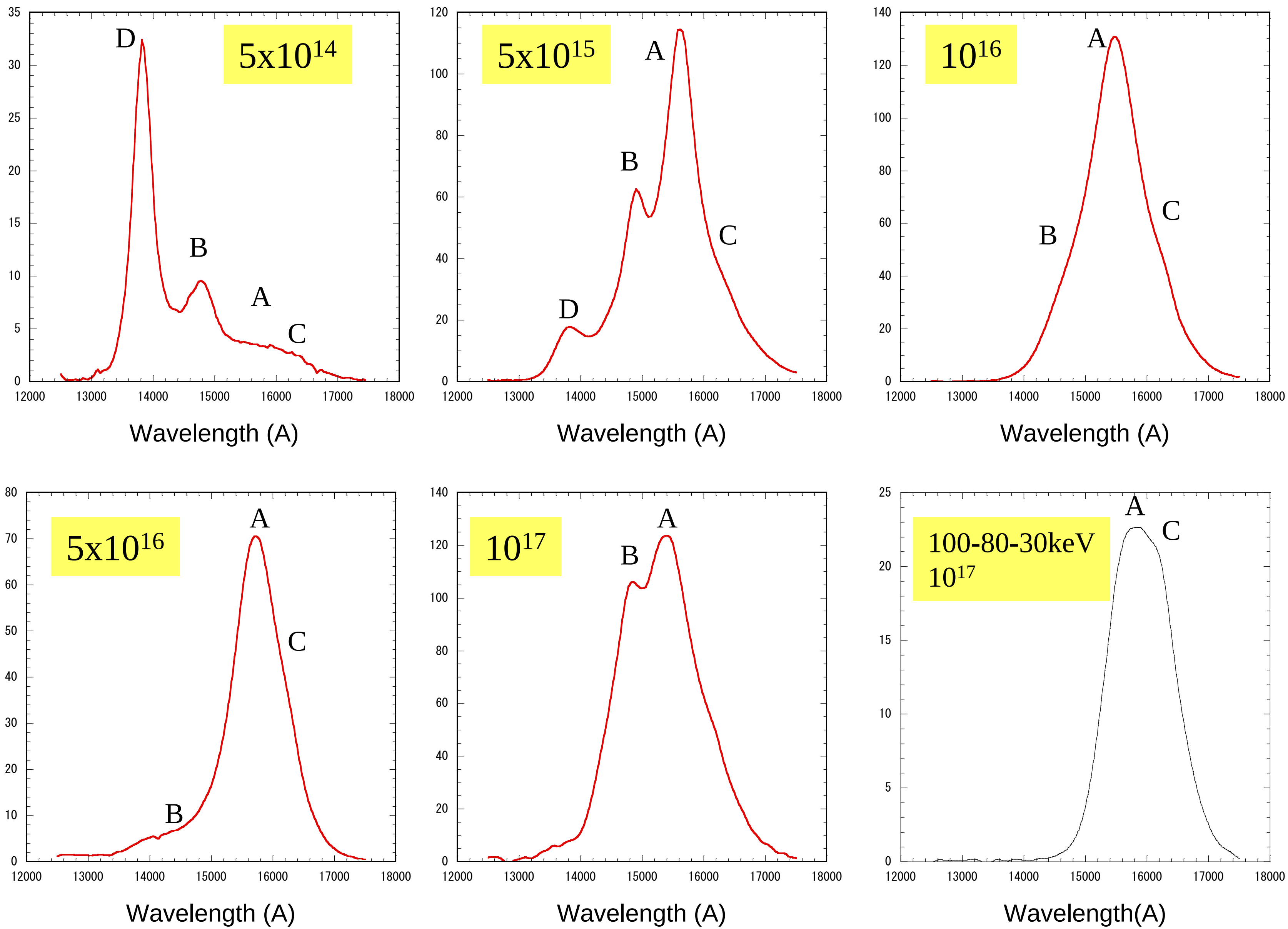

β-$FeSi_2$ NCs/Si nano-composite phase

HRSEM image

β-$FeSi_2$ NC

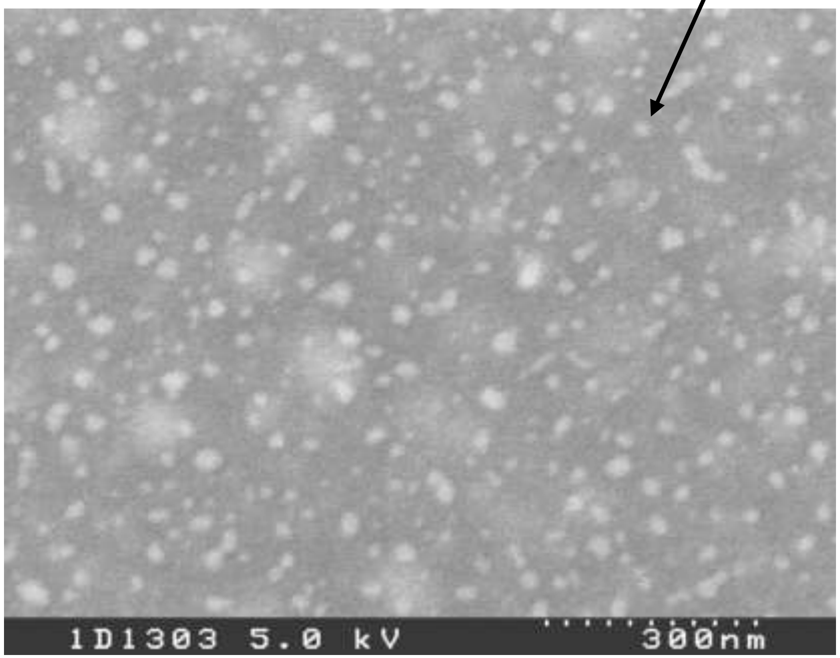

Size distribution of NCs

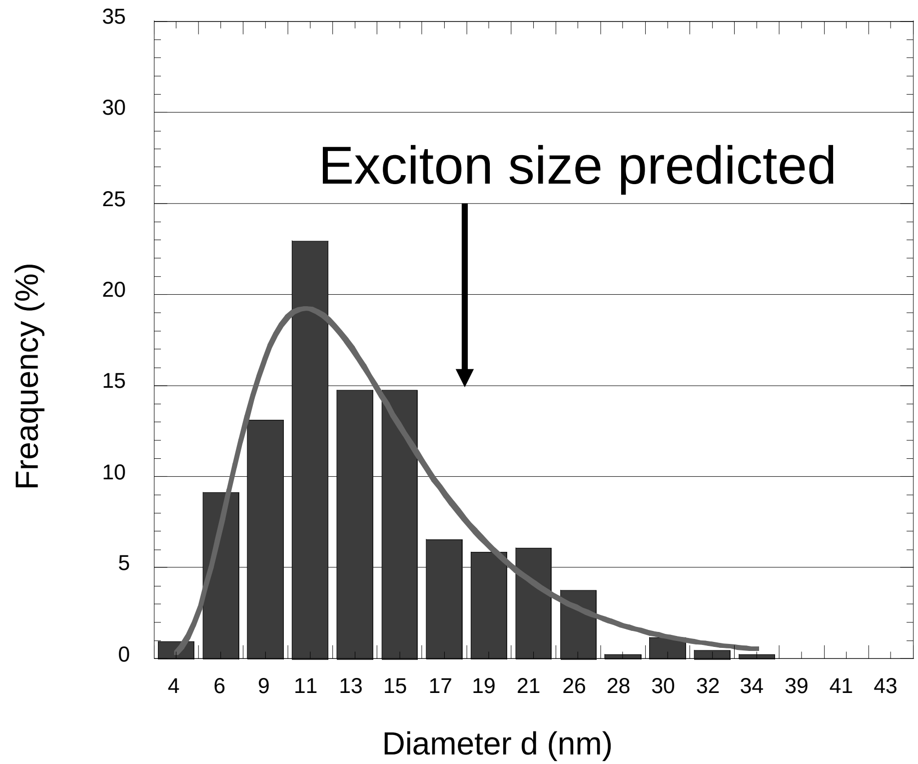

Note The average size of nanocrystals (NCs) is 11 nm, in which the exciton can be confined inside them. This situation brings high efficiency of radiative recombination of exciton. We will discuss effect of the exciton confinement on radiative efficiency later.

Y. Maeda et al.: physica status solidi (c) **9** (2012) 1888.

Intrinsic luminescence from β-FeSi2 nanocrystals(NCs)

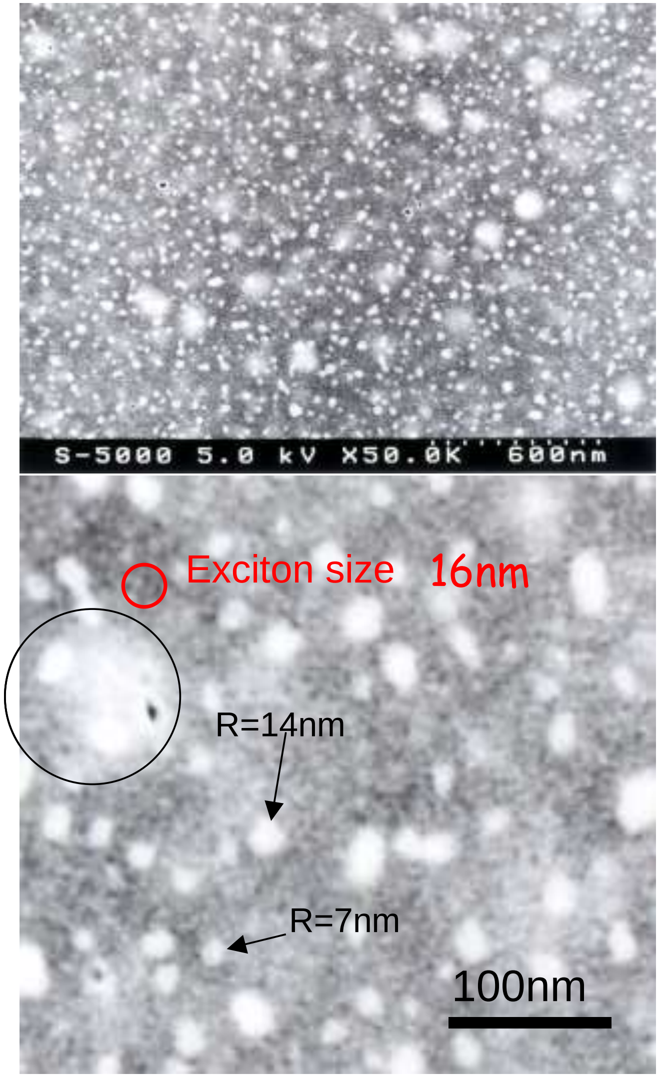

β-$FeSi_2$ NC/Si nano-composite phase

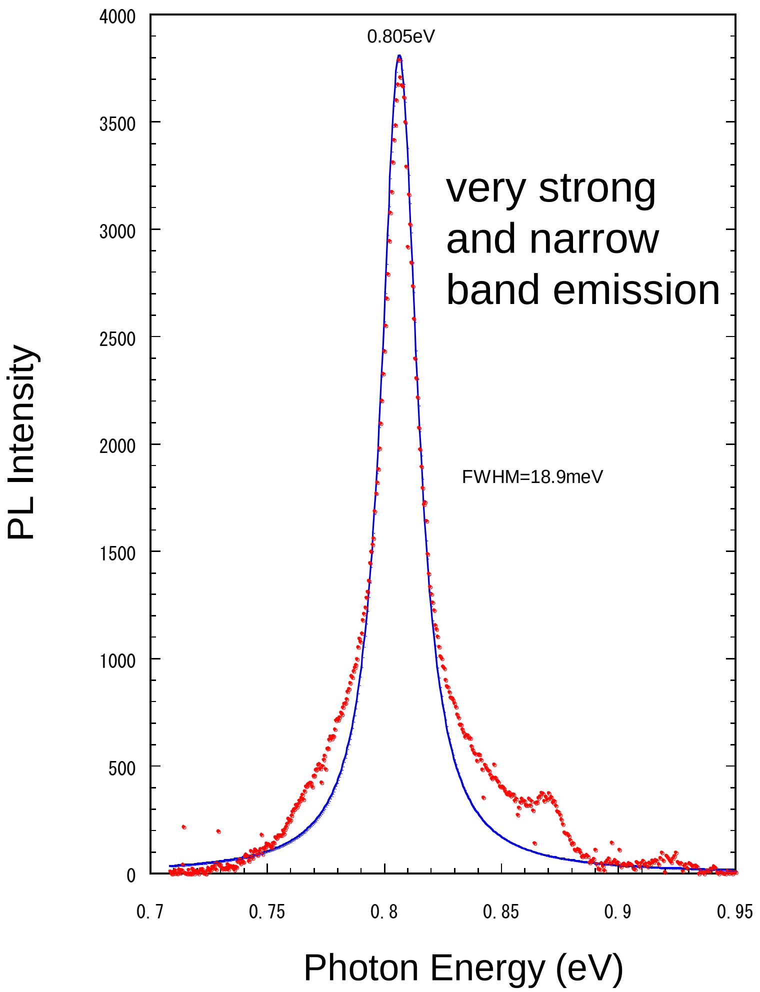

Note The nano-composite phase consisting of high density of β-$FeSi_2$ NCs embedded in the Si matrix indicated the intrinsic PL . Their sizes were close to the Winner-Mott type exciton size (~16 nm=2xa_B) in β-$FeSi_2$.

Empirical Varshni's law for interband radiative recombination

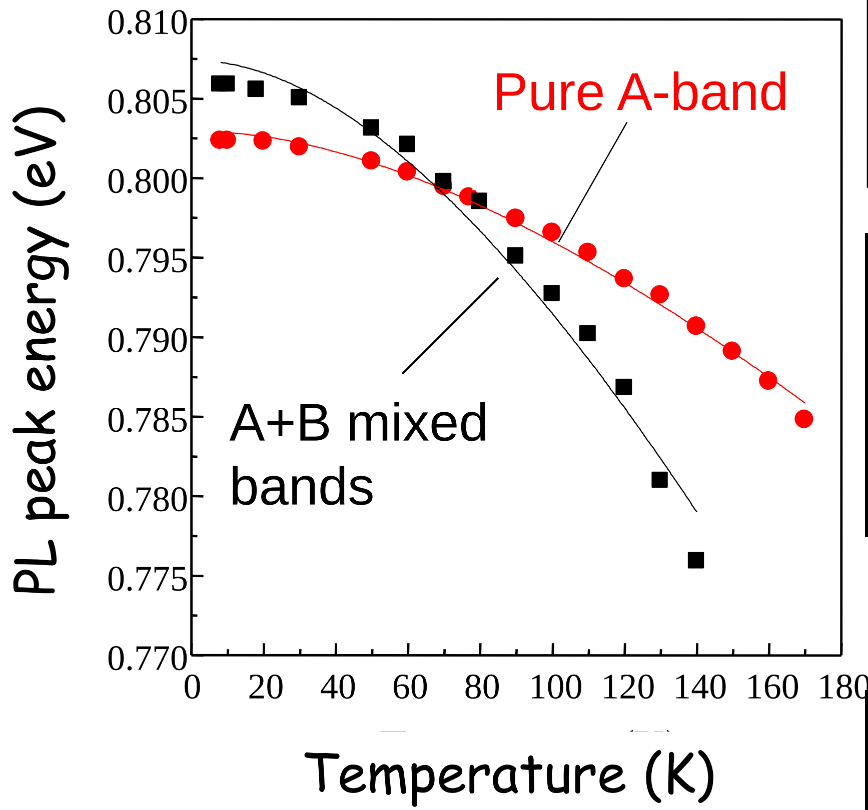

A: Intrinsic emission

A+B:Intrinsic & defect emissions

$$E_p(T) = E_p(0) - \alpha T^2/(\beta+T)$$

(Varshni's law)

	Ep(0) (eV)	α (x10⁻⁴)	β
IP	0.803	2.8	300
SP	0.8074	6.4	300
Si (ref.)	1.17	4.73	636

IBS β－$FeSi_2$

Yang, et.al (absorption)	0.9046	5.6	600
Martinelli (PL)	0.8052	4.2	600

Y. Maeda et al.: Thin Solid Films 461 (2004) 160.

Excitation power dependence of PL peak energy

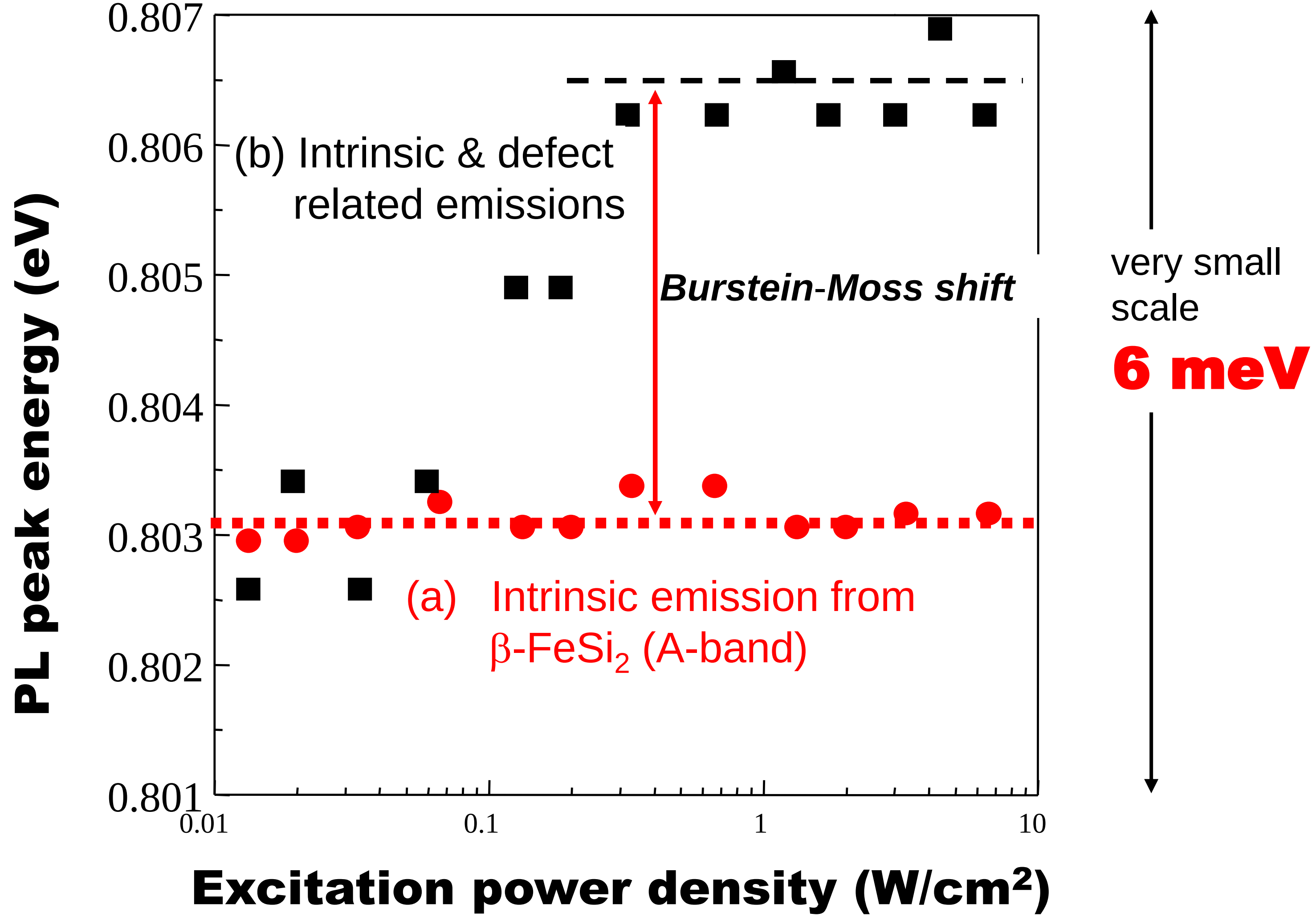

Note We can understand the difference between the intrinsic (A) and extrinsic or defect related band (B) luminescence by investigating the excitation power dependence.

Unique PL spectrum from β-$FeSi_2$ bulk crystals

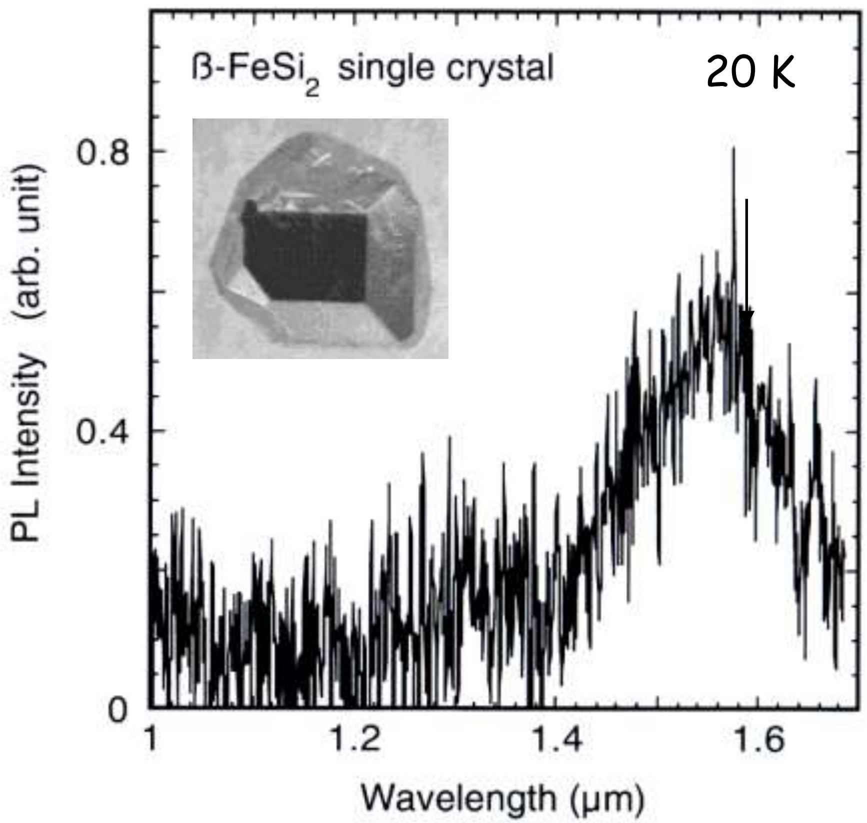

H. Udono et al.: Thin Solid Films 461 (2004) 182.

Crystal plate of β-$FeSi_2$

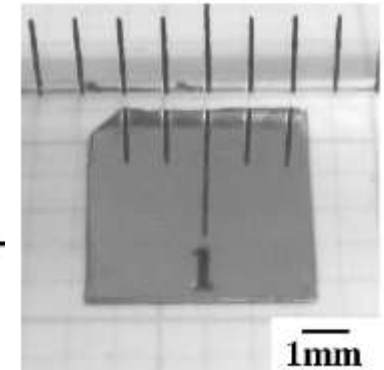

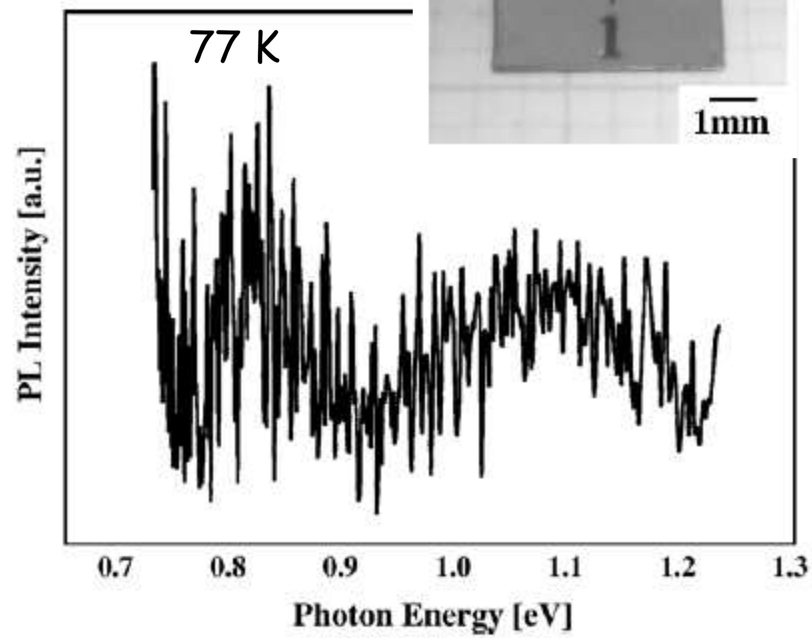

H. Tatsuoka et al.:
Thin Solid Films 515 (2007) 8268.

Unique PL spectra from the bulk crystal have been observed.
In this case, the PL cannot be affected by defects in Si substrates.
However, the present intensity is much smaller than those from thin film samples.
The reason for weak PLs may come from unavoidable and unintentional impurities.

3

Photoluminescence properties of β-$FeSi_2$/Si nano-composite phases

In this section, we discuss light emission due to exciton recombination related to material purity by using a simple model. The material purity required for sufficient efficiency of light emission will be roughly obtained.

Nano-composite phases

β-$FeSi_2$ nanocrystals embedded in a Si matrix

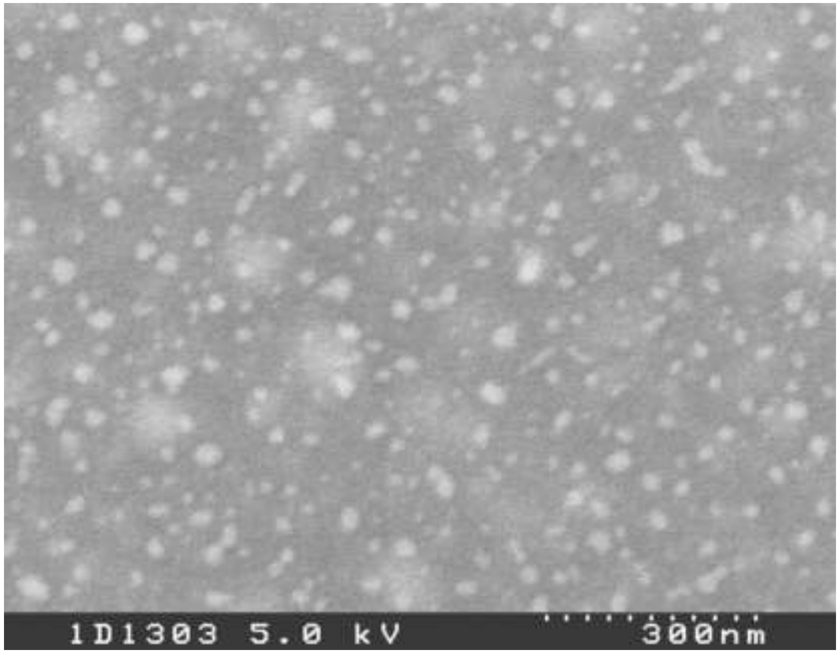

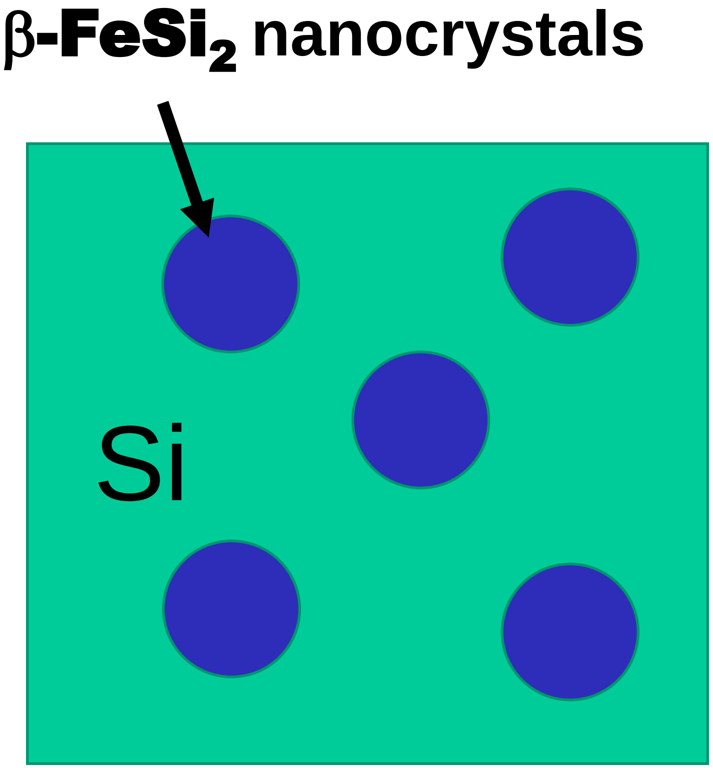

The average size of the nanocrystal = ~10 nm which depends on growth conditions.

Band-gap formation in $FeSi_2$

Note Deformation of g-$FeSi_2$ lattice by Jahn-Teller effect

⇒Band-gap formation between d bands : Semiconducting β-$FeSi_2$

This situation also means presence of large interaction between electrons and lattice in $FeSi_2$.

(a=b=c=5.43 Å)

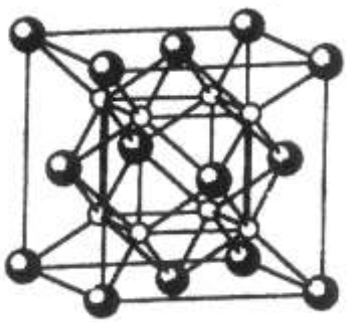

Metallic
γ-$FeSi_2$

a=b=c=5.43A
Si a=5.4306A

The γ-phase easily makes a coherent interface with Si. This condition can be applied to improvement of interface quality between β and Si.

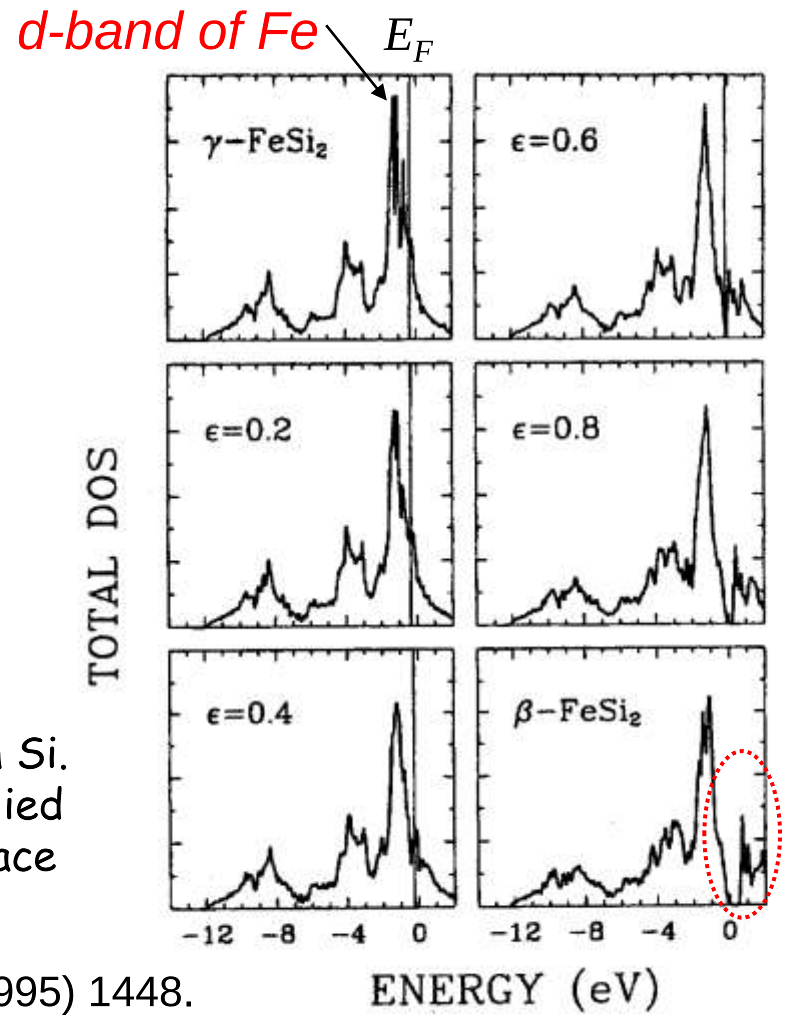

ε: Lattice distortion

Semiconducting
β-$FeSi_2$

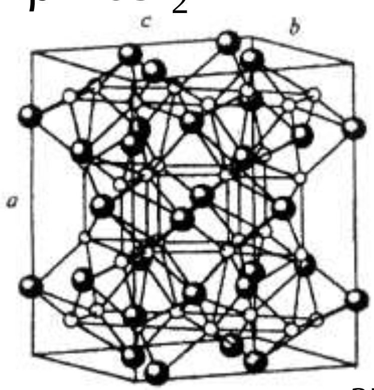

L. Miglio et al.: PRB 52 (1995) 1448.

Radiative recombination of β-$FeSi_2$ crystals

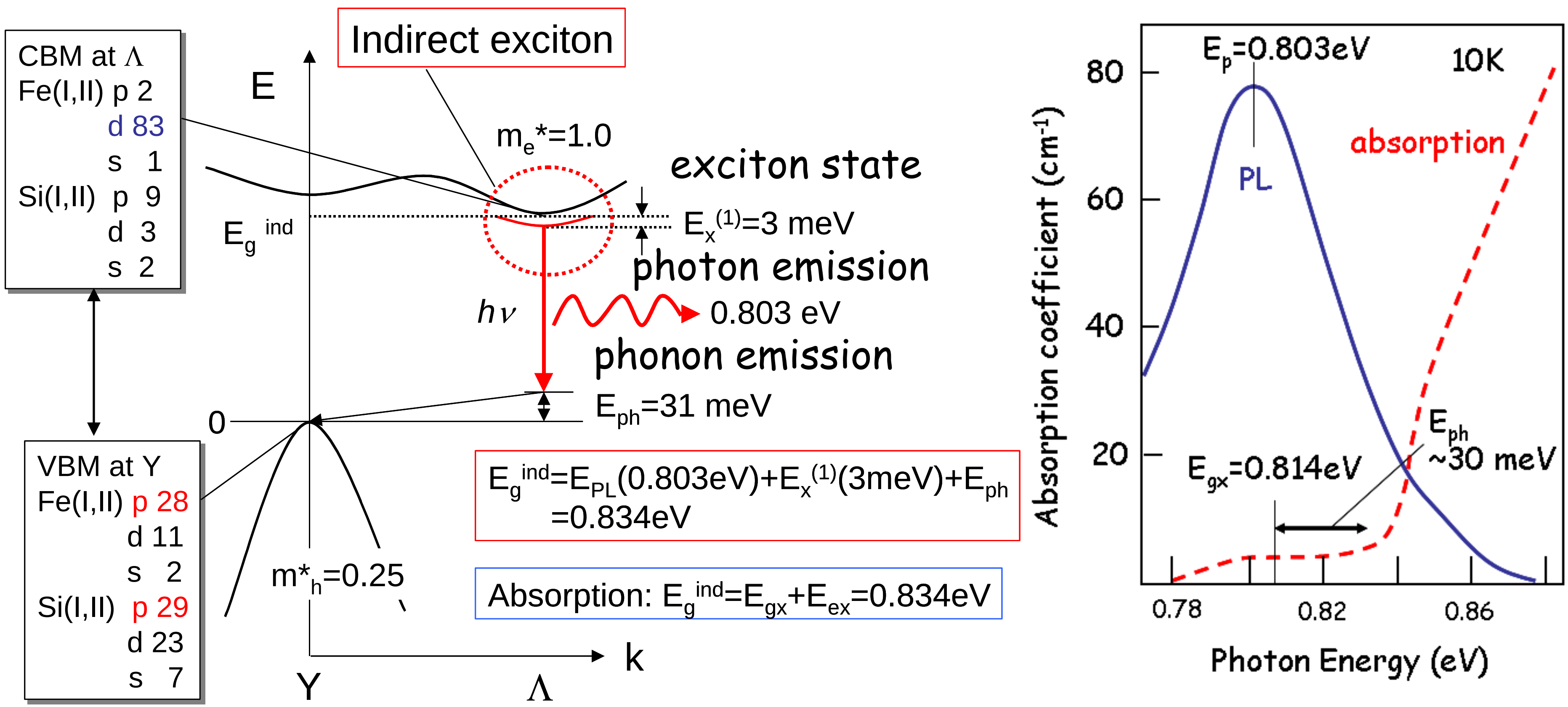

Note In β-$FeSi_2$ crystal, we can understand the radiative recombination of exciton due to interband transition with LO phonon emission from the minimum point on the L point on the conduction band to the Y point of the valence band.

Y. Maeda, Appl. Surf. Sci., **254** (2008) 6242.

Radiative and Non-radiative recombination processes

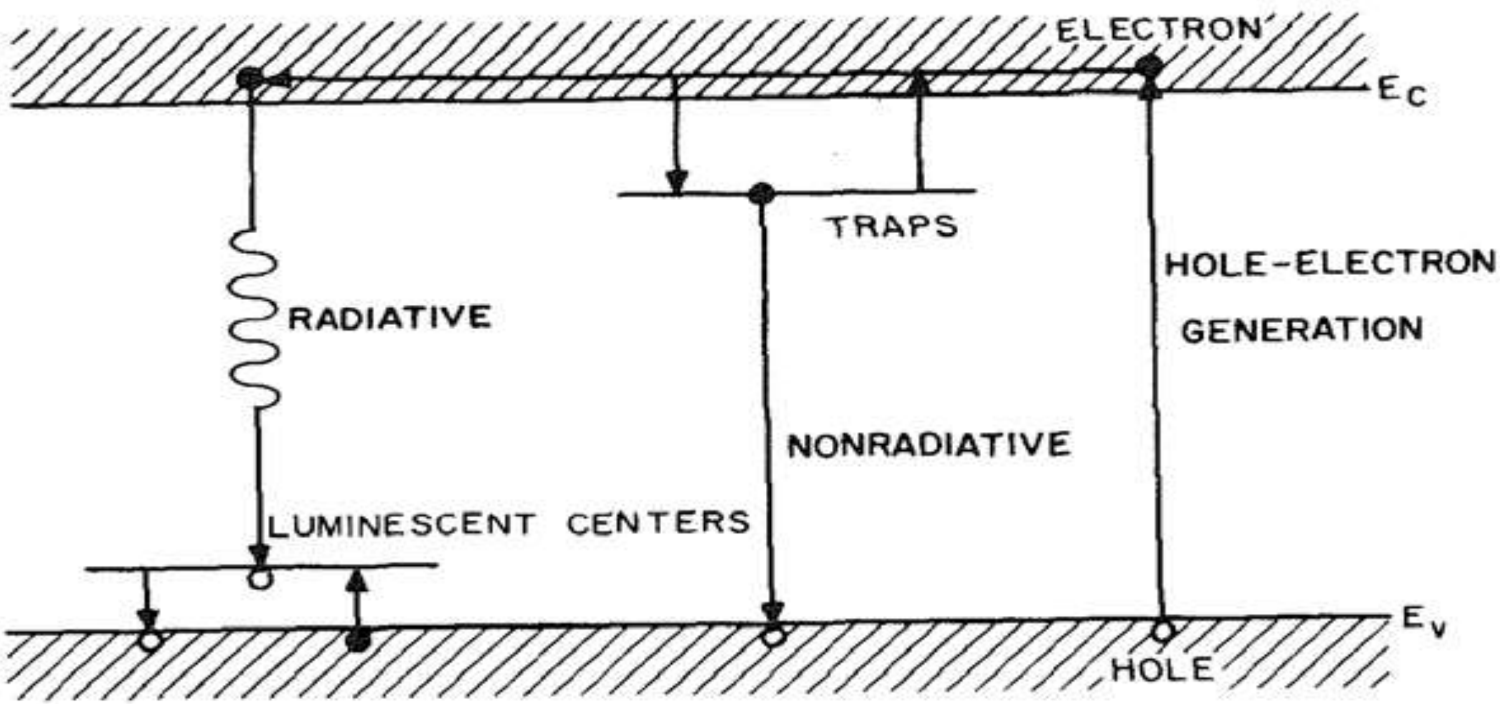

Representation of radiative and nonradiative recombinations. (After Ivey, F

Thermal resolution of excitons as a non-radiative recombination

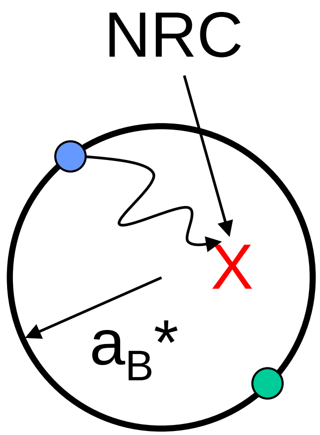

Wannier-Mott exciton

Non-radiative recombination centers (NRC)

Deep centers due to transition metal impurities

Atomic vacancy, defects etc.

$$(e\text{-}h)_{ex} \longrightarrow (e^-) \text{ in CB} + (h^+) \text{ in VB} + \text{heat}$$

N_T: Density of NRC

<n>: Number of NRC in the volume of exciton

a^*_B: Effective Bohr radius in a semiconductor

$$\langle n \rangle = \frac{4\pi}{3}(a_B^*)^3 N_T,$$

In case of <n>=1, we determine the critical radius $(a^*_B)_c$ by

$$1 = \frac{4\pi}{3}(a_B^*)_c^3 N_T, \quad (a_B^*)_c = \left(\frac{4\pi}{3} N_T\right)^{-1/3}$$

Calculation of effective Bohr radius in β-$FeSi_2$

$\varepsilon(0) = 29.9 \sim 32.5$: static dielectric constant

$\mu = 0.2 m_0$: reduced mass of electron-hole pair

$$a_B^* = 0.529 \times \varepsilon(0) \frac{m_0}{\mu} =\sim 8\, nm$$ 3 times larger than that in Si

The emission efficiency η is proportional to the density of exciton remaining $<n_{ex}>$after thermal non-radiative recombination

$$\eta \sim < n_{ex} > = \frac{{(a_B^*)_c}^3}{{a_B^*}^3} - < n_T >$$

Note In higher purity or less defective crystals, $(a^*_B)_c$ is larger, so that efficiency η becomes larger.

Possible conditions of crystal purity for exciton radiative recombination

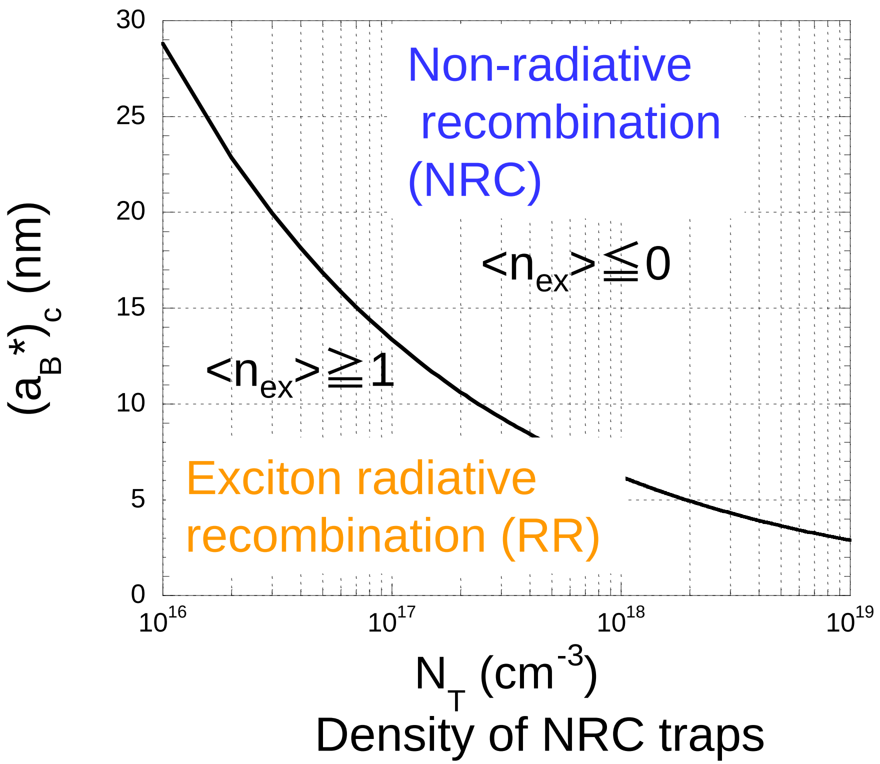

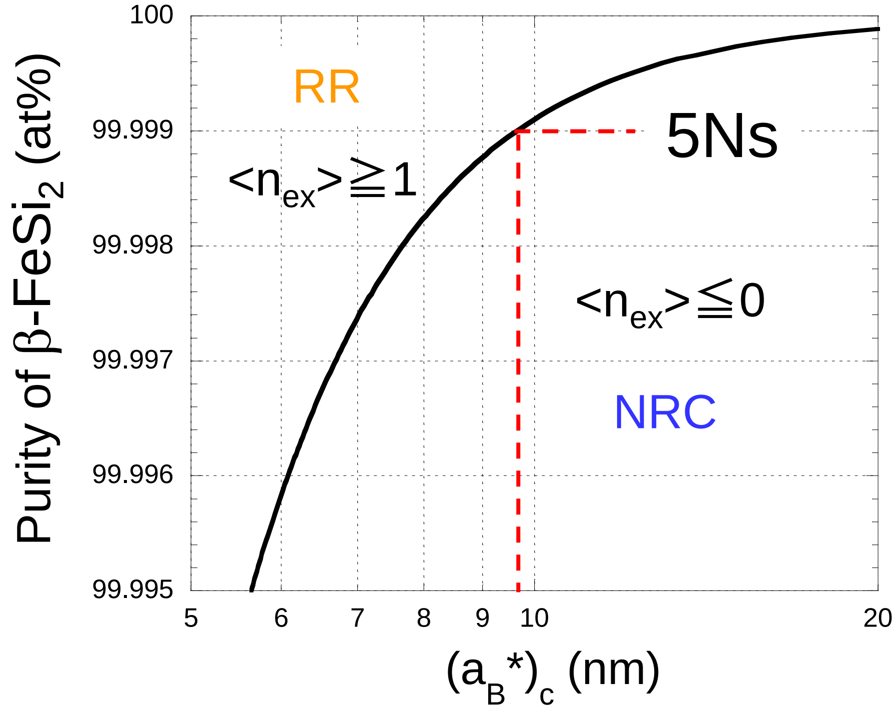

Note The exciton radius in β-$FeSi_2$ with a large static dielectric constant is so large that for exciton radiative recombination the purity of crystal should be higher than that of usual semiconductors with small static dielectric constants.

Radiative Efficiency and crystal purity

$$\eta \sim \langle n_{ex} \rangle = \frac{(a_B^*)_c^{\ 3}}{a_B^{*\,3}} - \langle n_T \rangle$$

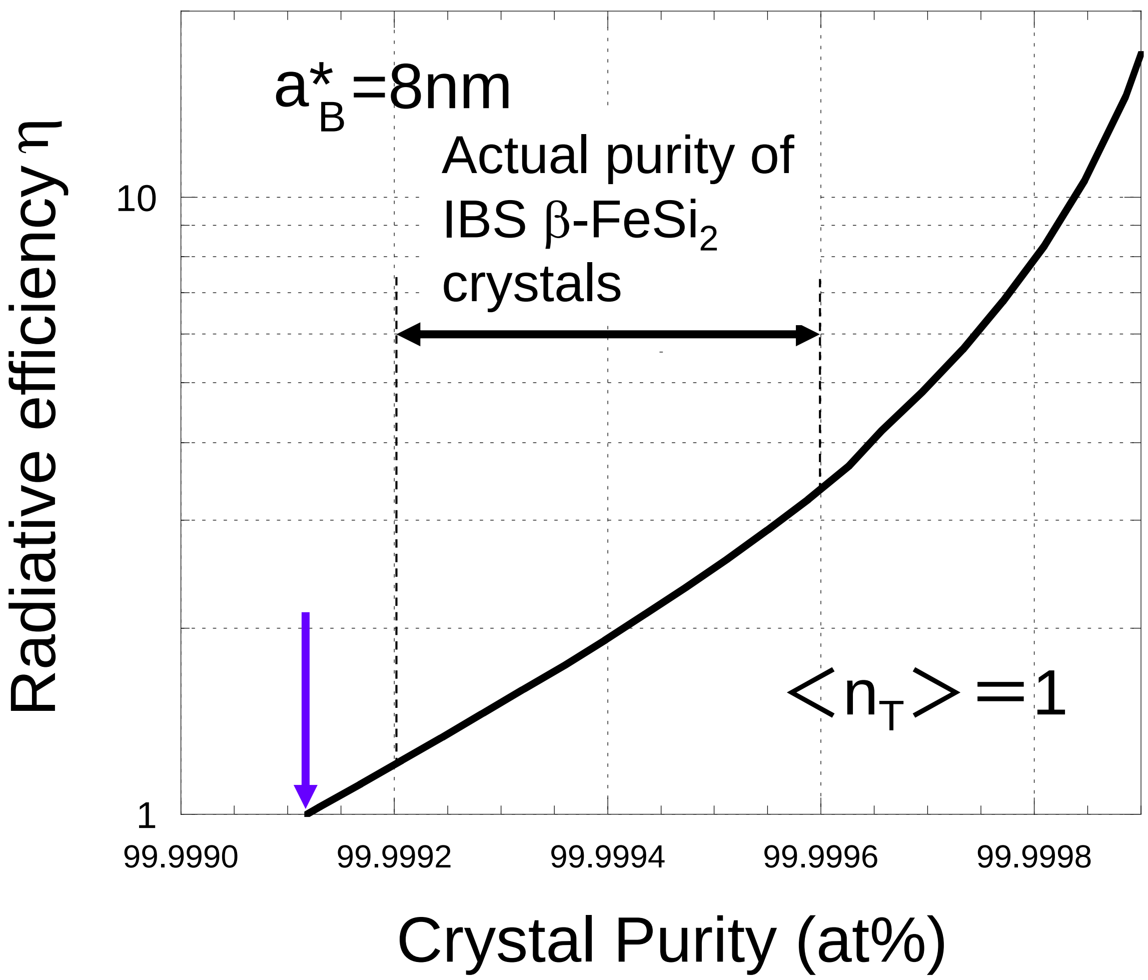

PL spectrum and its temperature dependence

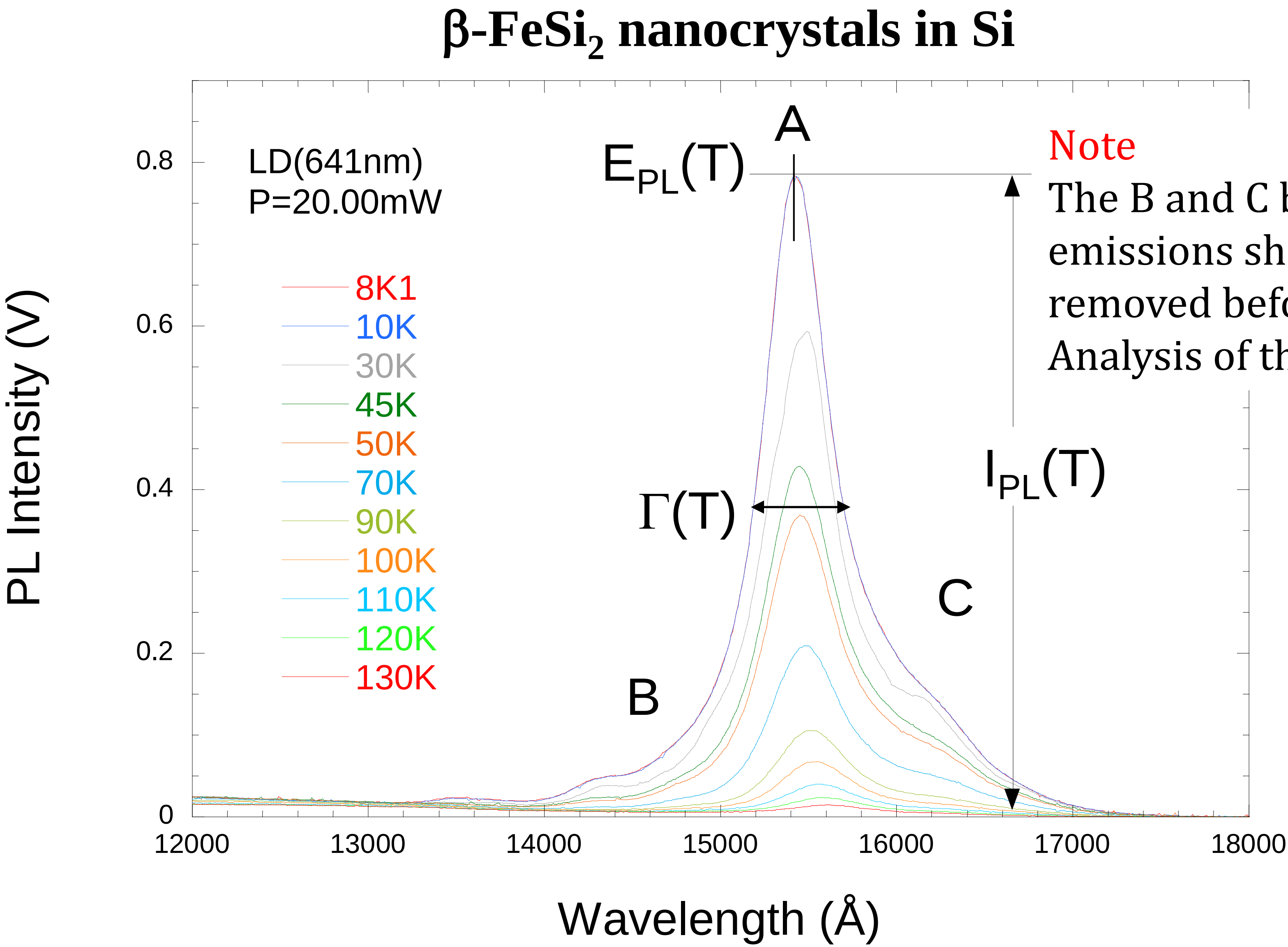

Note
The B and C bands emissions should be removed before Analysis of the spectrum.

Emission efficiency dominated by thermal quenching and crystal quality

Time dependent density for excitons

$$\frac{dN(t)}{dt} = -\left(\frac{1}{\tau_r}\right)N(t) - \sum_i \left(\frac{1}{\tau_{nr,i}(T)}\right)N(t) + G$$

Generation rate of excitons

Life time of radiative recombination

Life time of non-radiative recombination (NR)

$$1/\tau_{nr,i}(T) = (1/\tau_{nr,i}(0))\exp(-E_{A,i}/k_B T)$$

Activation energy into NR process

In a stationary state

$$N_s(T) = \frac{1}{1/\tau_r + \sum_i 1/\tau_{nr,i}(T)} G$$

Emission efficiency η(T)

$$I_{PL}(T) = N_s(T)(1/\tau_r) = \frac{1/\tau_r}{1/\tau_r + \sum_i 1/\tau_{nr,i}(T)} G$$

Internal quantum efficiency for light emission (Fundamental formula)

$$\eta(T) = \frac{1/\tau_r}{1/\tau_r + \sum_i 1/\tau_{nr,i}(T)}$$

τ_r: life time for a radiative recombination

τ_{nr}: life time for the non-radiative *i*-th process that is activated thermally

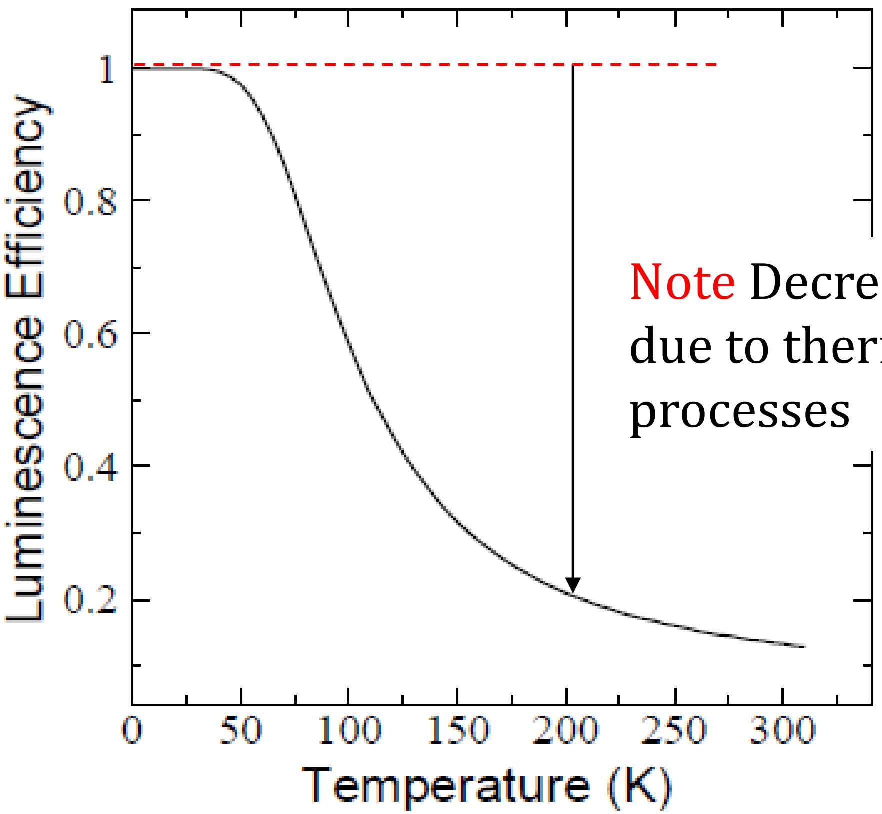

Note Decrease of radiative efficiency due to thermal activation to non-radiative processes

Analysis of radiative efficiency as a function of temperature

$$\eta(T) = \frac{1}{\left(1 + C_1 \exp(-E_1 / k_B T) + C_2 \exp(-E_2 / k_B T)\right)}$$

$$E_1 = E_T$$

$$C_1 = \tau_r N_T \sigma \underbrace{\left(\frac{3k_B T}{m^*}\right)^{1/2}}$$

Thermal velocity of electrons or holes

E_T: trap depth in energy
τ_r: life time of electrons or holes
N_T: density of trap for a non-radiative process
σ: Cross section of the trap
m: effective mass of electron or hole

$$\eta(T) = \frac{1}{\left(1 + \tau_r N_T \sigma \left(\frac{3k_B T}{m^*}\right)^{1/2} \exp(-E_T / k_B T) + C_2 \exp(-E_2 / k_B T)\right)}$$

$$E_2 = E_{ex} \quad \textit{for free exciton}$$

$$E_2 = E_{ex} + E_b \quad \textit{for bound exciton}$$

Actual case of analysis

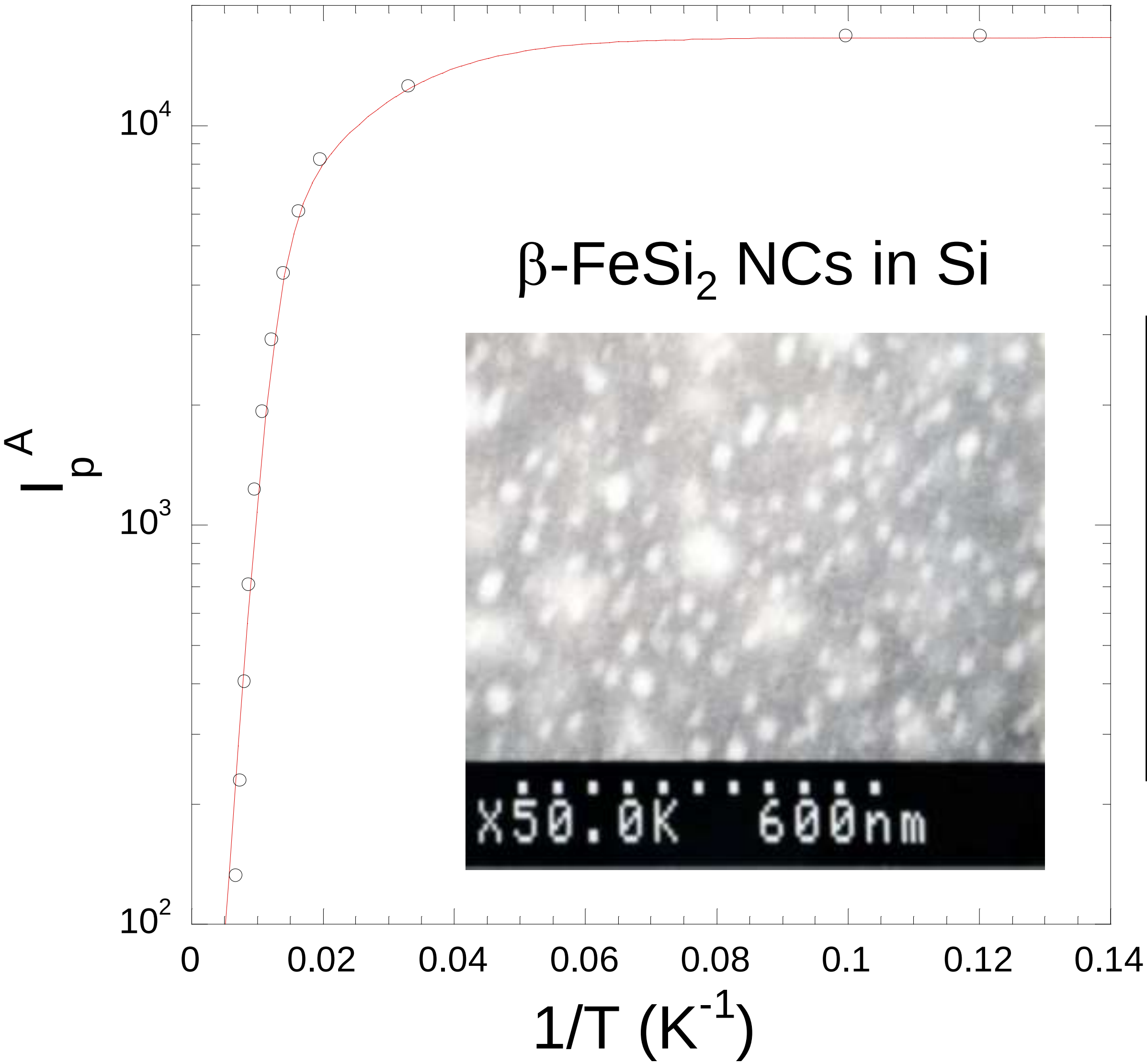

$$C_1{}^* = \tau_r N_T \sigma \left(\frac{3k_B T}{m^*} \right)^{1/2}$$

$C_1{}^*$	138.19
E_T (meV)	43.13
C_2	5.29
E_2 (meV)	7.43
I_{max}	16624

Some parameters required in calculations

(1) Life time of radiative recombination

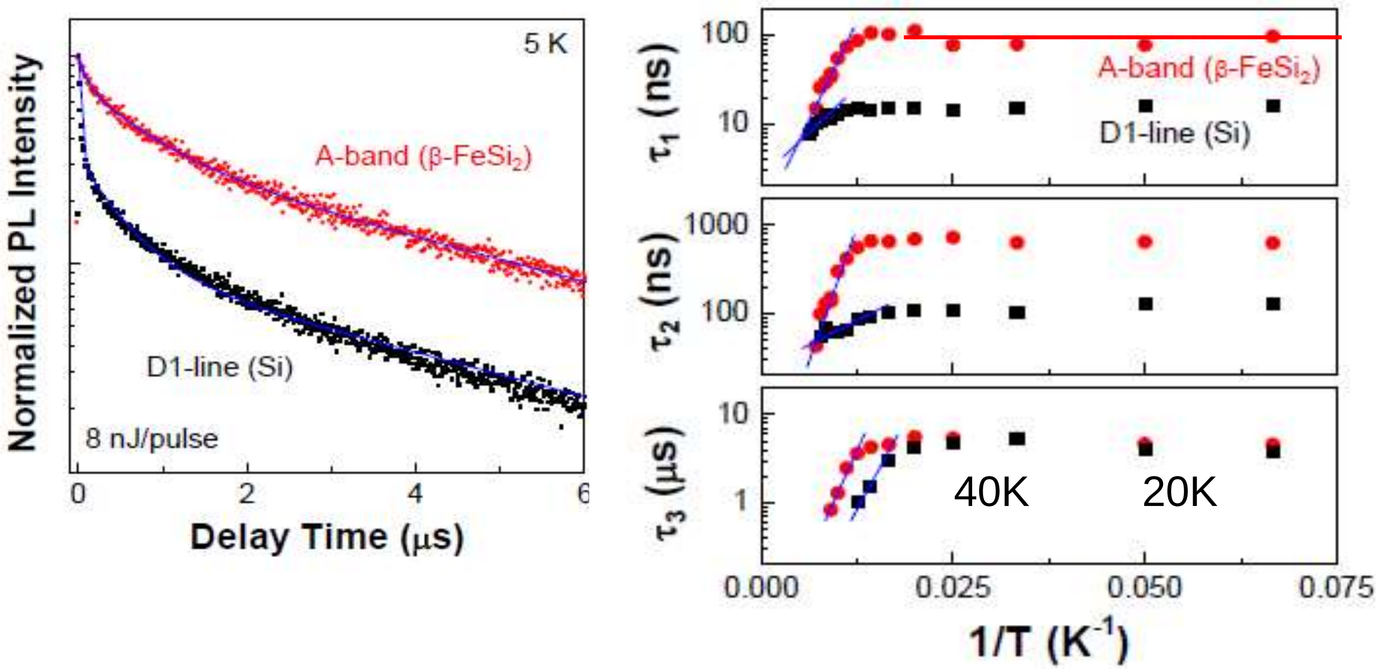

τ_r=100ns

T<100K

Y. Terai et al. JSAP Annual meeting

(2)Trap for minority carriers

$$\tau_r = \frac{1}{Bn} = \frac{1}{Bn_0} e^{E_D/k_B T}$$

Effective mass (Γ) $m_e^*=1.0m_0$

Cross section σ＝5.2×10^{-20} m^2 in p-type β-$FeSi_2$

Lefki et al.: J. Appl. Phys. 69(1)(1991)352.

Calculation results of N_T

β-FeSi$_2$ NCs Anneal conditions	N_T (cm^{-3}) calculated	Purity（at%） consent value
200keV 1e17 Fe 800℃/2h NCs	9.08×10^{18}	99.9657
200keV 1e17 Fe 800℃/6h NCs	3.90×10^{18}	99.9852
200keV 1e17 Fe DTT：500℃/4h＋800℃/6h NCs	3.90×10^{18}	99.9852
200keV 1e17 Fe DTT：500℃/8h＋800℃/6h NCs	2.75×10^{18}	99.9896
100keV 5e16 Fe 800℃4h Surface precipitates	4.67×10^{19}	99.8241
IBS β-FeSi$_2$* *Katsumata et al.：J. Appl. Phys. 80 (1996) 1784.	3.98×10^{19}	99.8500

How do we need purity of crystals toward RT emission?

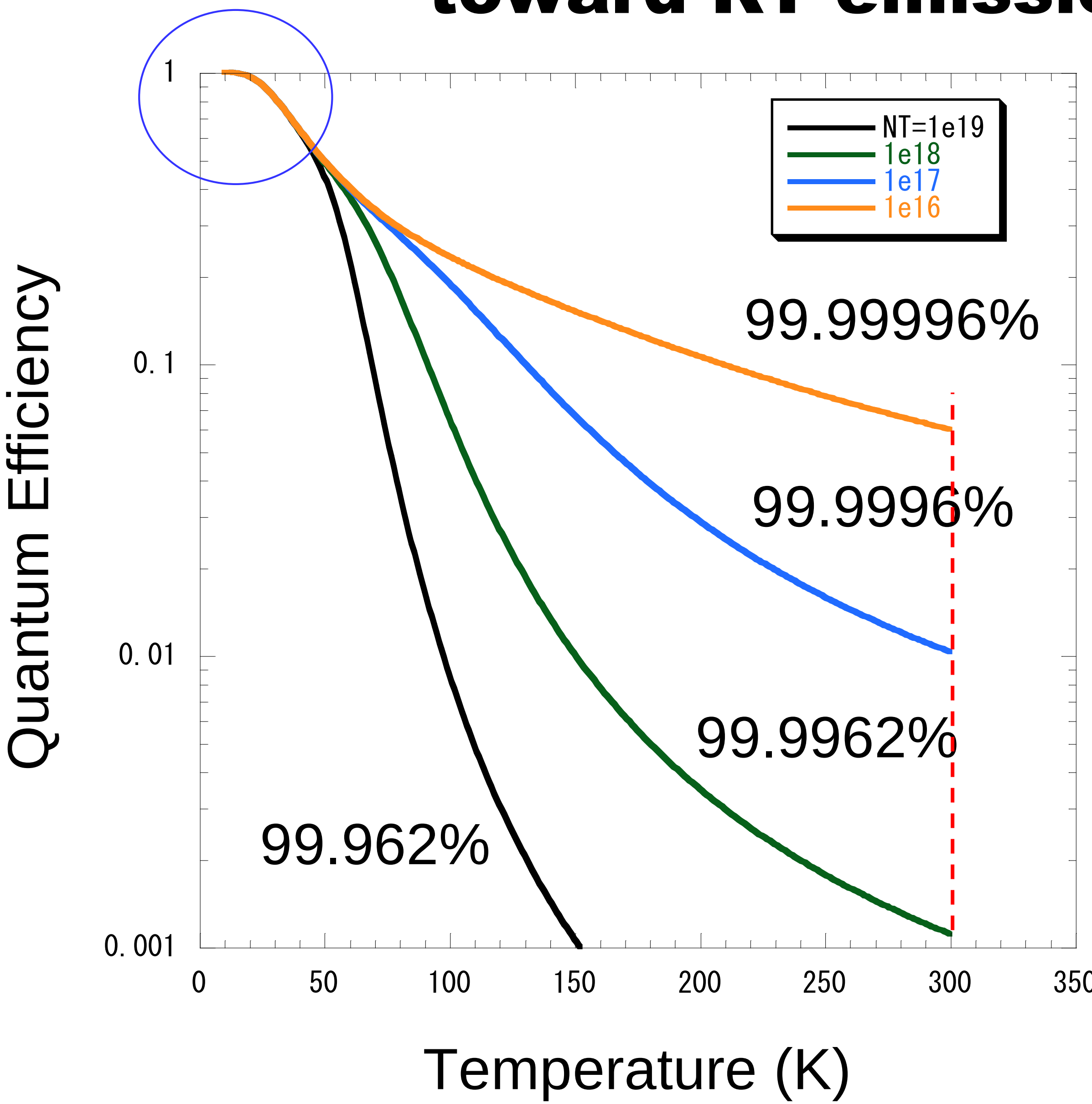

Consent purity

$N_T = C_{impurity}$

m^*	m_0
σ (m²)	5.2x10²⁰
E_T (meV)	50.0
C_2	10
E_2 (meV)	10

Note

At T>50K, a strong Dependence of the purity on a quantum efficiency of emission is expected.

Emission efficiency vs purity of crystals

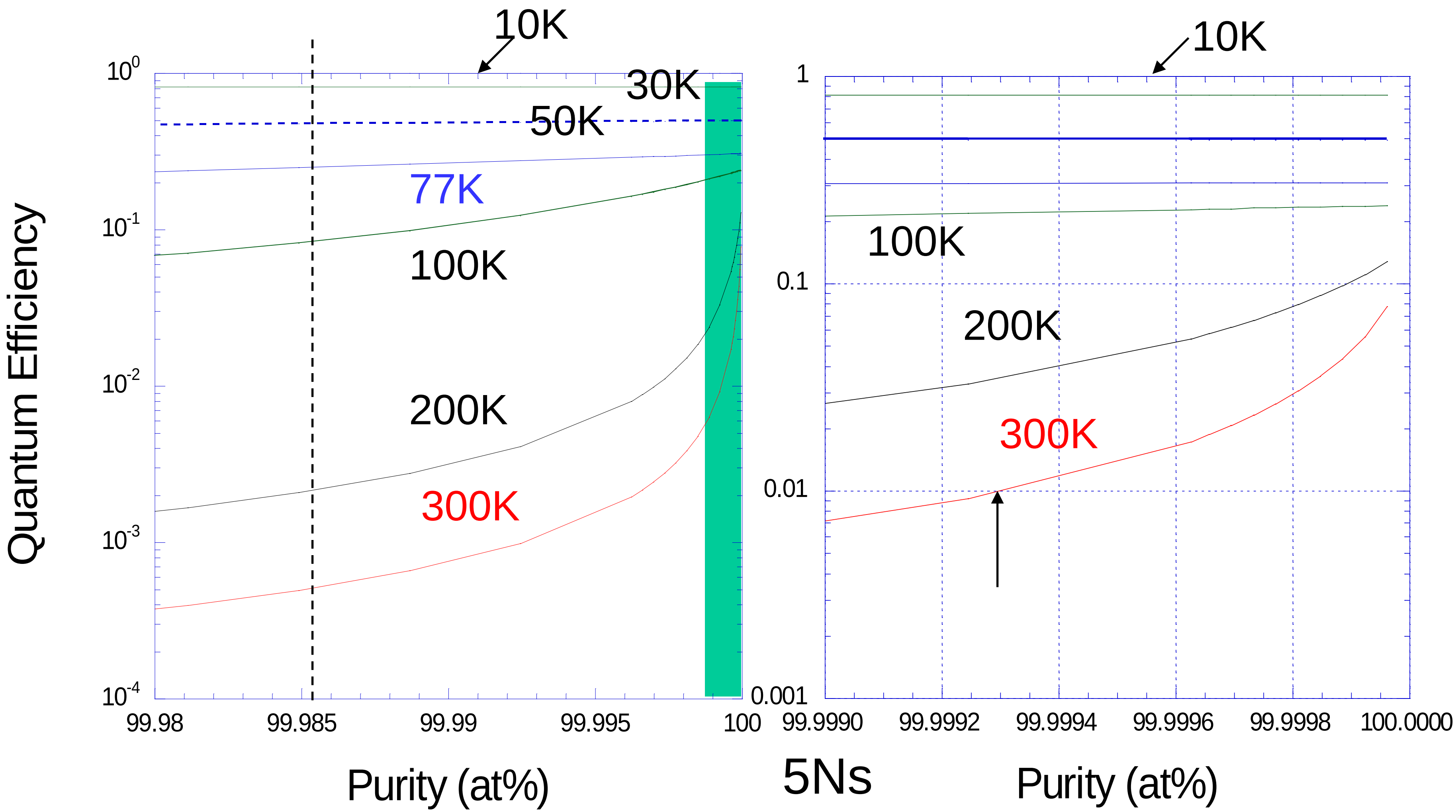

Note The purity is more than 5 nines 3, η≧1% at RT can be expected.

Analysis of temperature dependence of emission peak energy

We can get information of phonons relating to emission processes.

1. Varshni's empirical law

$$E_{PL}(T) = E_{PL}(0) - \frac{\alpha T^2}{T+\beta}$$

α : electron-lattice interaction constant (eV/K), β : Debye temperature in K (approx.)

2. Multiple phonon coupling model

$$E_{PL}(T) = E_{PL}(0) - \sum_{j=1}^{m} \frac{\alpha_j \Theta_j}{\exp(\Theta_j / T) - 1}$$

α_j : coupling constant of lattice with the i-th phonon,
$k_B\Theta_j$: average energy of the j-th phonon

3. Einstein model (Harmonic oscillator model)

$$E_{PL}(T) = E_{PL}(0) - S \cdot \langle E_{ph} \rangle \left[\coth\left(\langle E_{ph} \rangle / 2k_B T \right) - 1 \right]$$

S : Huang-Rhys factor, $\langle E_{ph} \rangle$: average energy of related phonons

$$S = -\alpha / 2k_B = -\alpha / 1.72 \times 10^{-4}$$

Physical meaning of Haung-Rhys S factor

The value of S corresponds to the average number of emitted phonons which should be required by the lattice relaxation from the point a at（q=0, E=E_0+Δ）to the point b at（q=q_0, E=E_0）

$$E_g = \frac{1}{2}M\Omega^2 q^2$$

$$E_e = \frac{1}{2}M\Omega^2 (q-q_0)^2 + E_0$$

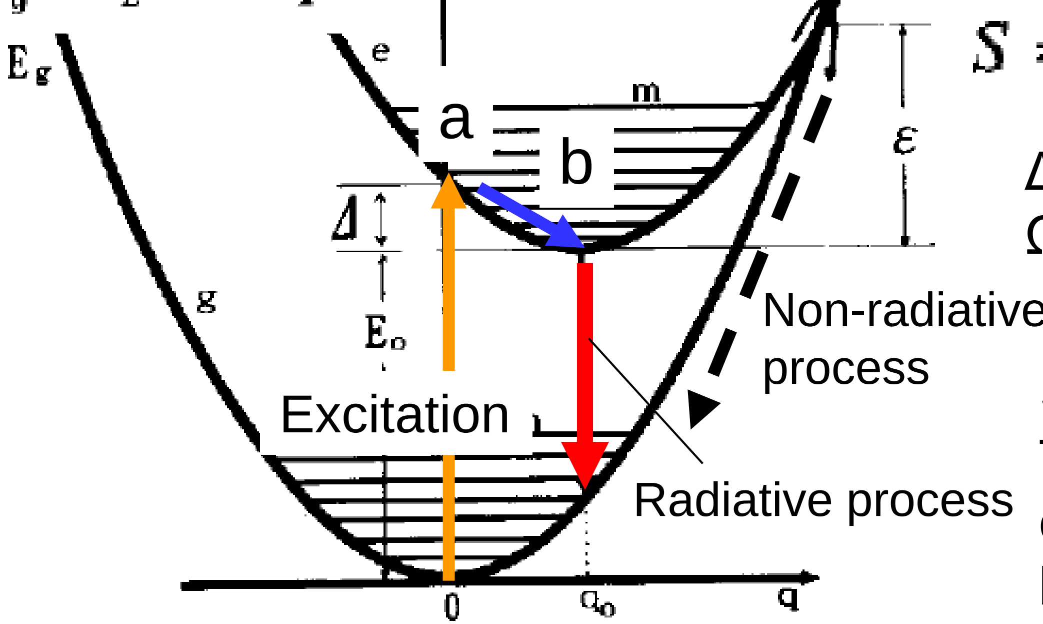

$$S = \frac{1}{2}M\Omega^2 q_0^2/h\Omega = \Delta/h\Omega$$

Δ：Lattice relaxation energy
Ω：average energy of phonon

S：smaller⇒Δ：smaller
The smaller Δ means electrons more weakly bounded at localized centers.

Adiabatic potential curves of a ground state and an excited state.

D. R. Vij ed.: Luminescence of Solids, (Plenum, 1998, New York) p.108.

Haung-Rhys factor and Spectrum shape

Poisson distribution $$I_{0,n} = e^{-S}\left(\frac{S^n}{n!}\right), \quad n = 0, 1, 2, \cdots$$

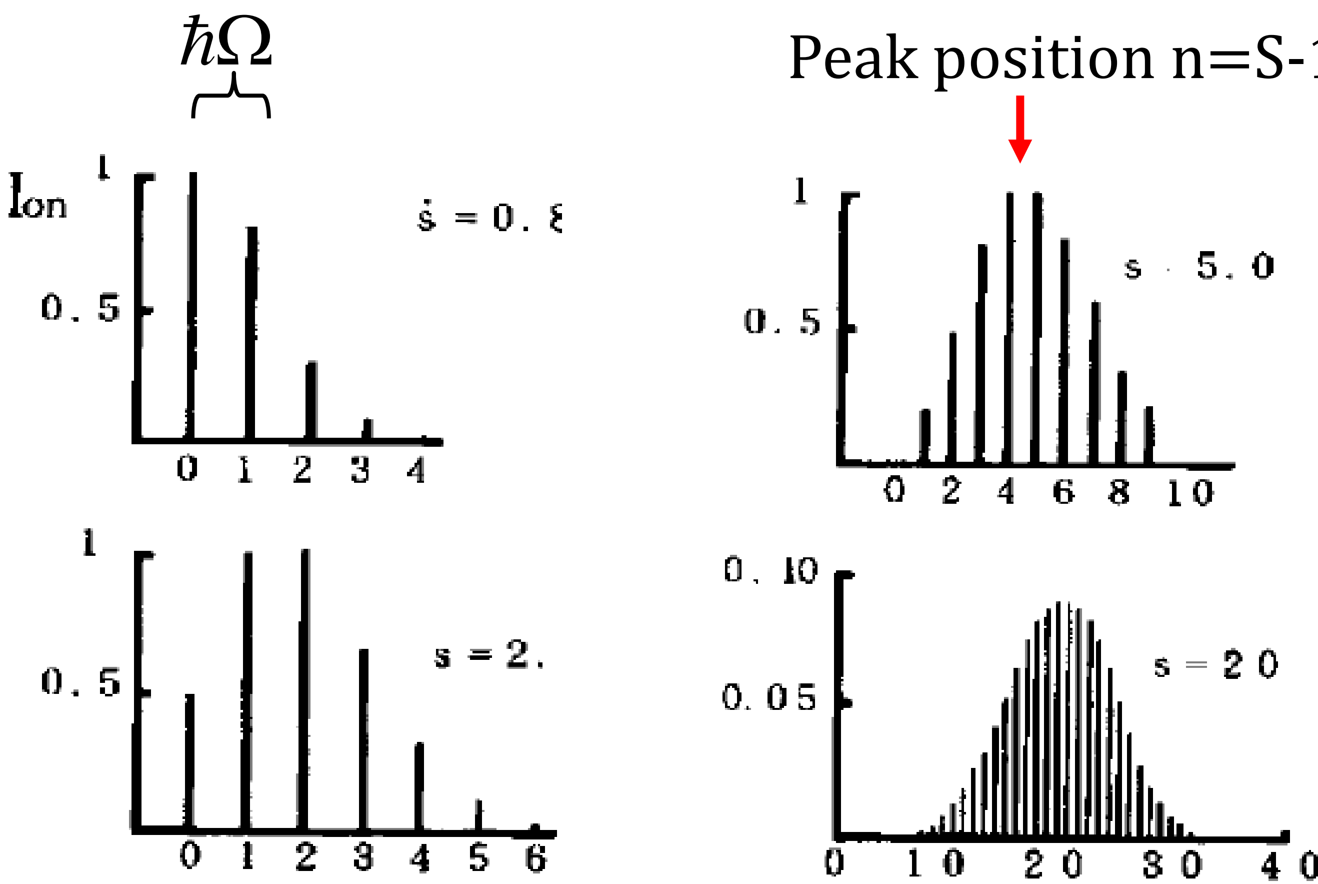

D. R. Vij ed.: Luminescence of Solids, (Plenum, 1998, New York) p.111.

Spectrum shape (1)

In the case of small S＝0.84,　＜E_{ph}＞＝47meV

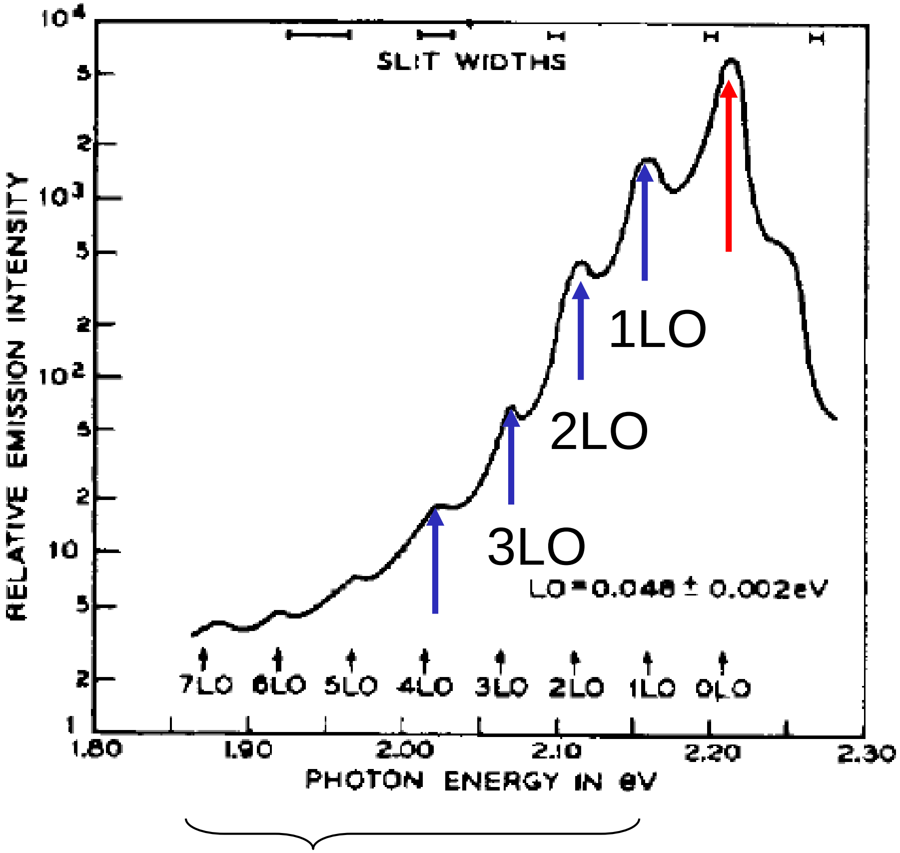

Phonon side band　Zero-phonon emission

Shallow DAP luminescence

Figure 11. Spectrum of edge emission (shallow DAP luminescence) in GaP:Si,S at 20 K (LO stands for longitudinal optical phonon energy). (Thomas *et al.*, 1964; with kind permission from the American Physical Society).

LO: Longitudinal optical phonon

Spectrum shape (2)

In the case of large S=~3, <E_{ph}>=26 meV

Mirror relationship

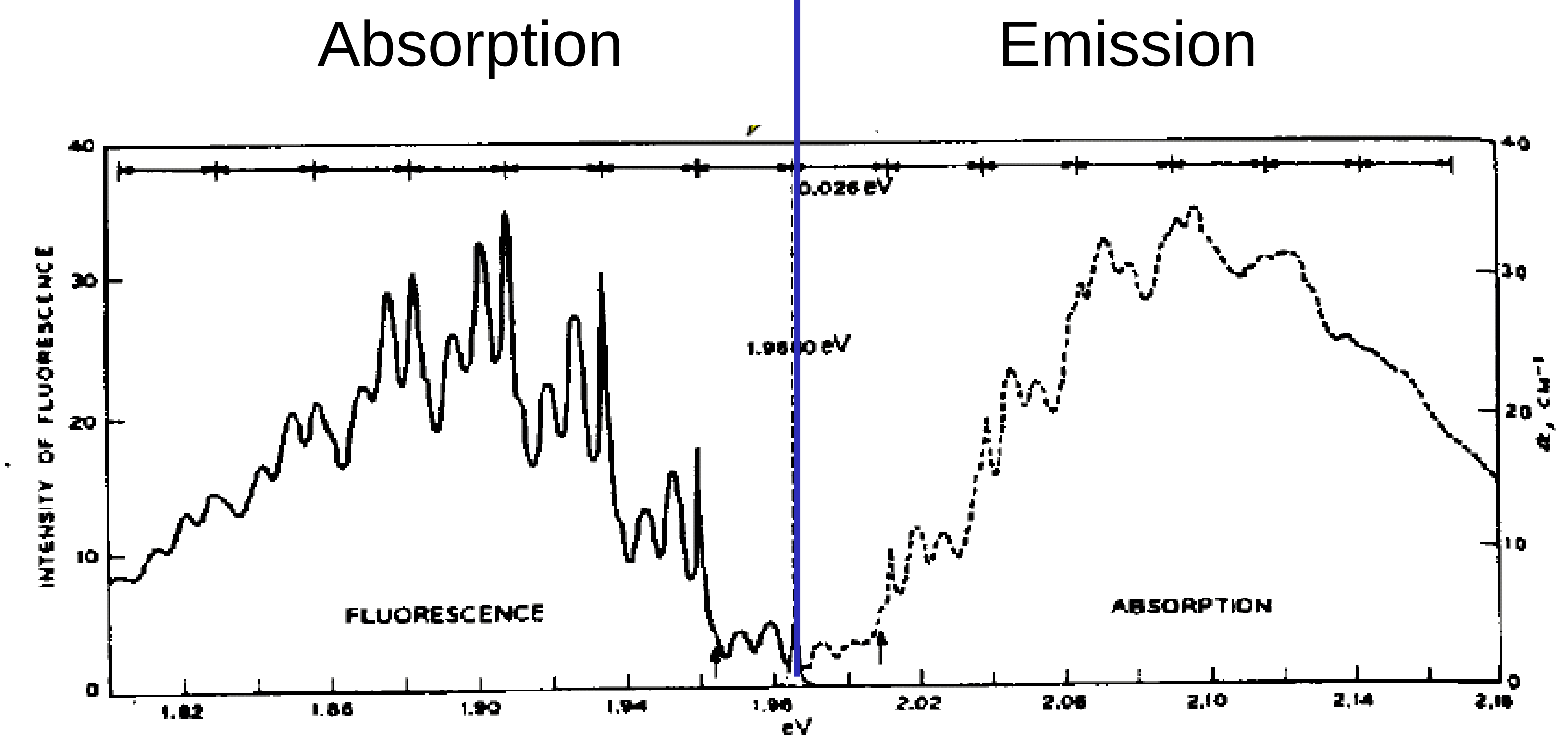

Figure 9. Absorption and fluorescence spectra of ZnTe: O at 20 K (Merz, 1968; with kind permission from the American Physical Society).

Analysis by multi-phonon model

$$E_{PL}(T) = E_{PL}(0) - \sum_{j=1}^{2} \frac{\alpha_j \Theta_j}{\exp(\Theta_j / T) - 1}$$

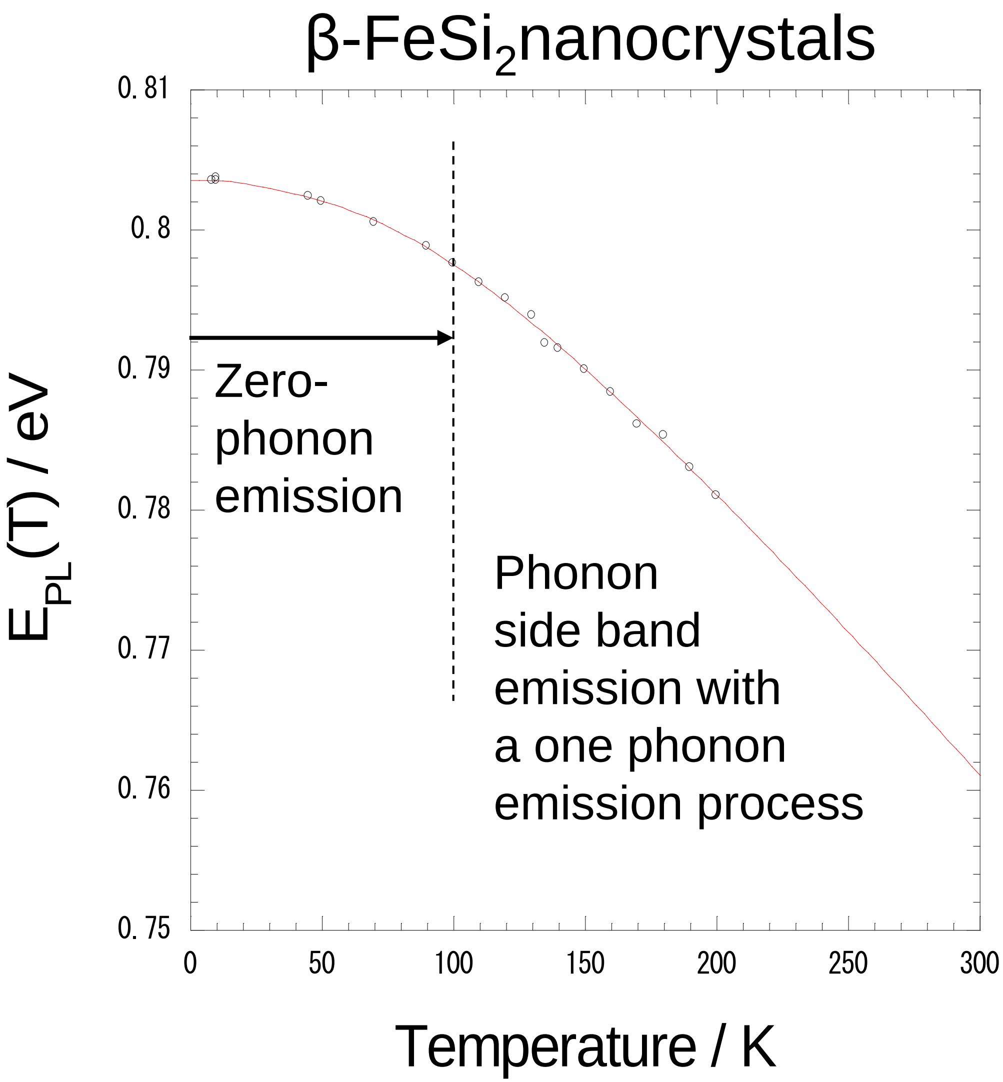

T>100K	
α_1	$1.76\text{x}10^{-4}$ (eV/K)
S_1	1.02
$\langle E_{ph}\rangle_1 = k_B\Theta_1$	27.7 (meV)
T<~50K	
α_2	$4.72\text{x}10^{-5}$ (eV/K)
S_2	0.275
$\langle E_{ph}\rangle_2 = k_B\Theta_2$	4.27 (meV)

LO phonon : E_{LO}=31meV

β-$FeSi_2$: **S factor reported**

Samples	S	$\langle E_{ph} \rangle$meV	Ref.
(a) Optical absorption measurements			
Single crystal	2.2 (id) 2.4 (d)	2.7 2.9	(1)
IBS sample	2.15	34.5	(2)
Polycrystal films	6.22	71.0	(3)
(b) PL measurements			
IBS nanocrystals	0.97~ 1.02	4~30	Un published
IBS films or precipitates	1.2~8	10~20	Un published

(1) H. Udono et al.: Thin Solid Films 461 (2004) 182.
(2) Z. Yang et al.: J Appl. Phys. 78 (1995)1945.
(3) C. Giannini et al.: Phys. Rev. B 45 (1992) 8822.

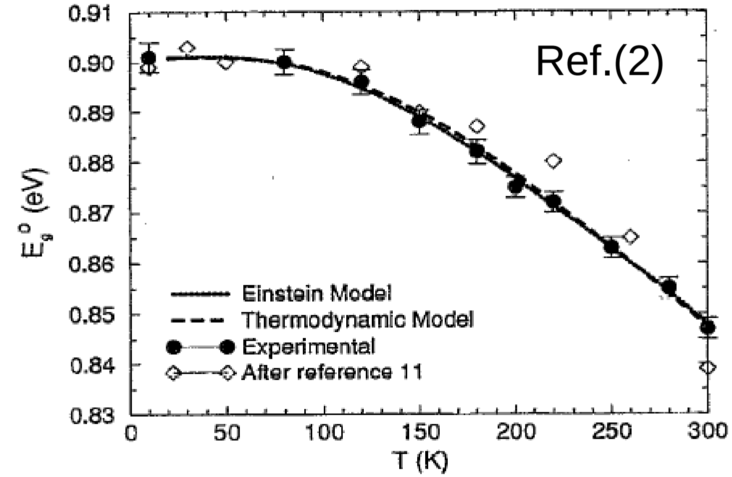

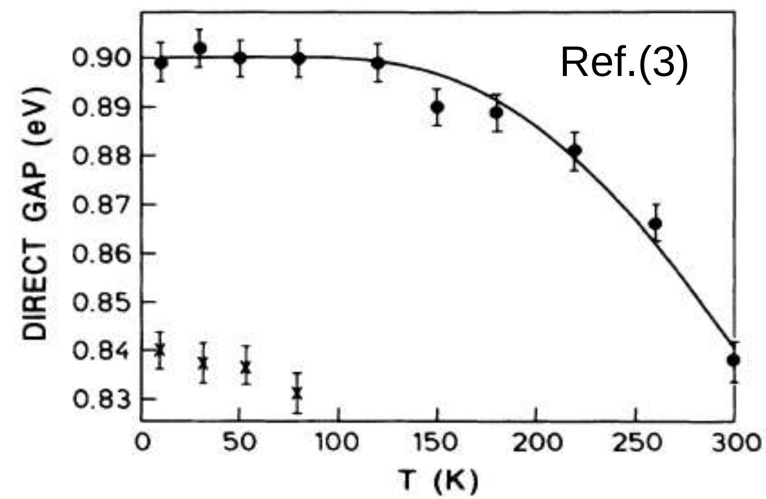

Crystal Si: S=1.49

A Debye-Waller factor

Note Computing the Debye-Waller factor, we can know an intensity ratio of the zero-phonon emission to the phonon side band emissions. This ratio determines the spectrum shape.

$$R_0(T) = e^{-S(1+2\langle n \rangle)},$$

Planck function for phonon statistics

$$\langle n \rangle(T) = \frac{1}{\exp(\hbar\omega_{ph} / k_B T) - 1}$$

$$= \frac{1}{\exp(\langle E_{ph} \rangle / k_B T) - 1}$$

Debye-Waller factor R_0 vs S factor

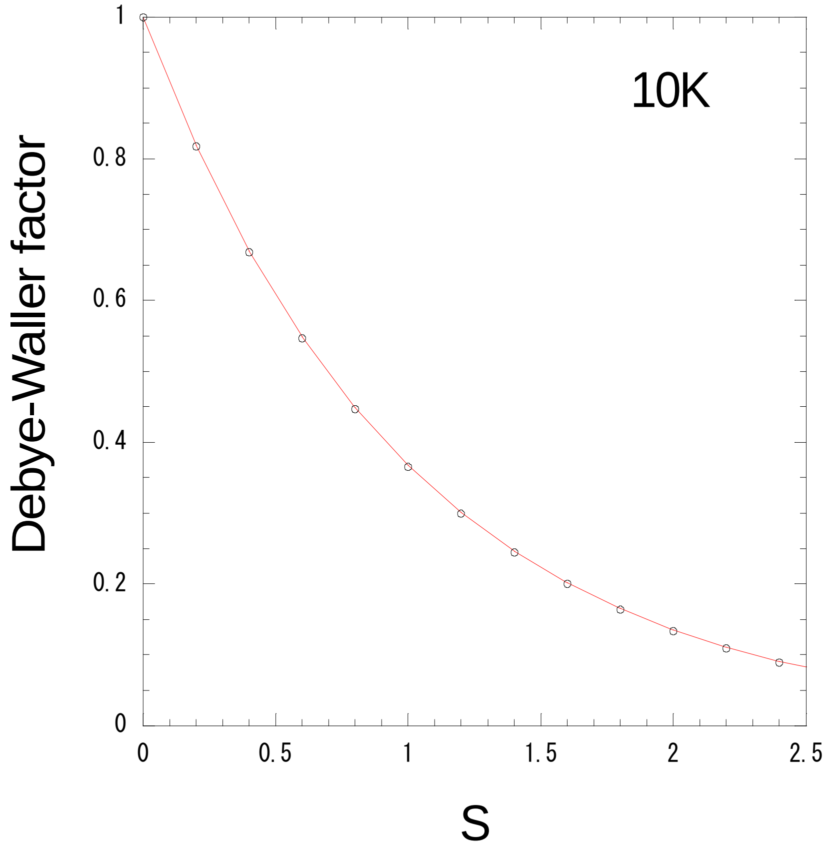

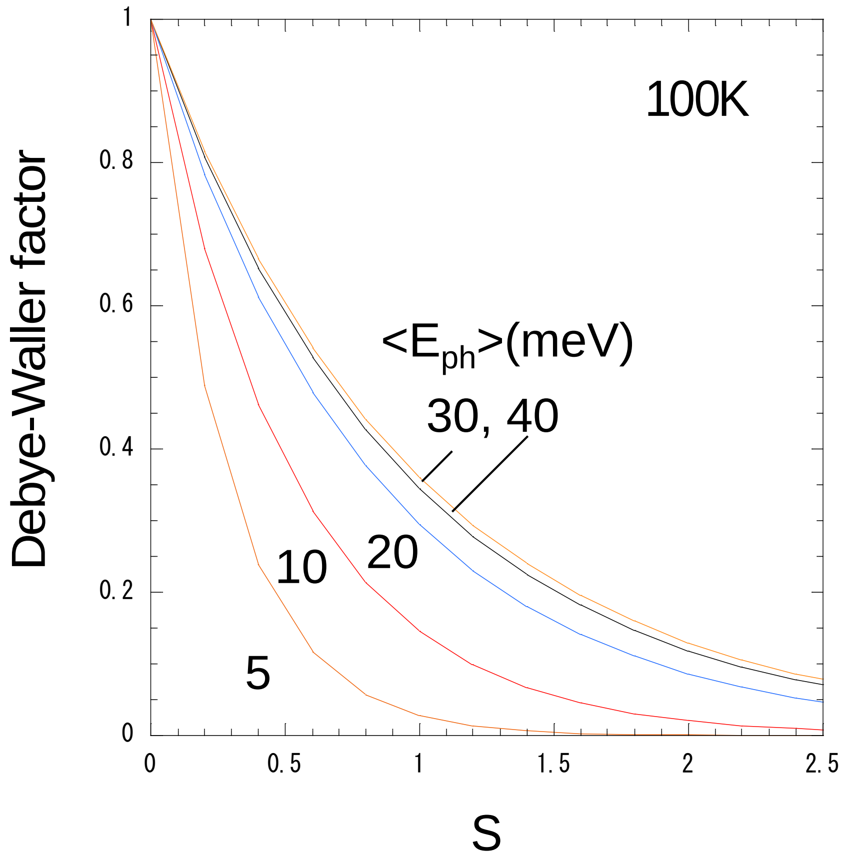

Note As the S factor is larger, the R_0 factor (contribution of the zero-phonon emission) is smaller. As the average energy of phonon relating to optical transitions is smaller, the R_0 factor is smaller at the same S factor. It suggests that the R_0 factor can be regarded as an evaluation parameter of thermal quenching of the emission intensity.

Emission spectrum

（Case of S near 1.0）

β-$FeSi_2$ nanocrystals

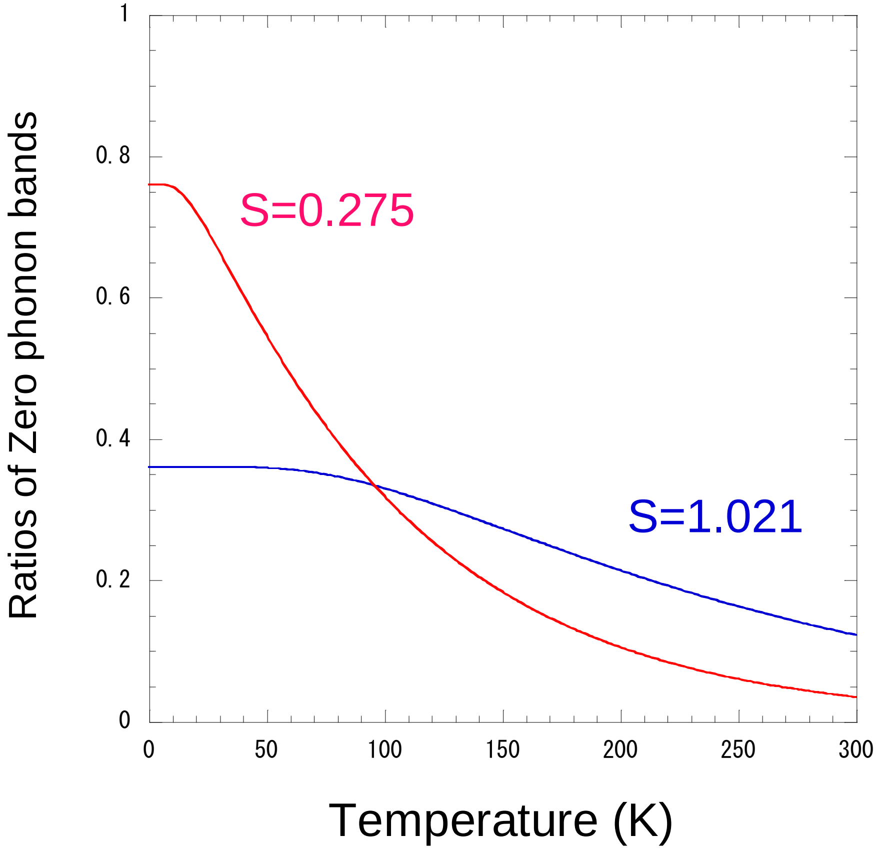

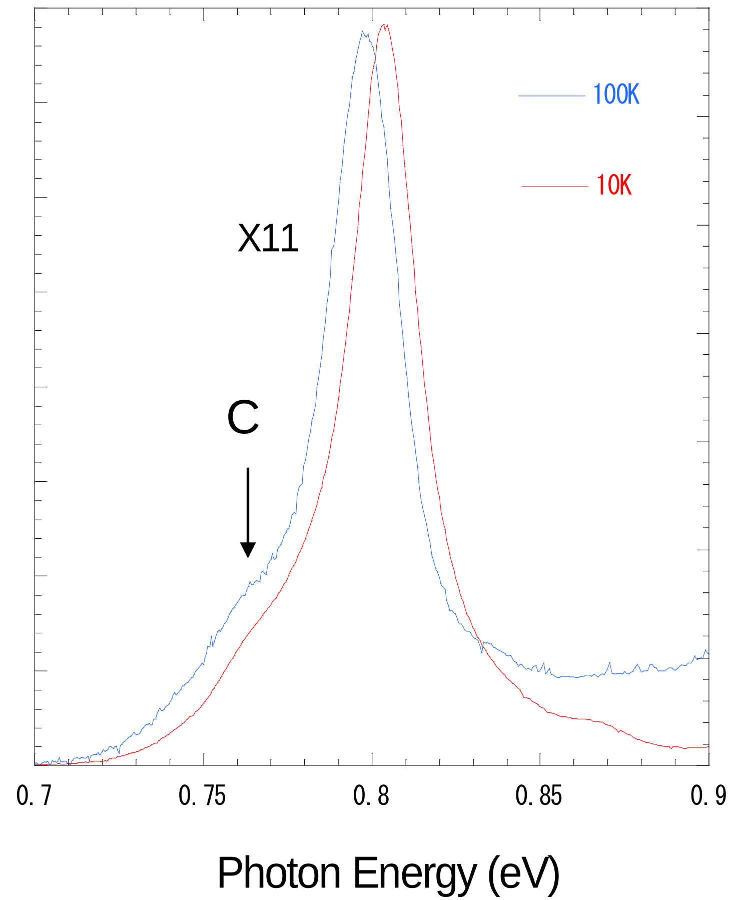

Note Above 100 K, the electron-lattice interaction becomes larger and the S factor also larger, so that contribution of phonon side bands is larger to the radiative process.

Emission spectrum

（Case of Large S）

PL spectrum from β-$FeSi_2$ precipitates

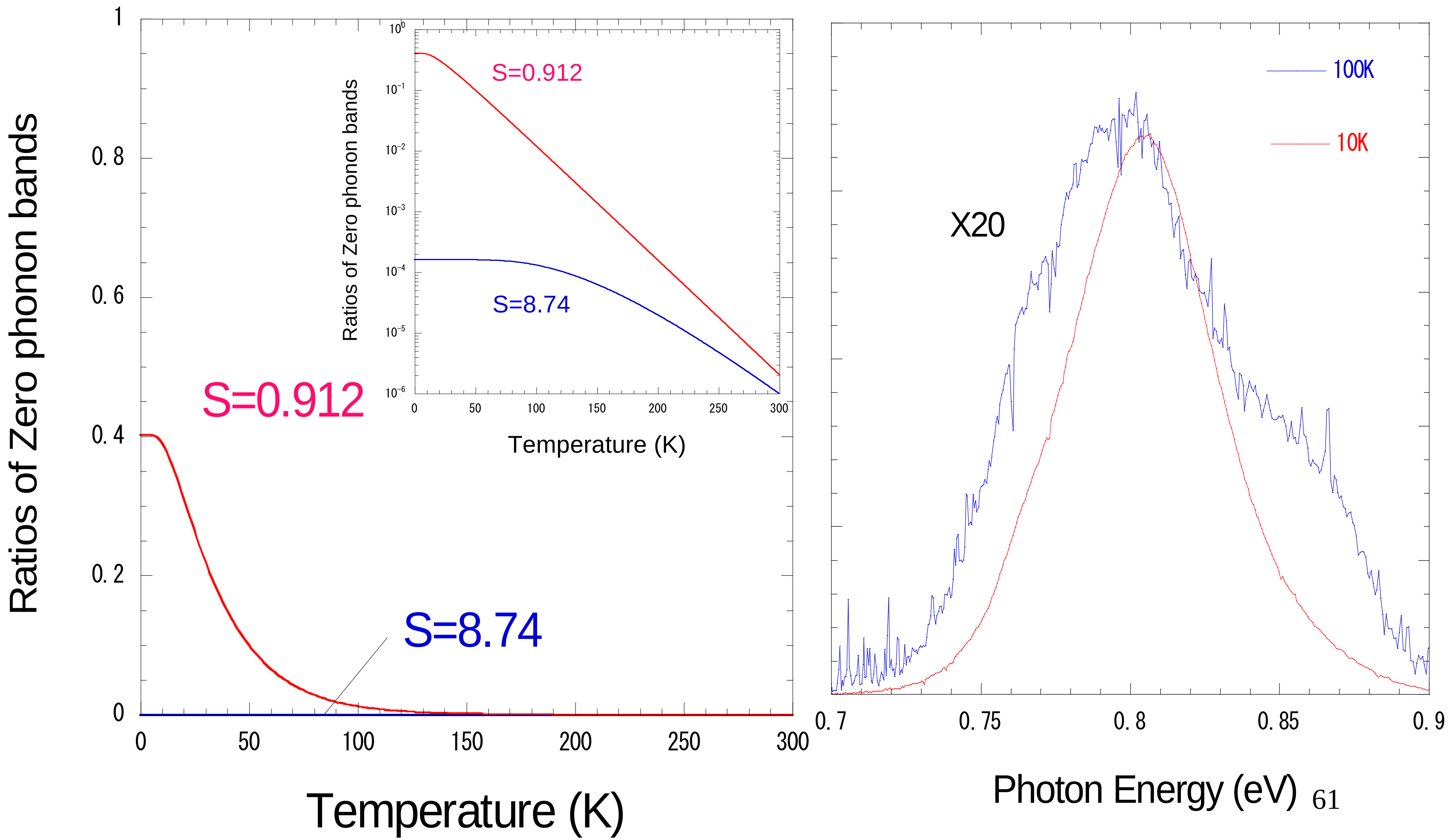

Emission spectra corresponding to S factors

Note : Zero-phonon emission line+Phonon side bands

$$I_{0,n} = e^{-S}\left(\frac{S^n}{n!}\right), \qquad n = 0, 1, 2, \cdots$$

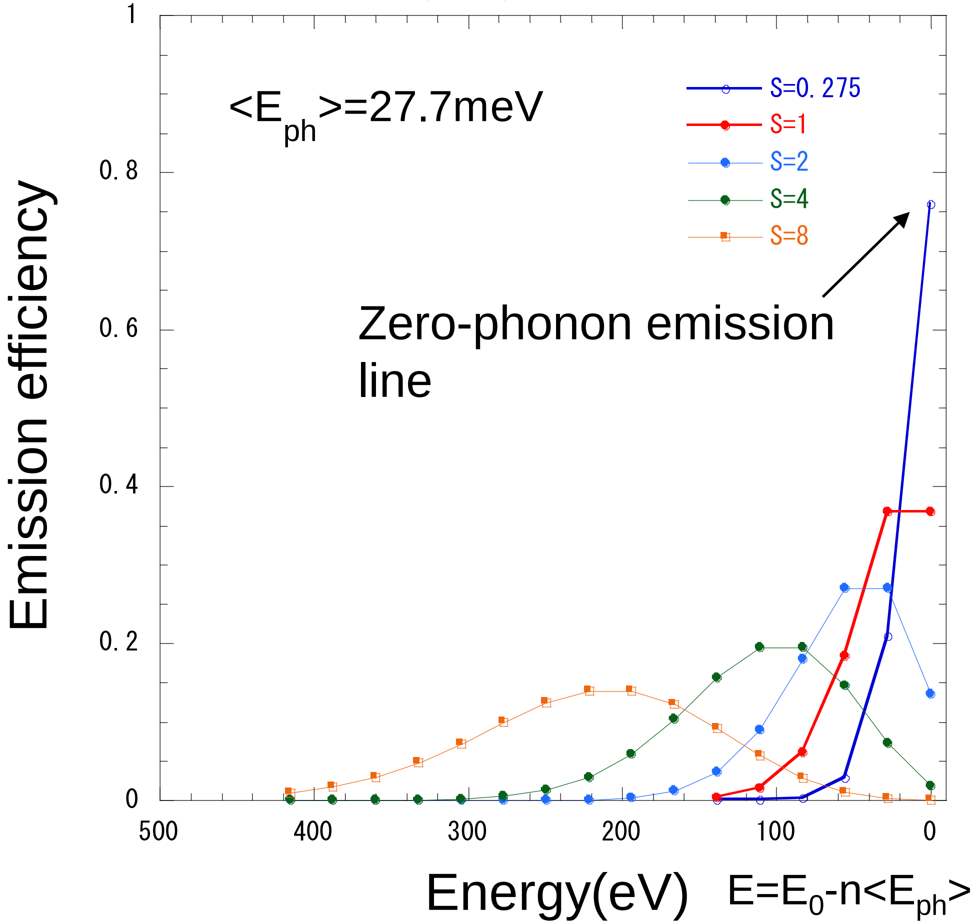

Radiative processes with a large Huang-Rhys factor S indicate

(1) Decease of zero-phonon emission intensity

(2) Red shift of apparent emission peak

(3) Decrease of total emission intensity

(4) Increase of emission band widths

Analysis of spectrum shape

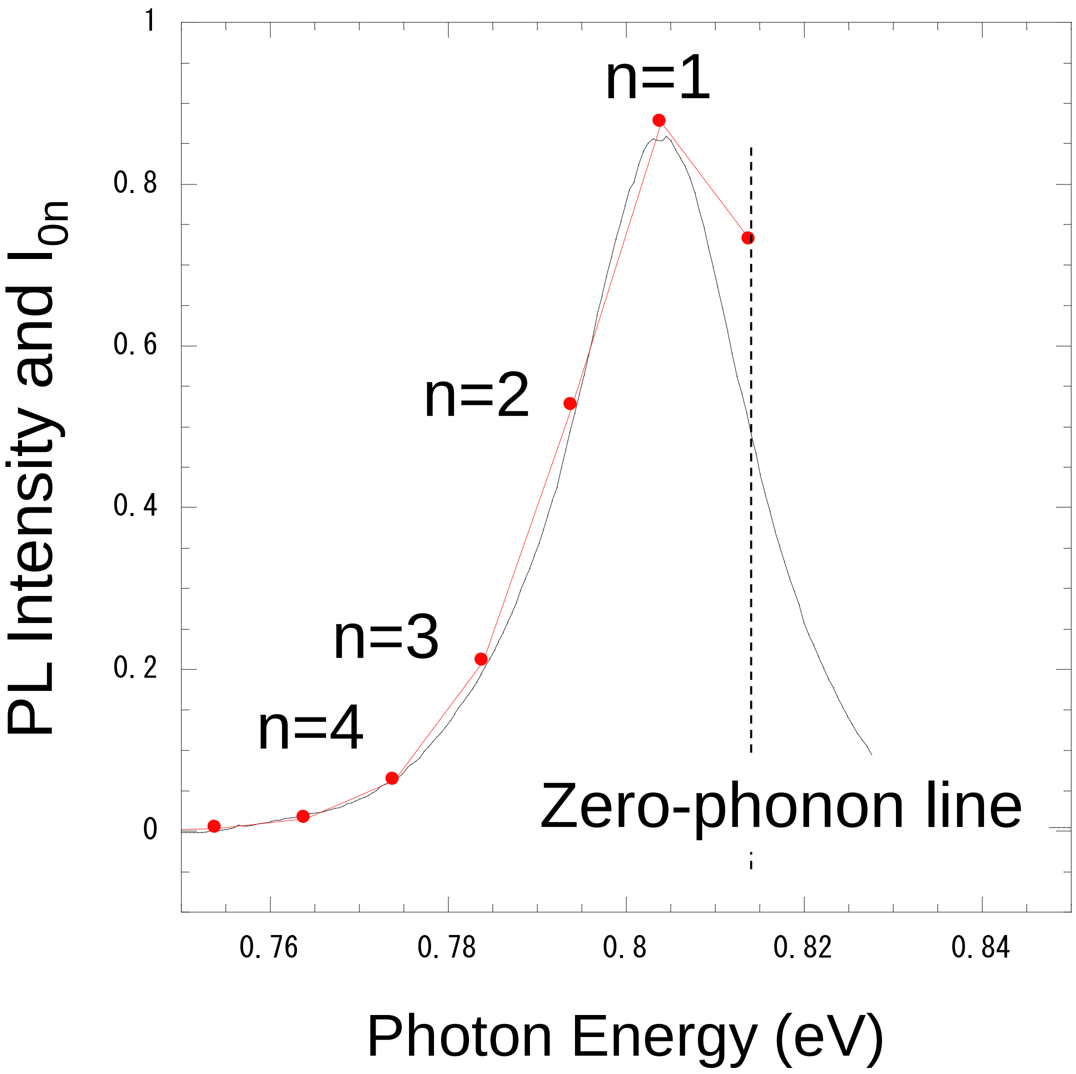

S=1.1

$\langle E_{ph} \rangle$=10meV

The A band emission

=Zero-phonon line

+phonon side bands

at n=1,2,3,4…….

Emission efficiency and S factor

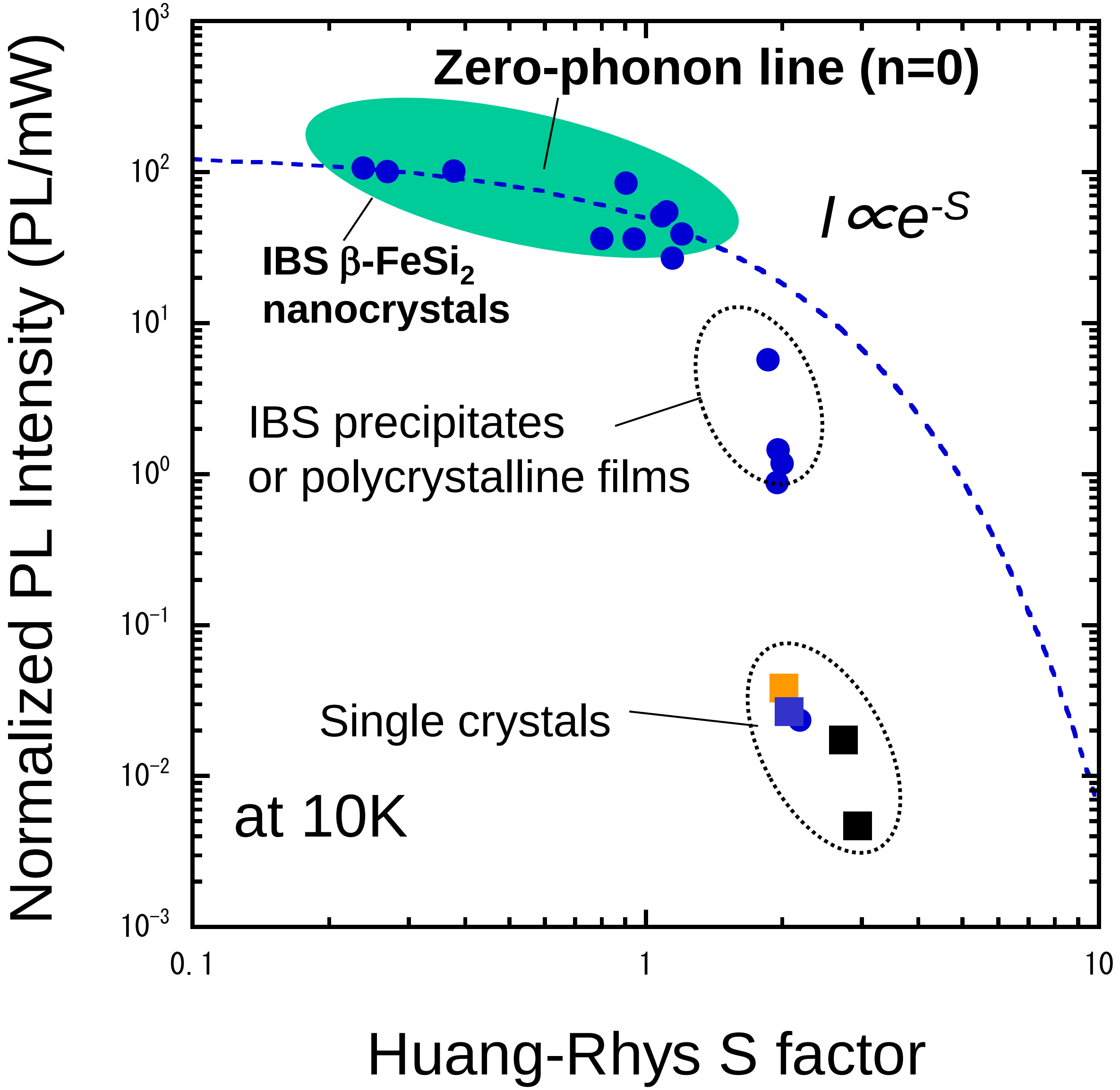

CSSE
Kyusyu Institute of technology

4

Some example of enhancement of PL from β-$FeSi_2$/Si

In this section, we report some cases about how enhancement of the PL intensity from β-$FeSi_2$ crystals has been realized.

Keywords to understand are

Improvement of defective heterointerface,
Si vacancy in the lattice,
and Band-diagram at the heterointerface.

PL enhancement of β-$FeSi_2$ by long hours of annealing

Reduction of interfacial defects and PL enhancement

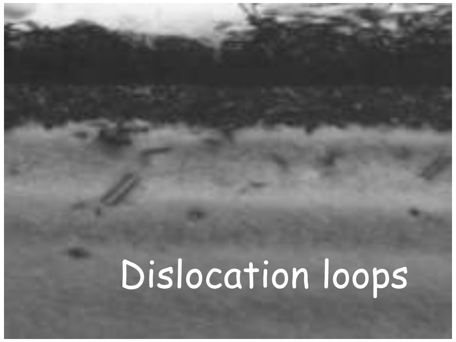

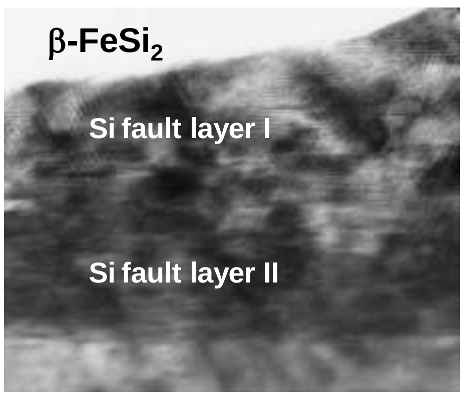

Annealing time: 2 h

Anneal temperature=800°C

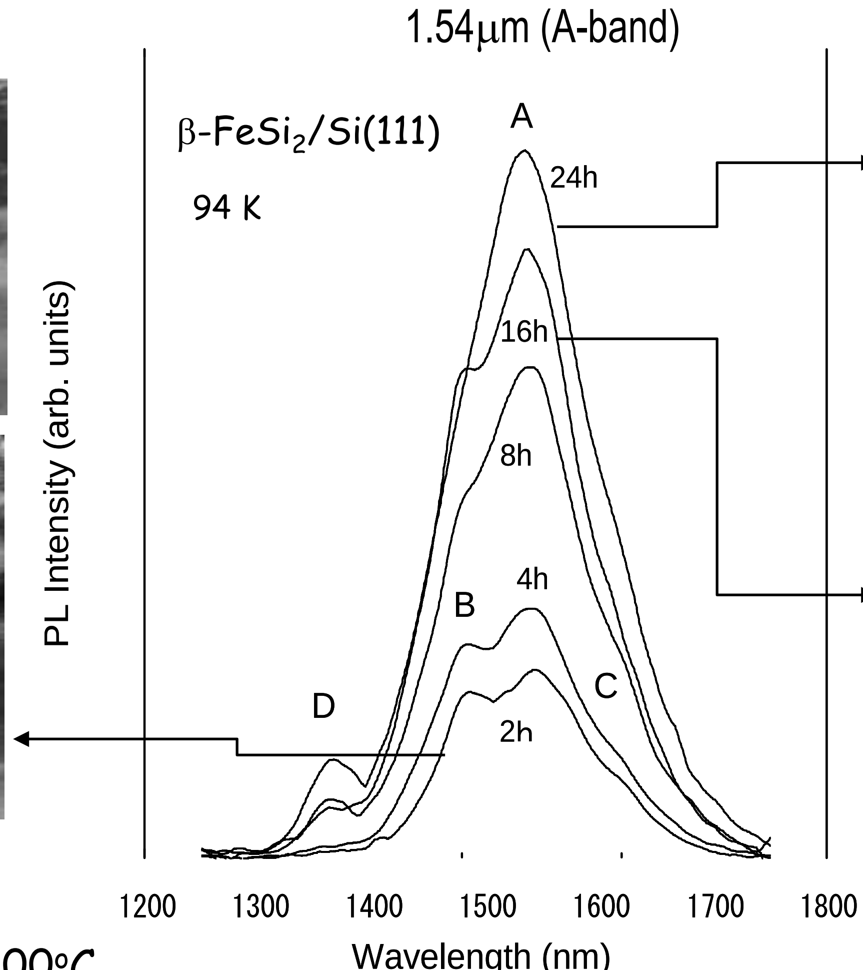

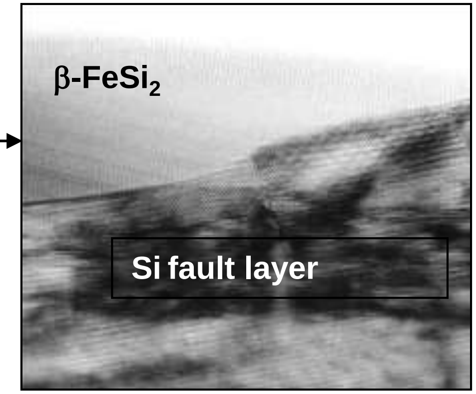

24 h

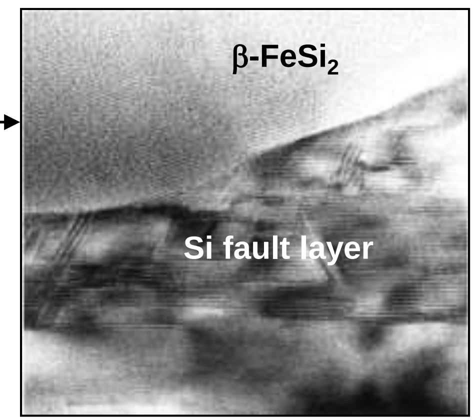

16 h

Y. Maeda et al., Thin Solid Films 461 (2004) 160.

Note In many cases, we need post-annealing at high temperature after deposition in order to obtain high quality crystals. Long hours of annealing is effective to reduce interfacial defects with nonradiative recombination centers and the efficiency of intrinsic PL can be improved.

Photoluminescence spectra affected by interfacial conditions

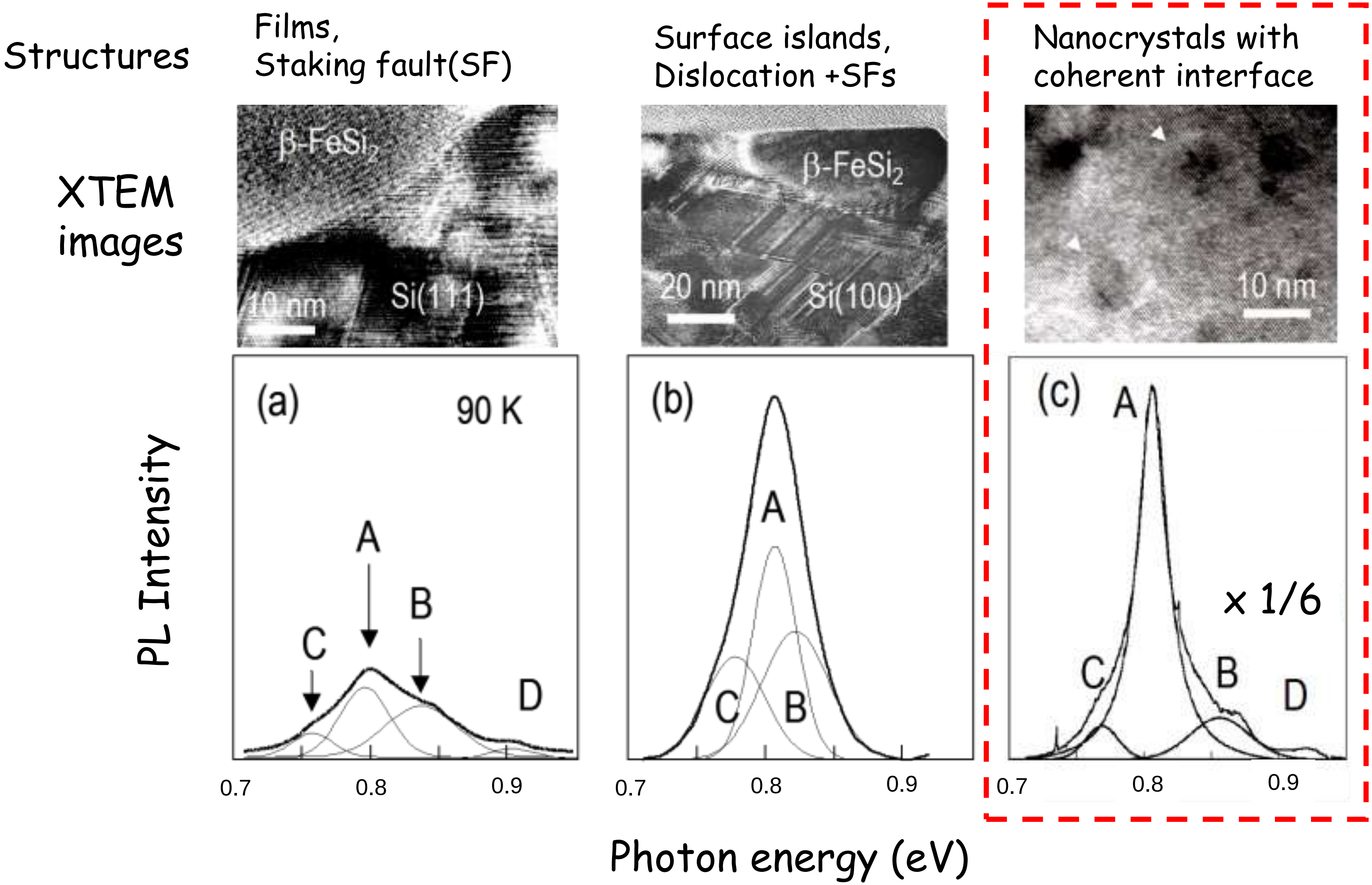

Note

A-band: intrinsic emission from β-$FeSi_2$

B, C-bands: defect-related emission

D-band: Carbon-related emission at the surface.

Importance of coherent Interfaces for luminescence

Coherent interface realized at

β-$FeSi_2$(220),(202)//Si(111)

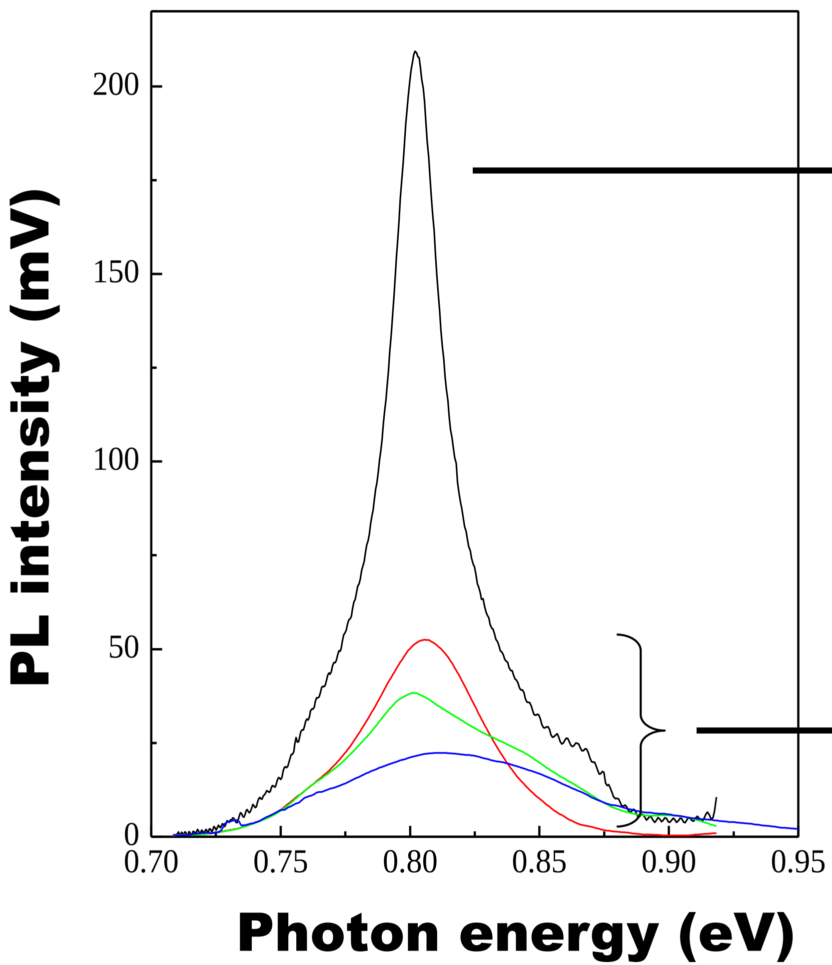

Nanocrystals
Nano-composite phase

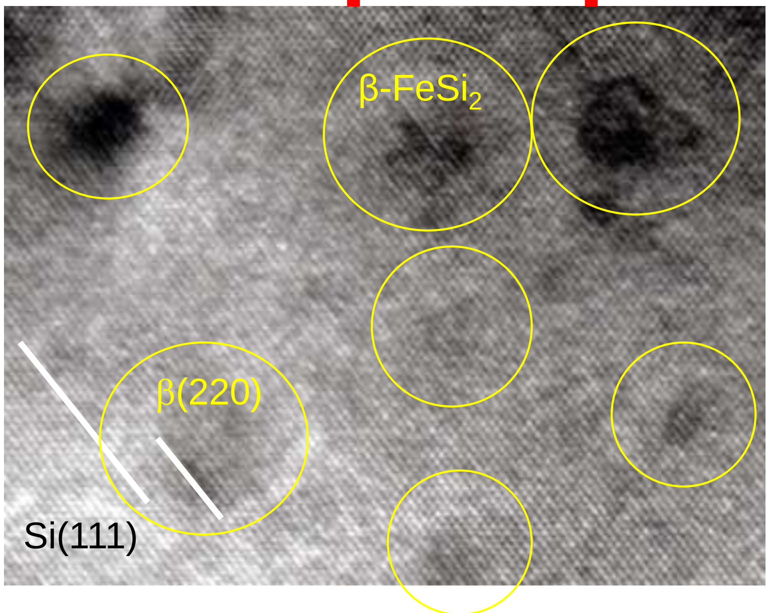

Large size precipitates

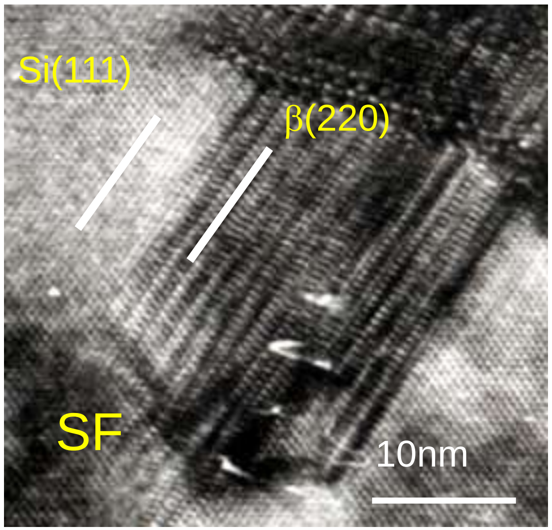

Lattice strains
stacking fault
dislocations

Orthorhombic β-$FeSi_2$: Unit Cell

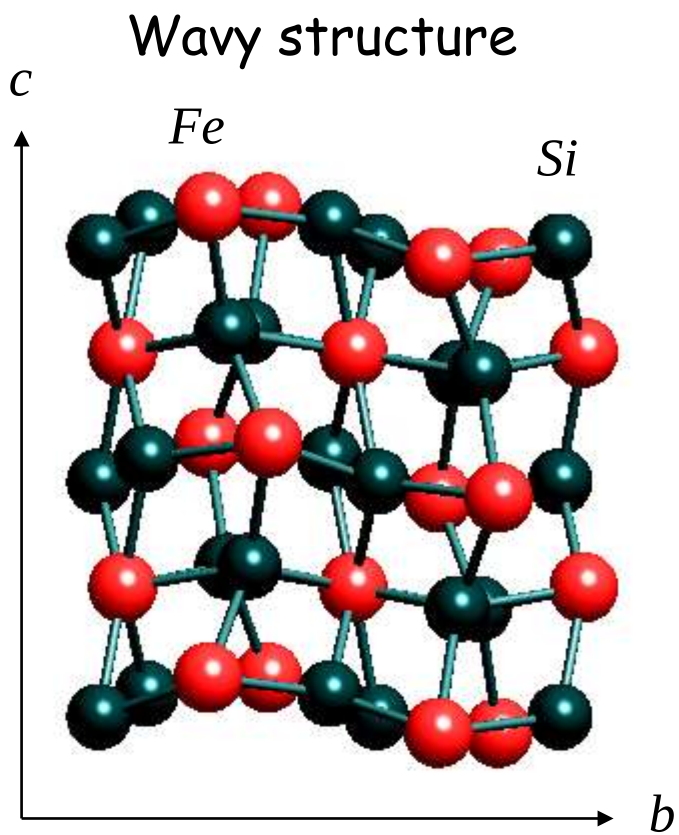

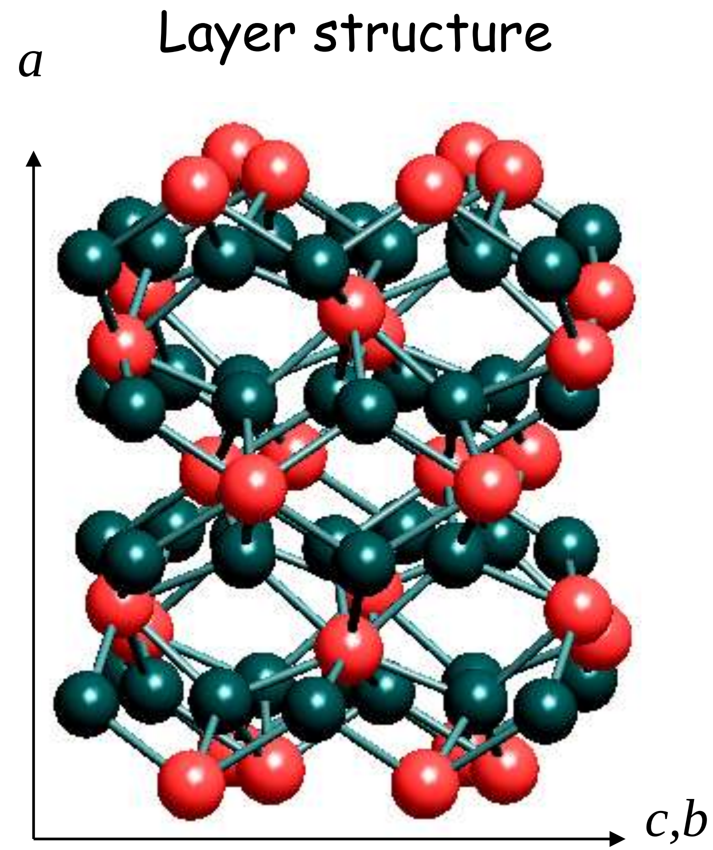

a=9.8792A, b=7.7991A, c=7.8388A
Si a=5.4306A √2xa=7.6789A

Note The lattice structure shows different view on each plain. A formation energy of Si vacancy is smaller than that of Fe vacancy, therefore, a large amount of Si vacancy forms in the lattice.

Enhancement of 1.54 μm photoluminescence observed in Al-doped β-$FeSi_2$

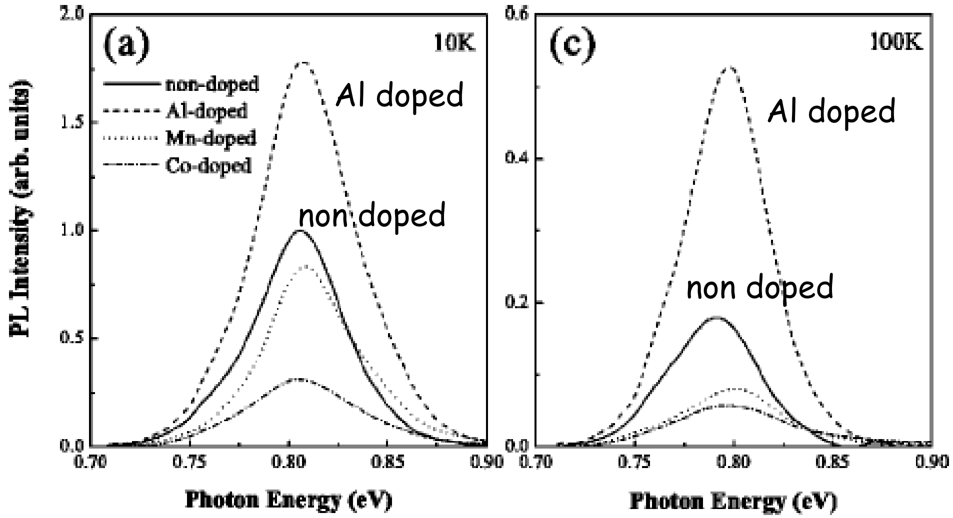

Al doping is very effective to enhance the PL intensity of defective samples.

Al atoms can diffuse inside of β-$FeSi_2$ and occupy Si vacancies, so that the vacancy sites which are nonradiative recombination centers can be reduced much effectively.

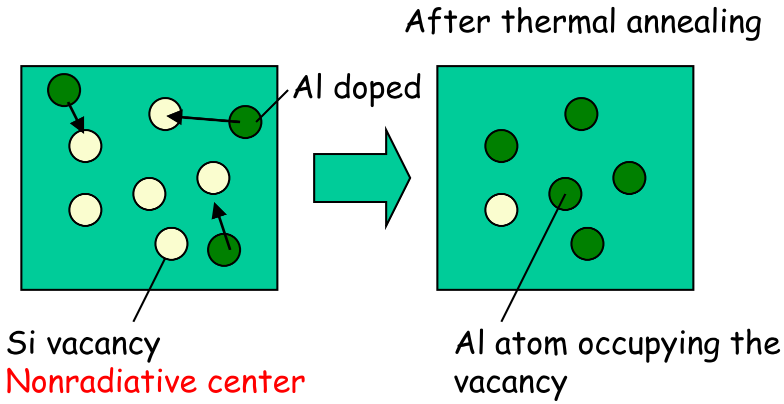

Y. Terai and Y. Maeda, Appl. Phys. Lett. 84 (2004) 903.

β-$FeSi_2$ nanocrystals cases

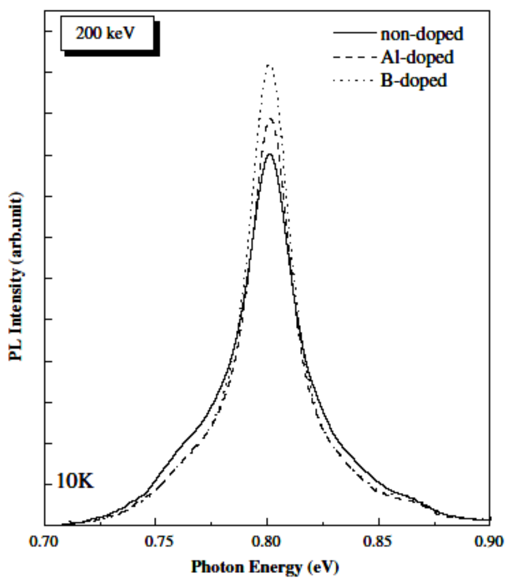

Fig. 3. PL spectra from the doped β-$FeSi_2$ precipitates embedded in Si matrix (200-keV sample). The samples were annealed at 800°C for 8 h.

Al or B doping is not effective for PL enhancement because of less defective structures of nanocrystals.

Y. Terai and Y. Maeda, Optical Materials 27 (2005) 925.

TEM observation of IBS Al-doped β-$FeSi_2$/Si photodiodes

Al doping into IBS β-$FeSi_2$ can enhance epitaxial growth on Si

SF//<111>

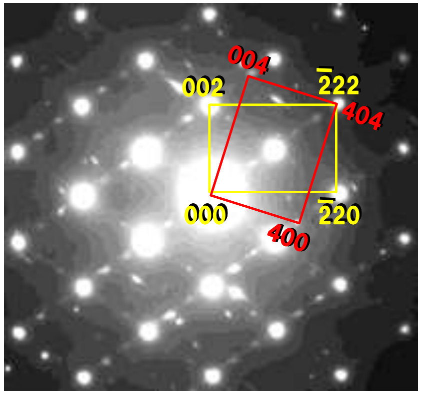

Epitaxial relationships:

β-$FeSi_2$ (101), (110) // Si($\bar{1}$11),
β-$FeSi_2$ [010], [001] // Si[110].

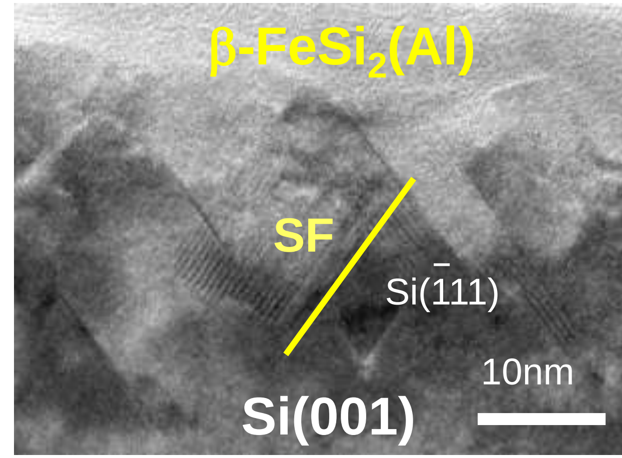

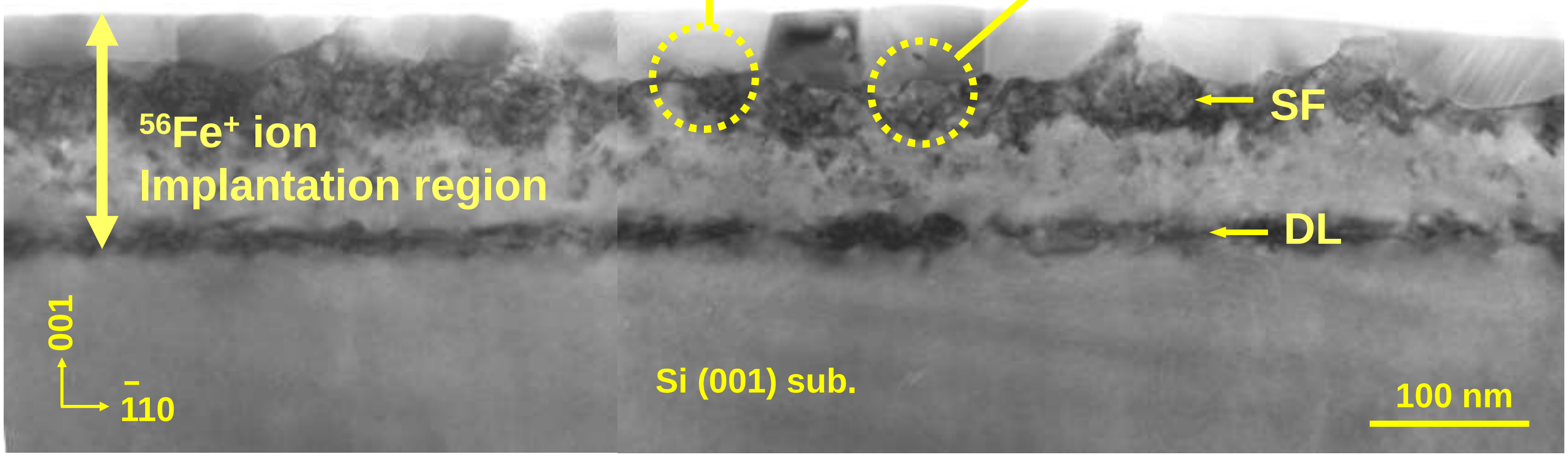

XTEM image (FEI Tecnai F20)

SF: Stacking Fault, DL: Dislocation Loop

after Y. Maeda *et al.*: Jpn. J. Appl. Phys. **44** (2005) 2502.

Improvement of surface morphology with many pin holes by doping Al

(a)Al-doped β-$FeSi_2$

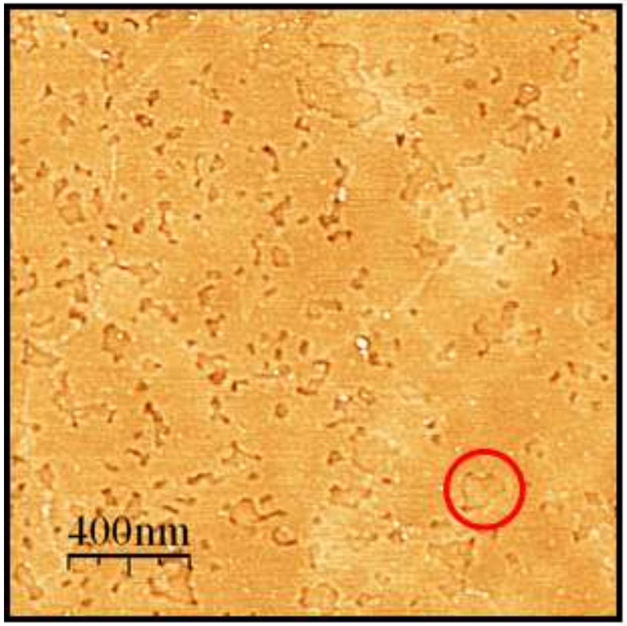

(b) non-doped β-$FeSi_2$

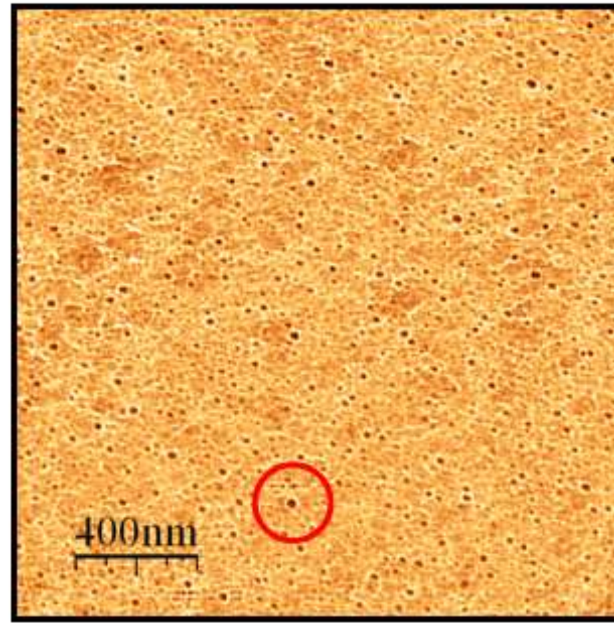

Growth of large grains

Epitaxial interface

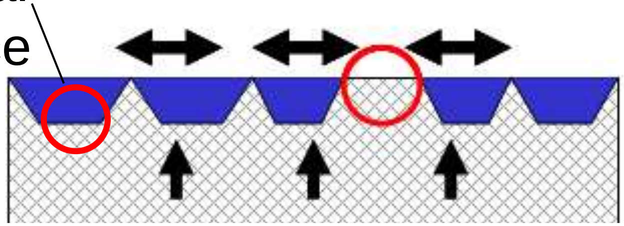

Solid phase epitaxy (SPE) also is enhanced by Al

Growth of fine grains with small pinholes

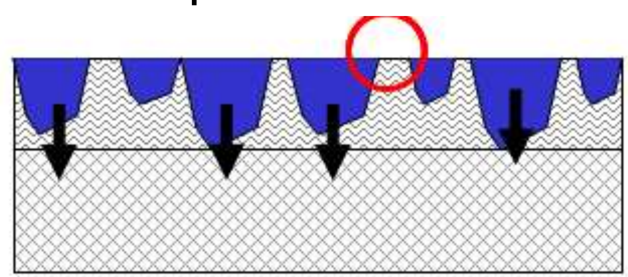

Photoluminescence from CVD β-$FeSi_2$ films highly oriented on Si substrates

β -$FeSi_2$(100)//Si(100)

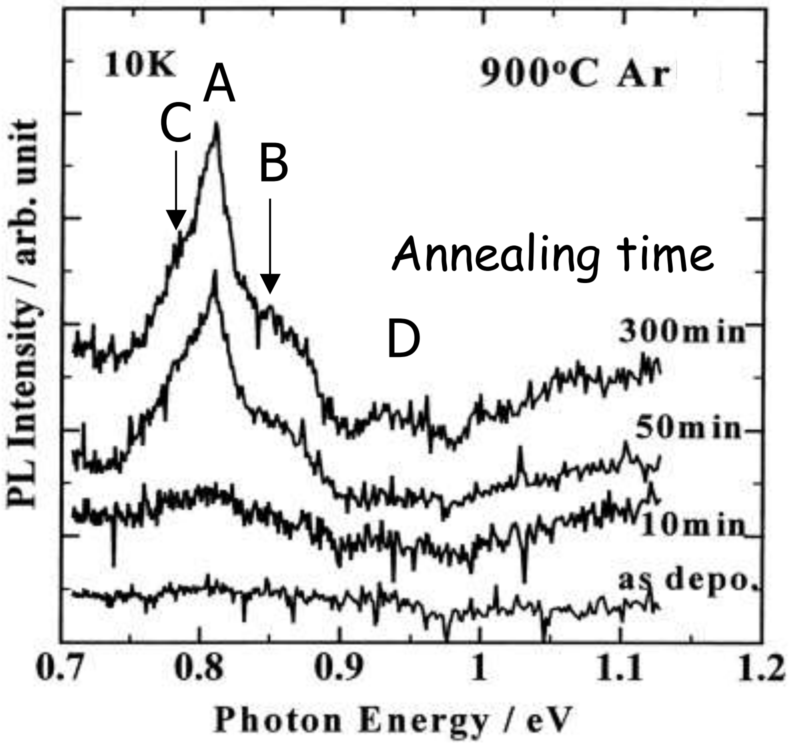

β -$FeSi_2$(101)//Si(111)

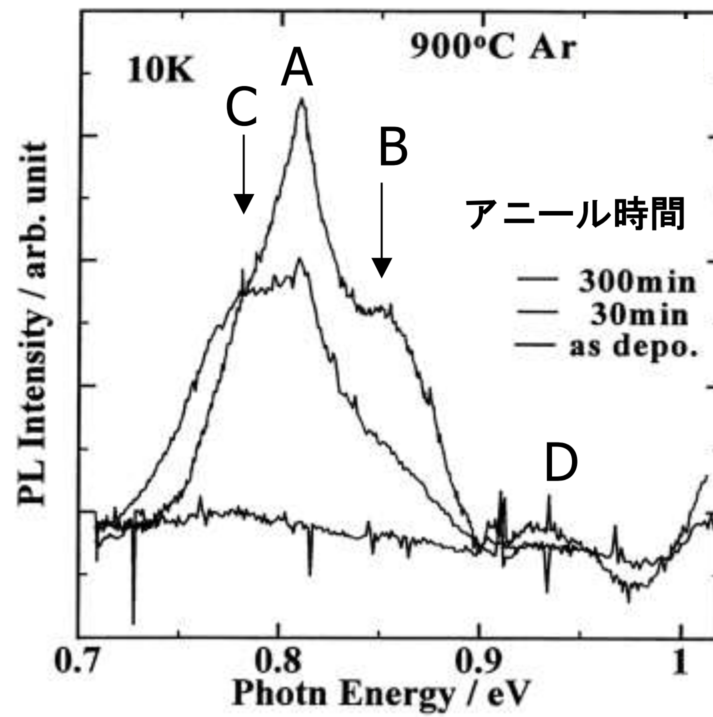

after K. Akiyama, PhD. Thesis (Tokyo Tech.)

1.54 μm photoluminescence from β-$FeSi_2$ as-deposited film

β-$FeSi_2$ films grown on the Cu mediated surface can emit 1.54μm light without any annealing at high temperature. This is the first PL observation from the as-deposited films. This shows importance of interfacial quality for luminescent processes.

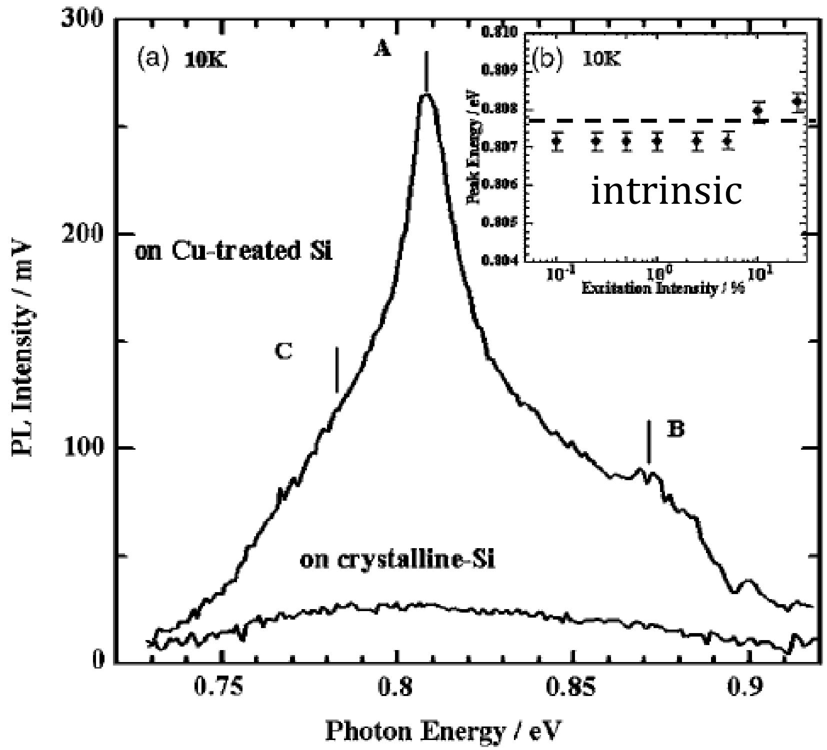

K. Akiyama, Appl. Phys. Lett. 91 (2007) 71903.

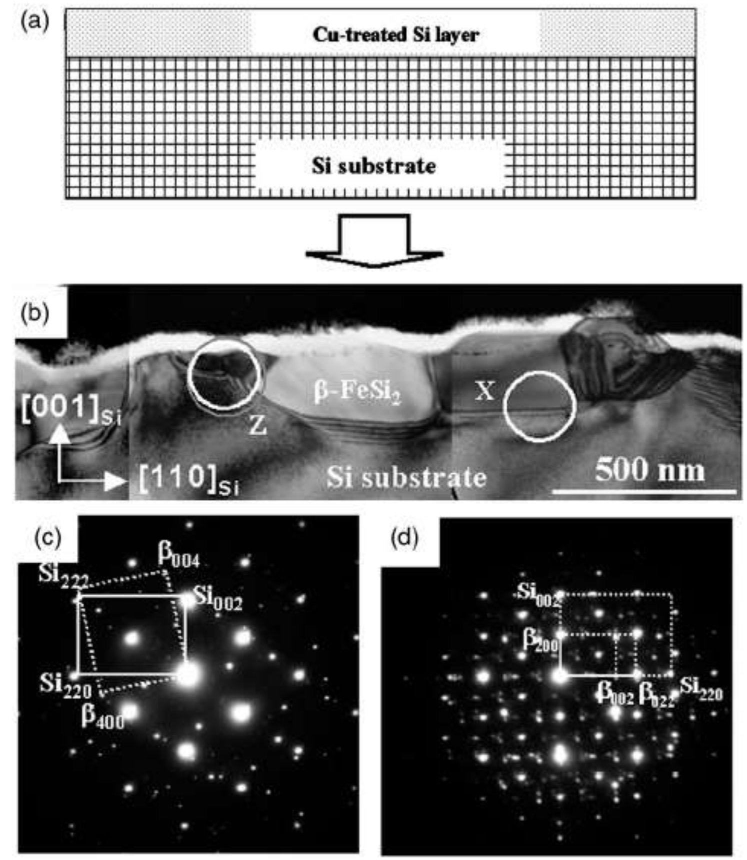

Coherent interfaces between β-$FeSi_2$ grains and Si can be grown.

PL enhancement by isolating β-$FeSi_2$ layers from implantation damage layers

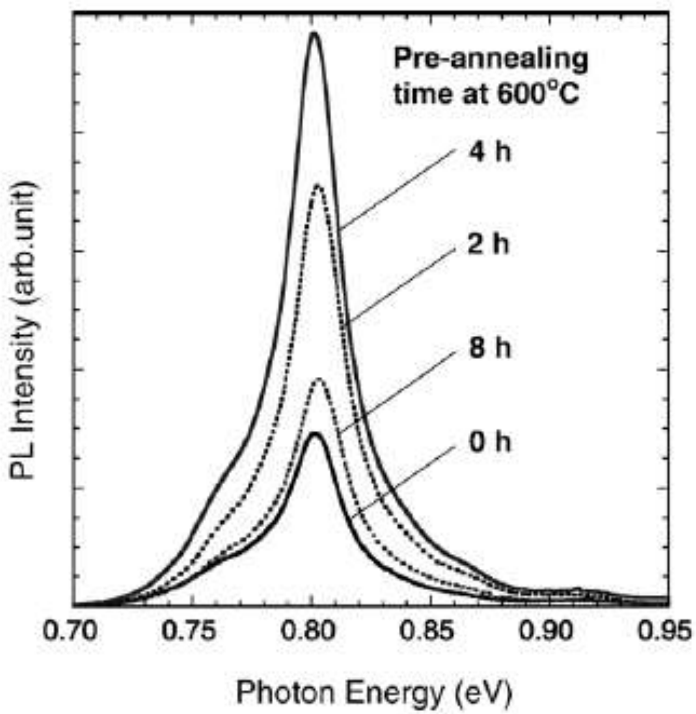

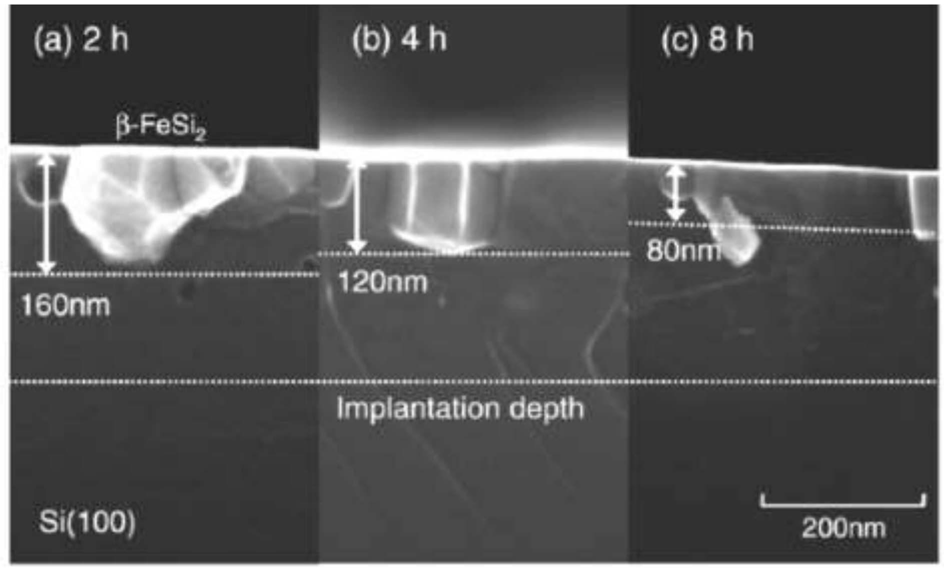

too thin

Nonradiative recombination at the interface can be eliminated.

Surface nonradiative recombination affects a PL efficiency.

The pre-annealing at 600°C is very effective to cause surface segregation of Fe atoms implanted deeply into Si substrates and β-$FeSi_2$ precipitates at the surface where is isolated from implantation damage layers. The best case of pre-annealing for PL enhancement was 4 h.

Y. Ando et al., Thin Solid Films 515 (2007) 8133.

Radiative and nonradiative recombinations in IBS samples

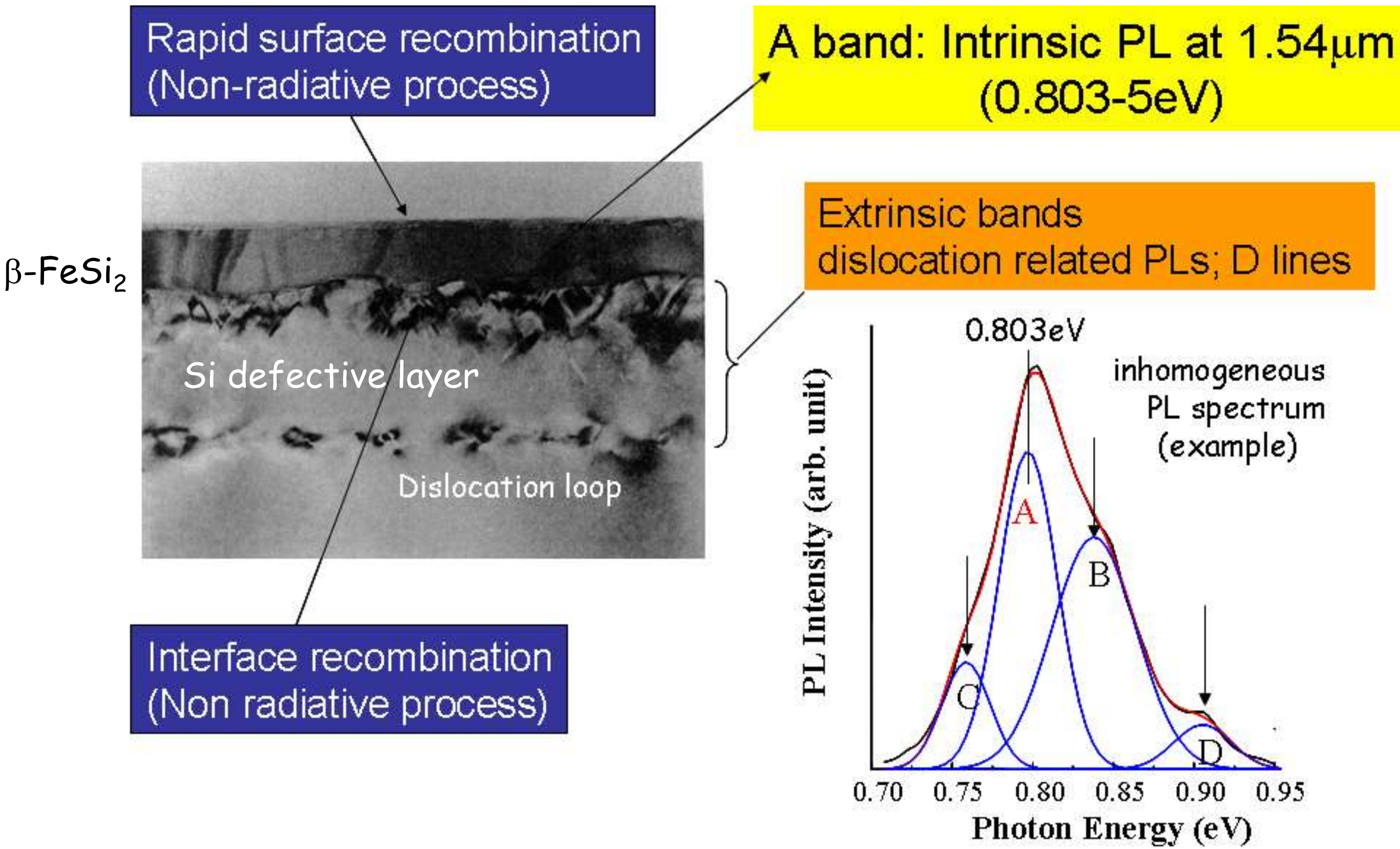

The usual IBS samples with incoherent interfaces and dislocation loops in initial damage layers show inhomogeneous PL spectra, where the A band PL has some defect-related bands around it. The A band PL can be increased by reducing nonradiative processes at the surface and the incoherent interface. This situation has confused correct understanding of nature of the intrinsic luminescence.

Dislocation free PL spectrum in IBS samples

(Y. Gao *et al.*: Appl. Phys. Lett. **83** (2003) 42.)

PL spectra obtained from IBS samples with no dislocation loops which result in D-line emissions.

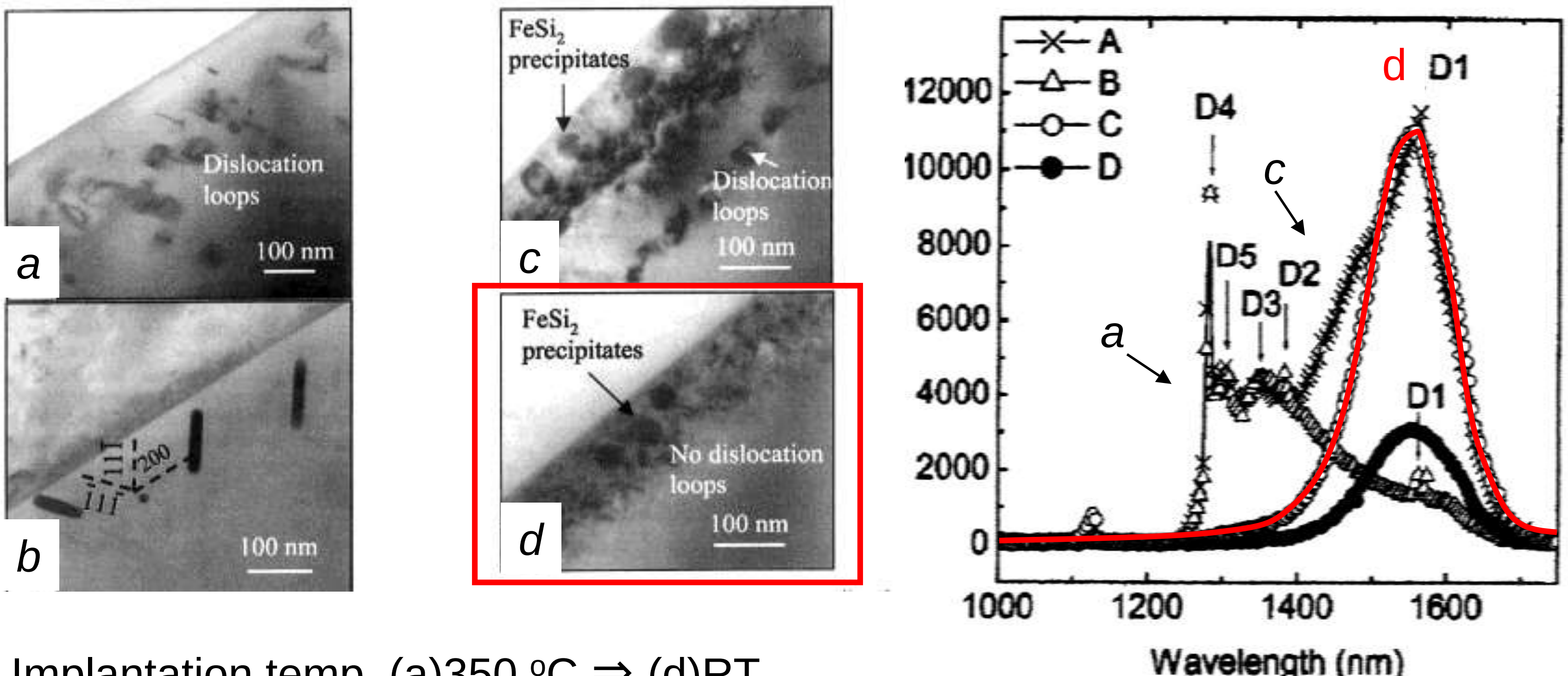

Implantation temp. (a)350 °C ⇒ (d)RT

Prof. Wang's group found the IBS process where dislocation loops (DL) did not form in Si substrates. They observed the intrinsic PL (red line) from b-$FeSi_2$ precipitates under much less influence of DLs. It is easy to see a complicated situation where both PLs overlap each other at the same energy region.

Introduction

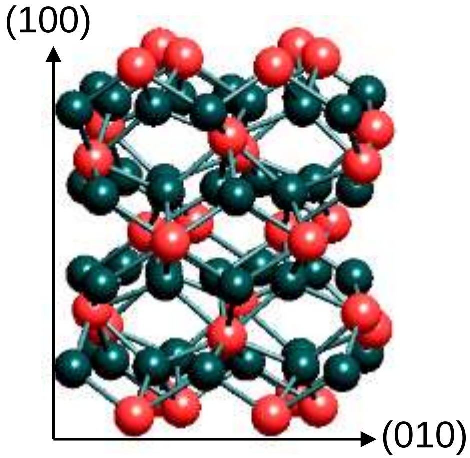

Semiconducting β-$FeSi_2$

IR light emission at the telecom wavelength, 1.55 μm

Large Optical absorption >10^5 cm^{-1}

Epitaxial growth on Si substrates

Optimal for applications to infrared optoelectronics and photonics

β-$FeSi_2$ nanocrystals (NCs) for IR light emitting*

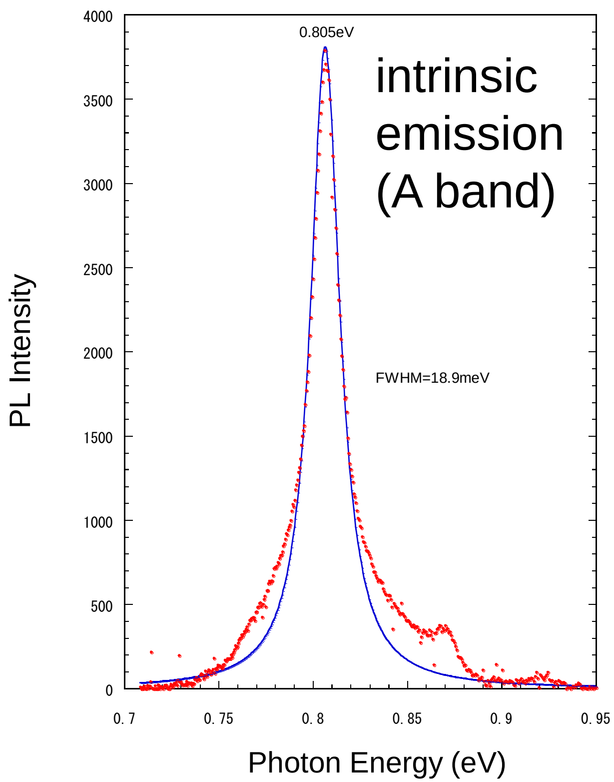

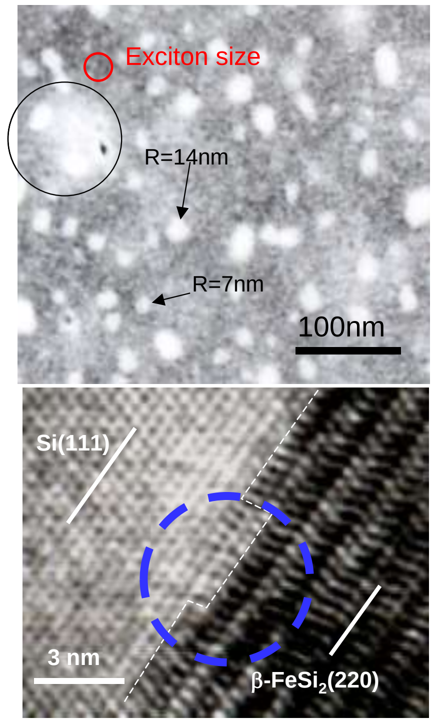

Strong intrinsic light emission observed from the exciton sized β-NCs embedded in Si.

The heterointerface was partially coherent and included some defective structures because of lattice mismatch with Si. These defects may control the efficiency of light emission.

*Y. Maeda: Appl. Surf. Sci. **254** (2008) 6242.

PL enhancement observed in Cu-doped β-NCs/Si nano-composite phase

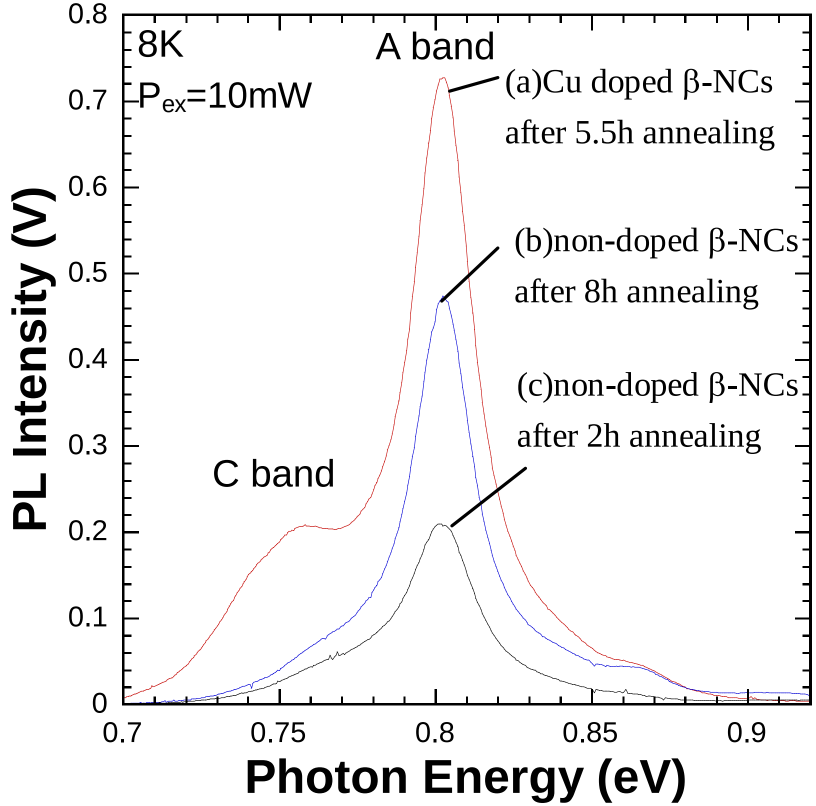

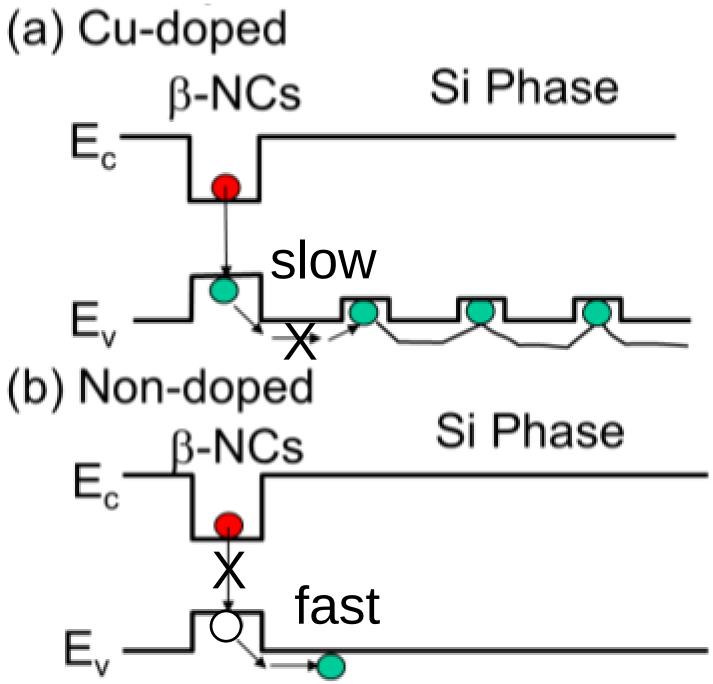

Note Dynamics of positive holes going out from β-NCs before radiative recombination dominates light emission efficiency. Cu in Si forms shallow traps of holes, so that transport rate of holes should be controlled by the repeated trap process. This dynamics may contribute to the PL enhancement.

Y. Maeda et al., Phys. Stat, Sol. (c) (2014) (in press). (E-MRS Proc. 2014 Spring)

Phys. Status Solidi C **9**, No. 10–11, 1888–1891 (2012) / **DOI** 10.1002/pssc.201200072

physica status solidi c
www.pss-c.com
current topics in solid state physics

Enhancement of IR light emission from β-$FeSi_2$ nanocrystals embedded in Si

Note The γ-β phase transition can be applied to enhancement of PL intensity.

Yoshihito Maeda[*,1], Kentaro Nishimura[1], Takahito Nakajima[1], Bui Matsukura[1], Kazumasa Narumi[2], and Seiji Sakai[2]

[1] School of Energy Science, Kyoto University, Sakyo-ku, Kyoto 606-8501, Japan
[2] Advanced Science Research Center, Japan Atomic Energy Agency, Tokai, Ibaraki 319-1195, Japan

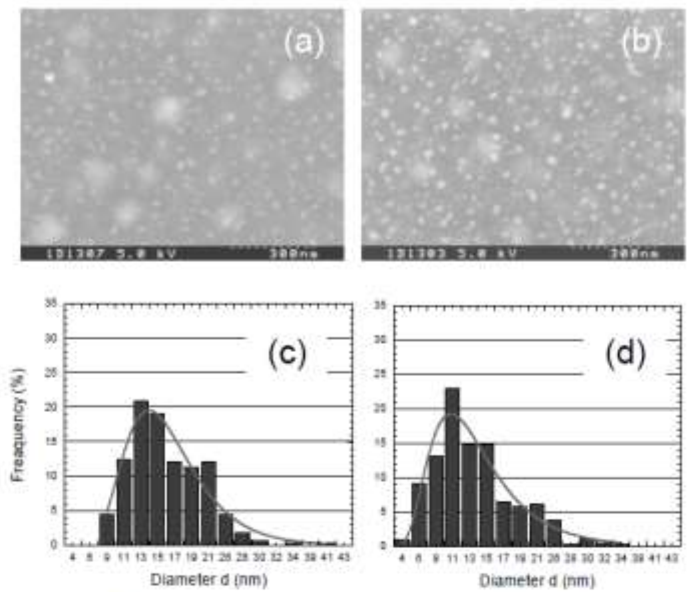

Figure 2 SEM images of β-nanocrystals precipitated in a Si matrix after (a) usual annealing at 800 °C for 2 h and (b) that at 400 °C for 4 h and 800 °C for 2 h. The size profiles are shown in (c) and (d) corresponding to the images (a) and (b), respectively. The profiles can be fitted by a logarithm Gaussian function.

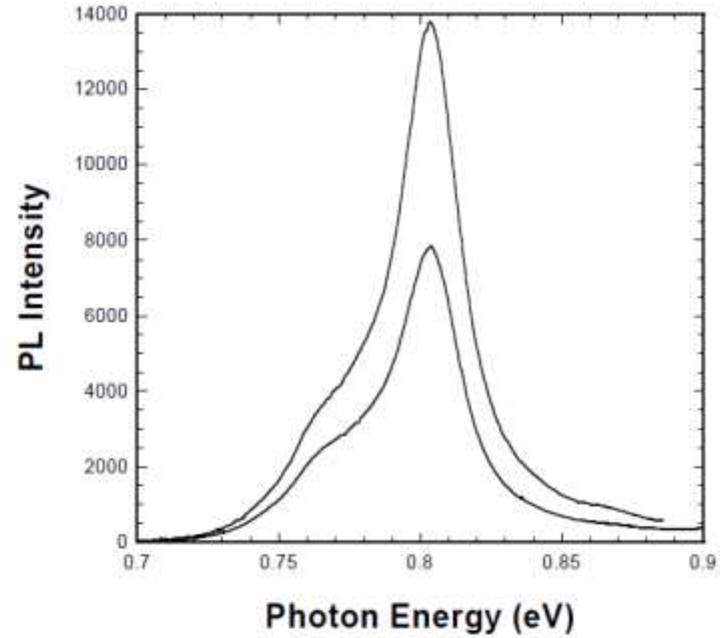

Figure 5 Enhancement of PL intensity by increasing the postannealing time from 2 h to 6 h. The preannealing time at 400 °C was 16 h. The optical gain of PL was improved from 1.25 to 2.1.

Why we focus on the γ-$FeSi_2$?

β-$FeSi_2$ nanocrystal (NC) formation by direct silicidation

ion implanted Fe + Si substrate->Silicidation $Fe+2Si=FeSi_2$->growth of β-NC

Light emission efficiency is controlled by interface defects

Crystallographic relation between γ-$FeSi_2$ and β-$FeSi_2$

metastable
CaF_2 structure
cF12
a=0.5431nm~Si

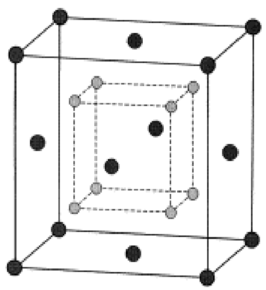

γ-β phase transition

above 600°C

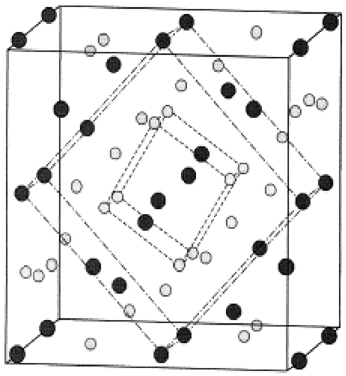

Cmca
a=0.9865nm
b=0.7791nm
c=0.7833nm

G. Shao, This Solid Films **519 (2011) 8446.*

After the transition, the following plane relationship can be maintained.

β(202),(220)//γ(111)//Si(111)

Our idea, Toward enhancement of the light emission efficiency, we employ the phase transition to improve the interface between β-NC and Si

In this study, we have investigated photoluminescence properties of the β-NCs which are formed by controlling the phase transition

Experiments

β-NCs preparations

High purity crystal growth by
Ion beam synthesis (IBS)

Ion implantation
Energy: 200keV, Dose : 10^{17}ions/cm^{-2}
Substrate: CZ-Si(100)
Post anneal
Double annealing process by RTA
(Rapid Thermal Annealing) in a vacuum.

Measurements

Structural observations
SEM, RBS
Optical measurements
Infrared photoluminescence (PL)
detected by LN_2 cooled Ge PIN PDs
Infrared reflection measurements

Fe channel RBS spectrum

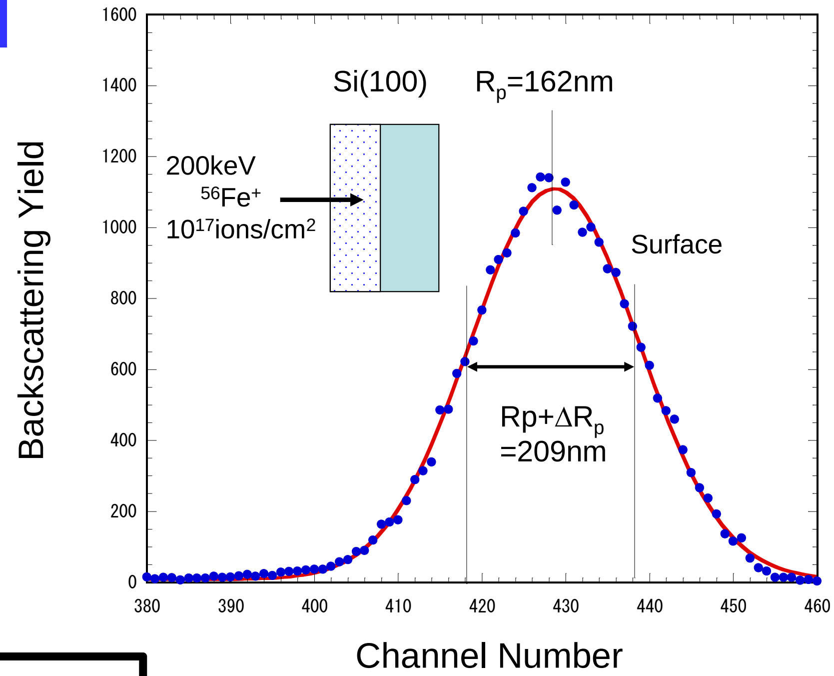

Profile of double annealing

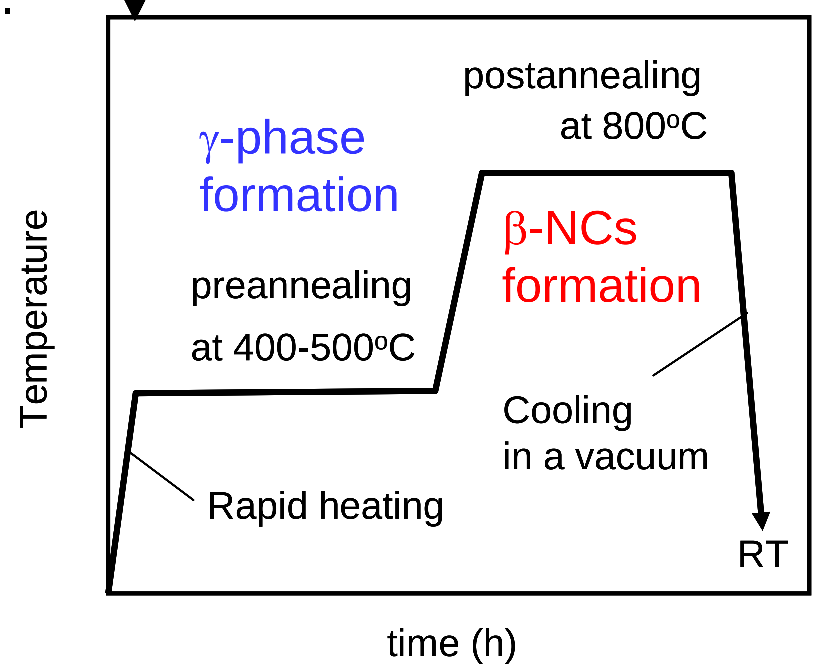

Toward enhancement of PL by controlling growth of β-$FeSi_2$ on Si(111)

Thin films or Precipitates	β-NCs
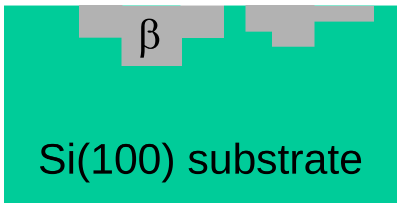	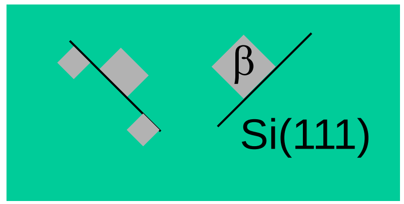

β(100)//Si(001)
δ=1.5~2.1%
	β(101),(110)//Si(111)
	δ=1.45~2.0%

IBS conditions	
Shallow implantation (E<100keV)	Deep implantation (E~200keV)
Thermal anneal	
Temp.<600-800°C	Temp.>750°C
PL properties	
Weak & broad peaks with defect related emissions	Strong & sharp peak (Intrinsic A band)

New steps process

First step
Precipitation of γ-phase with epitaxy on Si(111) below 500°C.

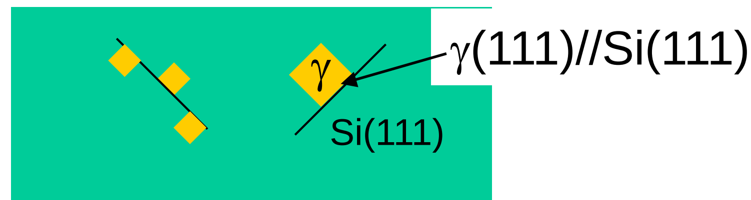

Second step
γ->β phase transition with epitaxy at 800°C

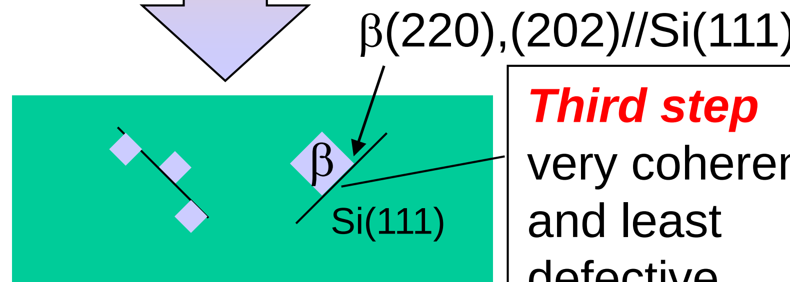

Third step
very coherent and least defective interfaces

*Theoretically, less defective interfaces were realized on β(202),(220)//Si(111).

Structures , Sizes, Phonon properties of β-NCs in Si

Single annealing at 800ºC

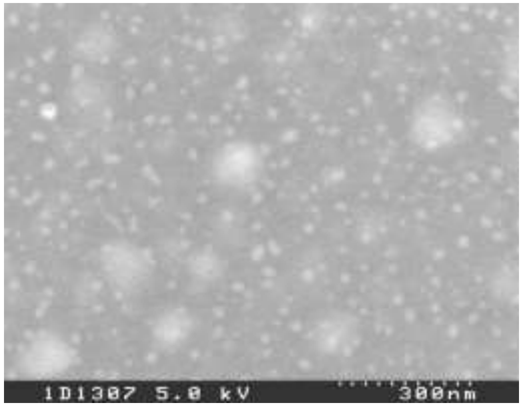

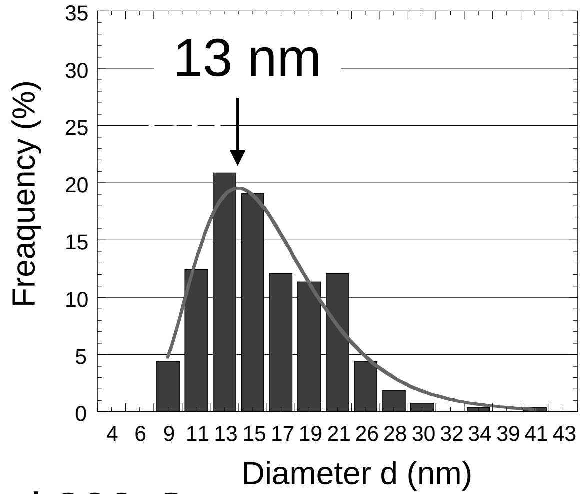

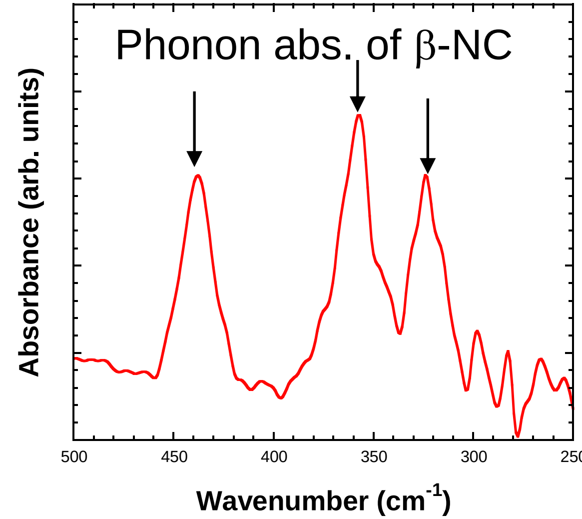

Double anneling at 400ºC and 800ºC

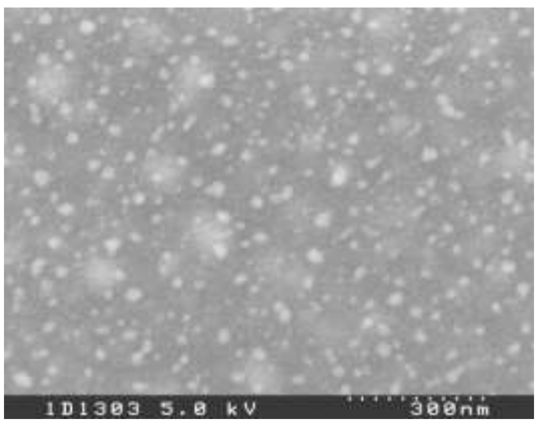

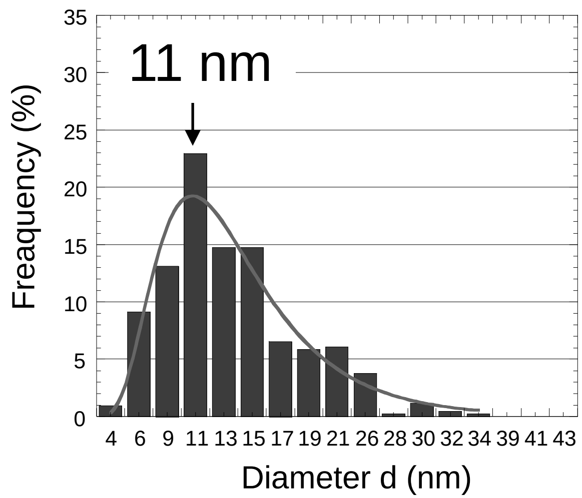

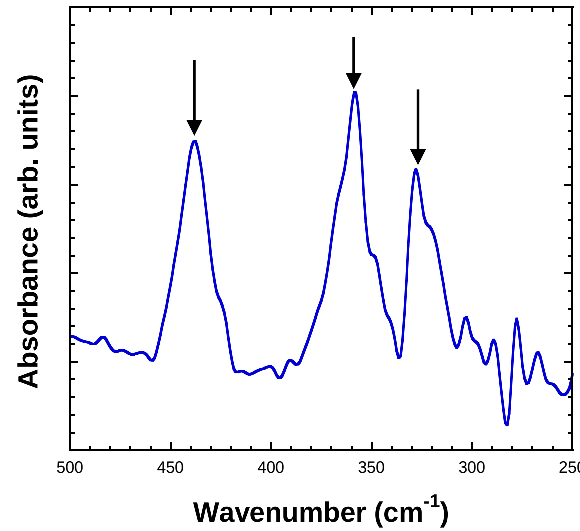

We confirmed that morphology of β-NCs formed in Si and their phonon properties showed no large differences in both annealing cases, ***except for size decrease***.

Photoluminescence spectra of β-NCs embedded in Si

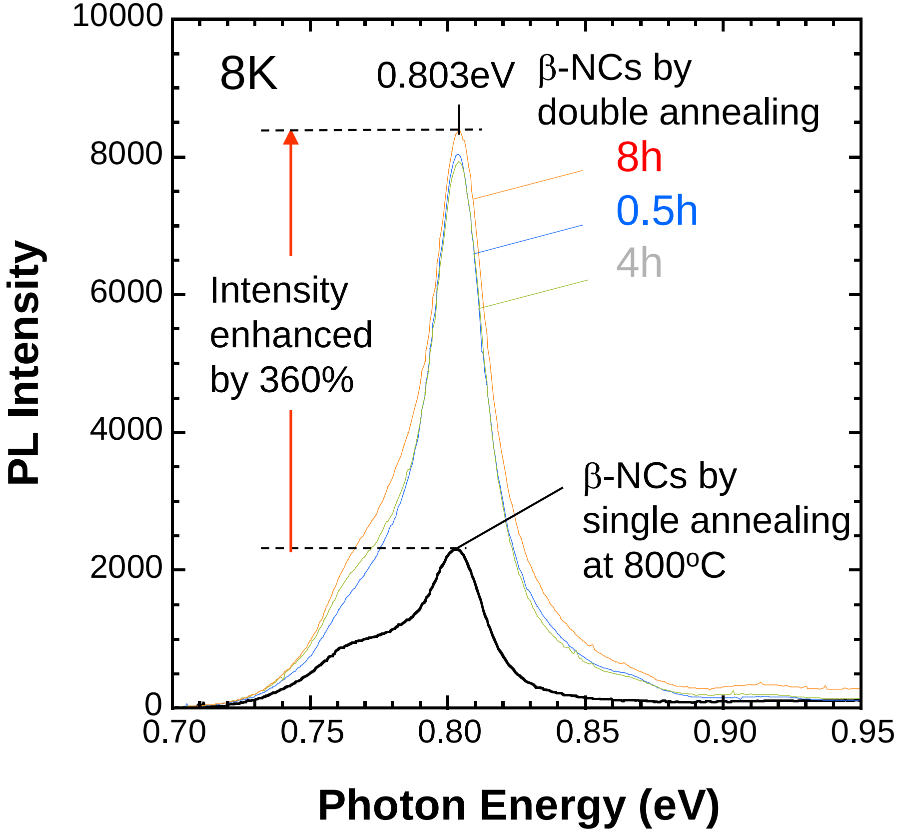

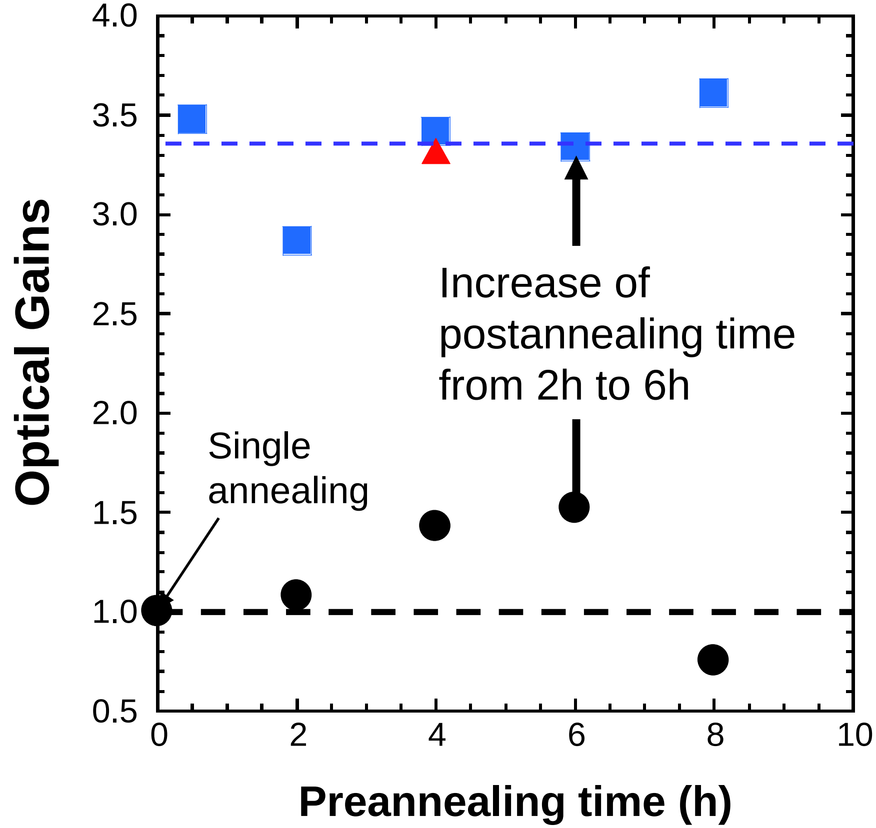

Comparison of PL intensities between β-NCs formed by single annealing and by double annealing. We observed 360% enhancement of PL peak intensity in the maximum.

Enhancement of PL intensity (optical gain) depended on the time of postannealing at 800ºC, where the phase transition to β-NCs was enhanced.

We confirmed that ***β–NCs formed by the phase transition have higher efficiency of light emission*** than β-NCs directly formed by silicidation.

Discussion

Possible reasons of the PL enhancement,

(1) Change of phonon states adapting a radiative indirect transition?

Answer NO! because of no change in phonon states.

(2) Realization of coherent interface between the β-NCs and Si?

Answer. Possible! because of epitaxy among β-, γ-phases and Si can be maintained even after the γ->β phase transition.

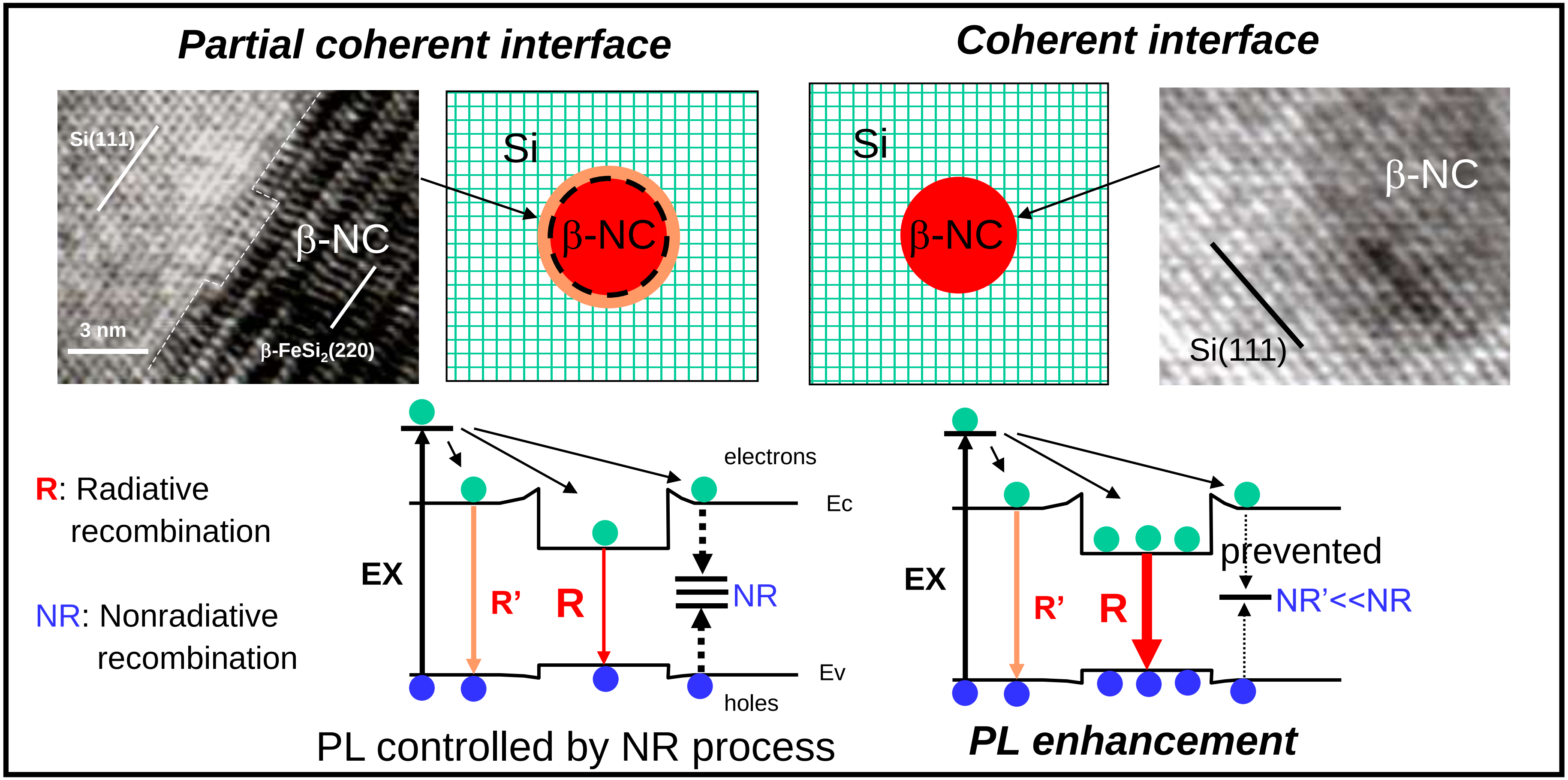

Phys. Status Solidi C 9, No. 10–11, 1884–1887 (2012) / **DOI** 10.1002/pssc.201200058

physica status solidi c
www.pss-c.com
current topics in solid state physics

Photoluminescence properties of carbon-doped β-$FeSi_2$ nanocrystals

Yoshihito Maeda[*,1], **Kentaro Nishimura**[1], **Takahito Nakajima**[1], **Bui Matsukura**[1], **Kazumasa Narumi**[2], **and Seiji Sakai**[2]

[1] School of Energy Science, Kyoto University, Sakyo-ku, Kyoto 606-8501, Japan
[2] Advanced Science Research Center, Japan Atomic Energy Agency, Tokai, Ibaraki 319-1195, Japan

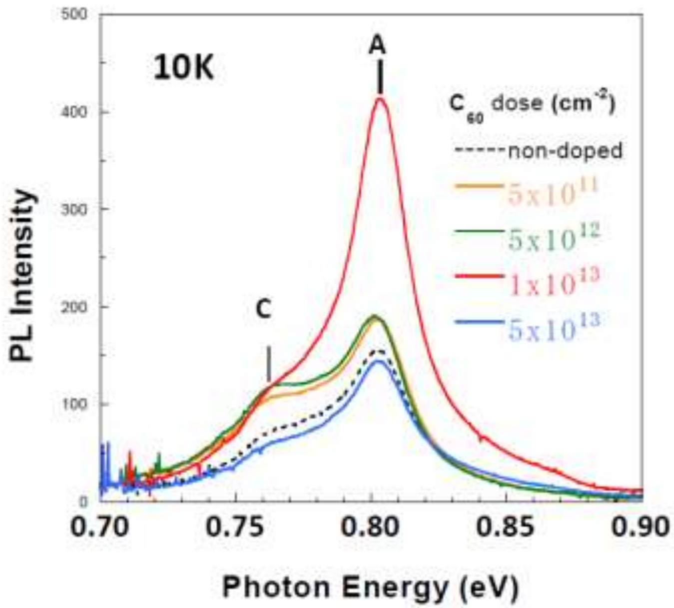

Figure 2 Photoluminescence spectra of non-doped and C-doped β-$FeSi_2$ nanocrystals. The symbols A and C denote emissions from the A band at 0.80 eV and the C band at 0.76 eV, respectively. The amount of carbon doped into the sample was expressed by the dose of C_{60} implanted into β-$FeSi_2$.

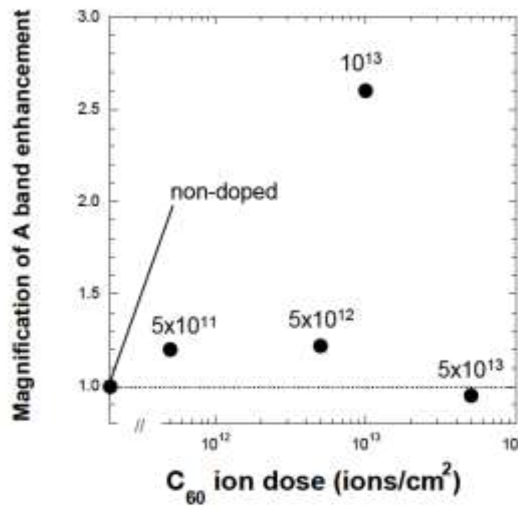

Figure 3 Magnification of enhancement of the A band intensity as a function of C_{60}^{+} ion dose.

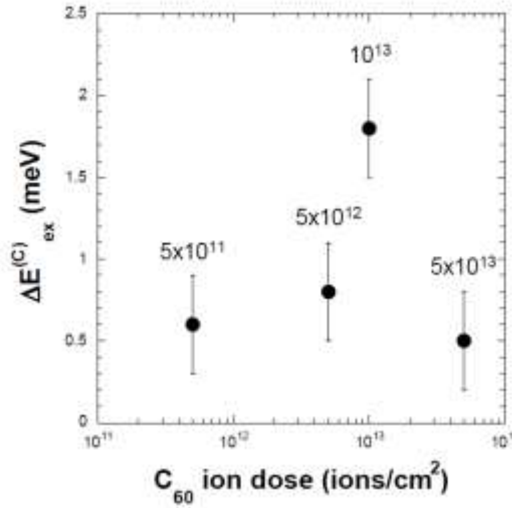

Carbon doping increases a binding energy of excitons, so that the A band PL an be enhanced.

CSSE
Kyusyu Institute of technology

5

Future study: enhancement of PL

In the final section, we report trial study of PL enhancement in order to reduce a thermal quenching effect which has been observed in β/Si heterostuructures.
This pronounced thermal quenching comes from situation of band offsets at the heterojunction.

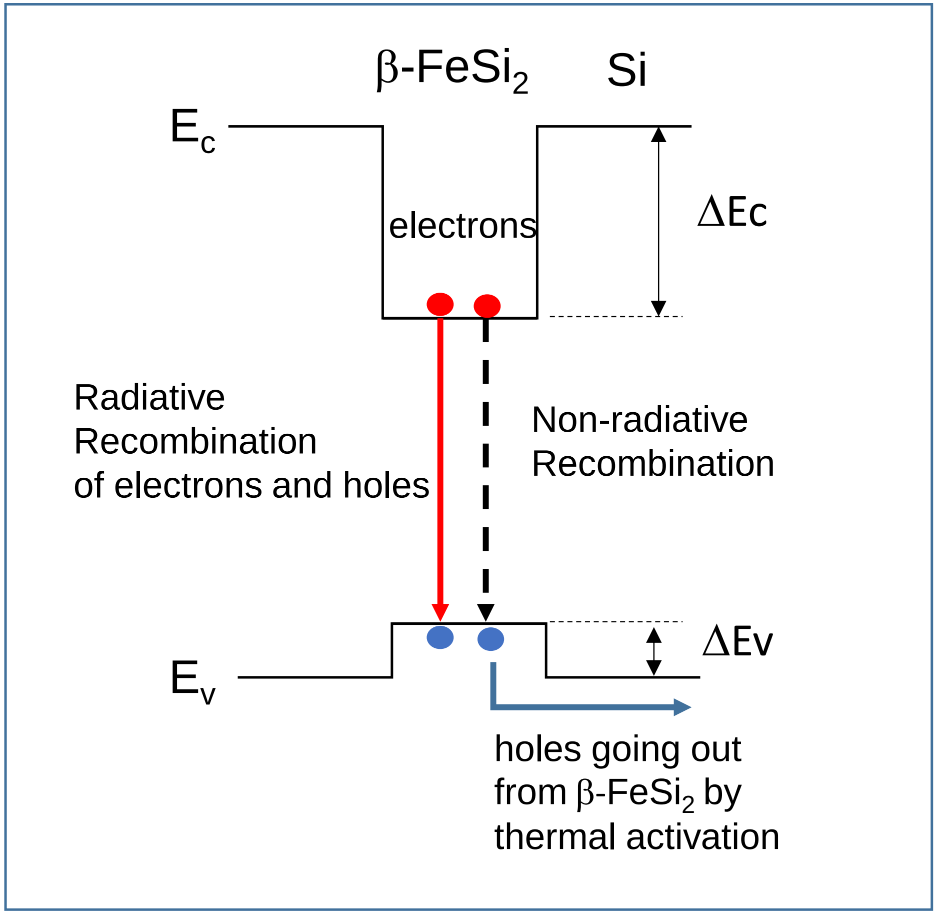

Band diagram in β-$FeSi_2$/Si heterointerfaces. ΔE_c and ΔE_v are band offset energies at the conduction and valence bands, respectively. Radiative recombination processes (RRP) between electrons at the conduction band and holes at the valence band and non-radiative processes due to escape of holes from β-$FeSi_2$ to Si. The RRP rate may be controlled by NRRP due to escape of holes.

Band offset problem at β-$FeSi_2$/Si heterojunction

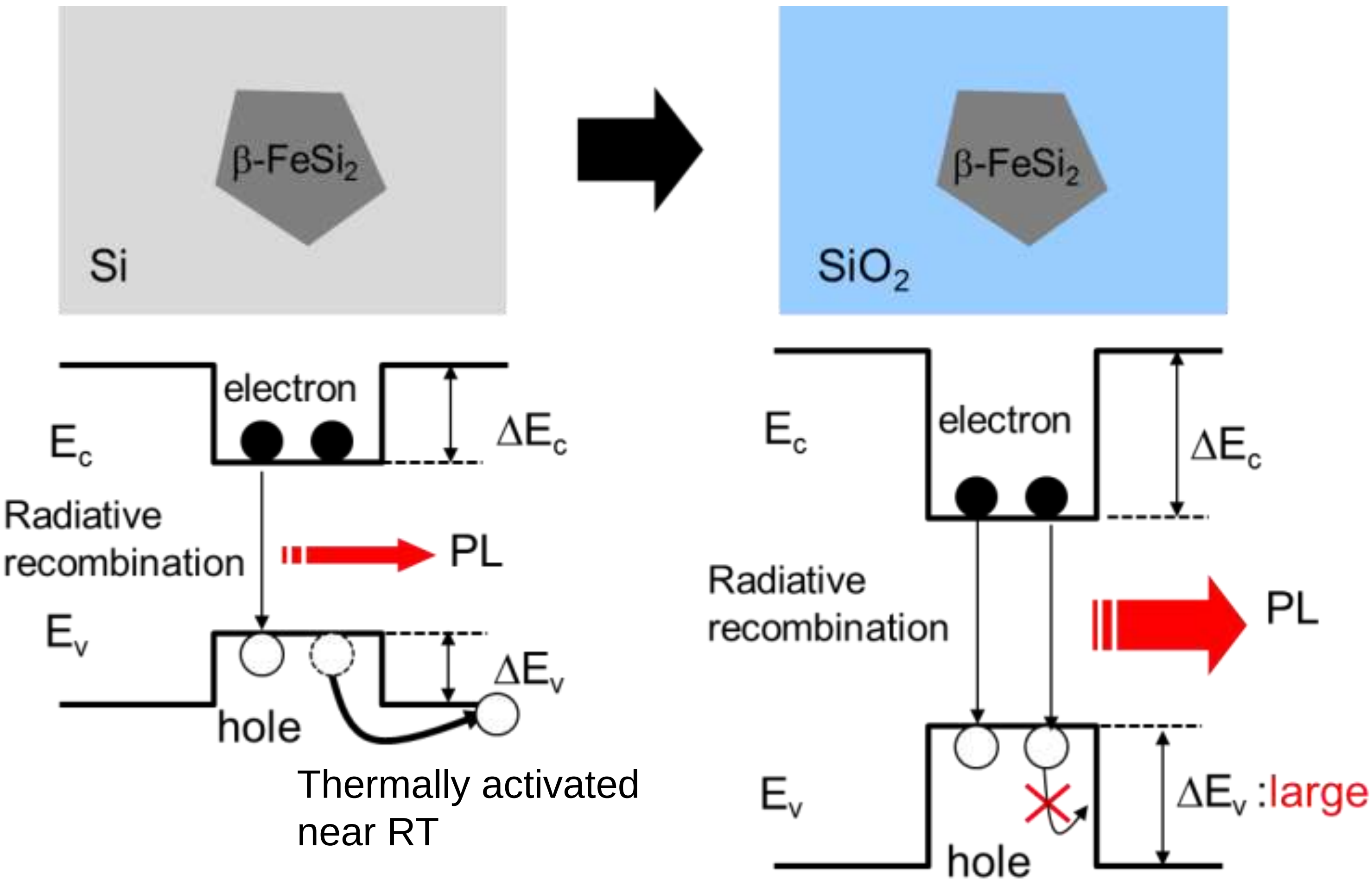

Note The valence band offset ΔEv at β-$FeSi_2$/Si heterojunction is small (~20meV), so that holes in β-$FeSi_2$ can be thermally activated into Si sides before radiative recombination near room temperature. Toward RT light emission, we need a heterojunction with large band offests like a β/SiO_2 heterojunction.

PL properties of β/SiO_2 heterostructures

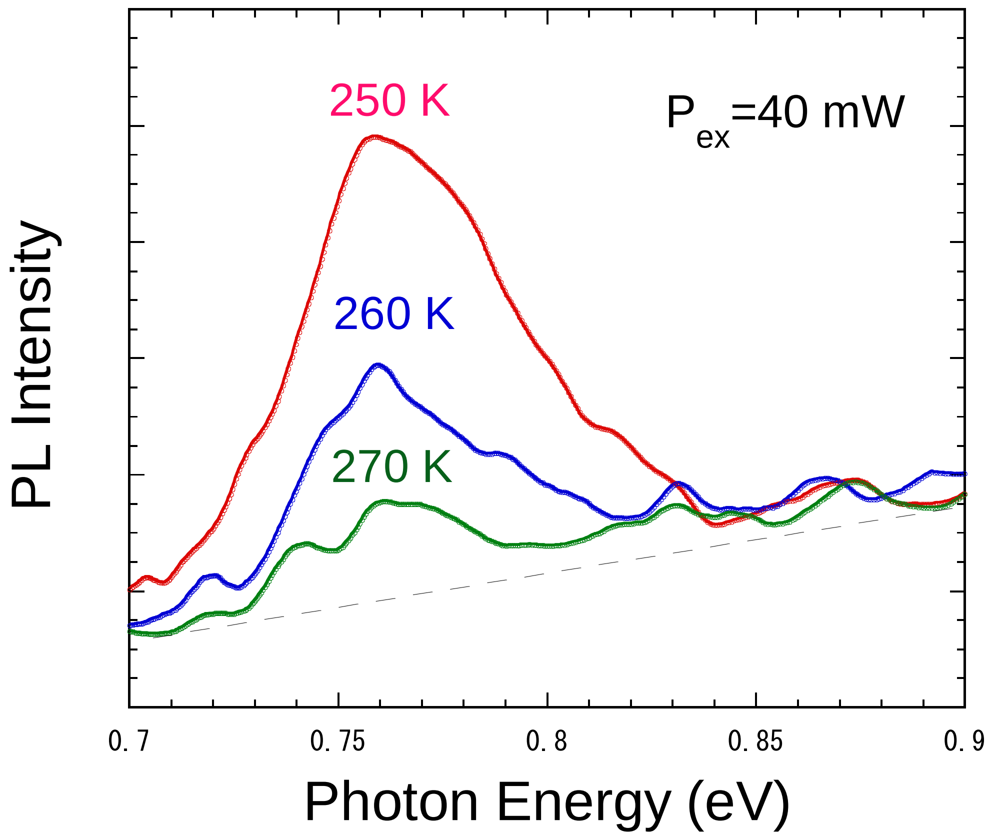

PL spectra from the oxidized non-composite phases near room temperature. The oxidation of β-NCs/Si nano-composite phase was carried out at 900^{o}C for 6 hours. The FTIR absorption measurements revealed that the Si phase was mainly oxidized. This means that a β-NCs/SiO_2 nano-composite phase forms. SiO_2 has a wide band-gap and makes large offset energies for both conduction and valence bands with β-$FeSi_2$. So we can expect sufficient confinement of electron-hole pairs at the β-NCs in the oxidized nano-composite phase. This situation may contribute to observable PL spectra near room temperature.

Analysis of reflection interferences

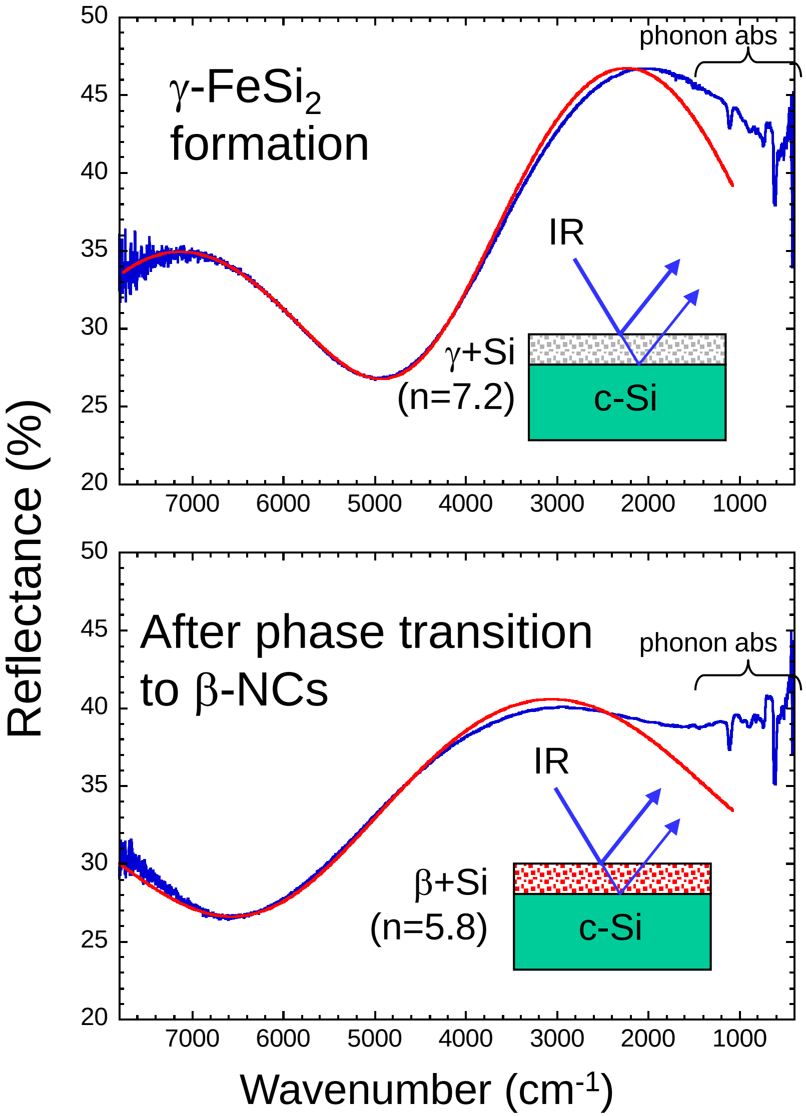

Changes of refractive index due to the γ->β phase transition can be calculated by analyzing the reflection interferences.

Volume fractions of each phase can be obtained from the change of refractive index.

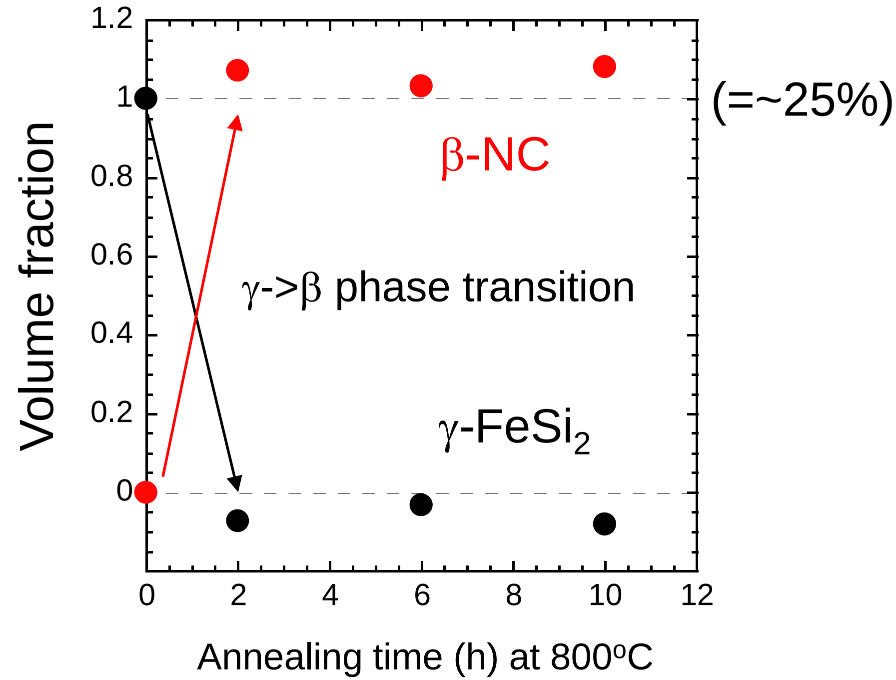

After postannealing at 800ºC, in the analysis errors, whole of the γ-phase formed by preannealing have transformed into β-NCs.